
Electronic Thesis and Dissertation Repository

8-14-2012 12:00 AM

The Contact Mechanics and Kinematics of Radial Head Implants

Hannah L. Shannon
The University of Western Ontario

Supervisor
Jim Johnson
The University of Western Ontario

Graduate Program in Biomedical Engineering
A thesis submitted in partial fulfillment of the requirements for the degree in Master of
Engineering Science
© Hannah L. Shannon 2012

Follow this and additional works at: <https://ir.lib.uwo.ca/etd>



Part of the [Biomedical Devices and Instrumentation Commons](#)

Recommended Citation

Shannon, Hannah L., "The Contact Mechanics and Kinematics of Radial Head Implants" (2012). *Electronic Thesis and Dissertation Repository*. 745.
<https://ir.lib.uwo.ca/etd/745>

This Dissertation/Thesis is brought to you for free and open access by Scholarship@Western. It has been accepted for inclusion in Electronic Thesis and Dissertation Repository by an authorized administrator of Scholarship@Western. For more information, please contact wlsadmin@uwo.ca.

The Contact Mechanics and Kinematics of Radial Head Implants

(Spine title: The Contact Mechanics and Kinematics of Radial Head Implants)

(Thesis format: Integrated Article)

by

Hannah L. Shannon

Graduate Program in Biomedical Engineering

A thesis submitted in partial fulfillment
of the requirements for the degree of
Master of Engineering Science

The School of Graduate and Postdoctoral Studies
The University of Western Ontario
London, Ontario, Canada

© Hannah L. Shannon 2012

CERTIFICATE OF EXAMINATION

Supervisor

Examiners

Dr. Jim Johnson

Dr. Trevor Birmingham

Dr. Graham King

Dr. Abbas Samani

Supervisory Committee

Dr. George Athwal

Dr. George Athwal

The thesis by

Hannah Louise Shannon

entitled:

The Contact Mechanics and Kinematics of Radial Head Implants

is accepted in partial fulfillment of the
requirements for the degree of
Masters of Engineering Science

Date

Chair of the Thesis Examination Board

ABSTRACT

A number of commercially available radial head (RH) implants are used for the management of RH fractures. The optimal shape of a RH implant to restore joint mechanics to the native state has not been established. This work compares radiocapitellar contact and kinematics for three implant designs as well as the native RH. These implants include an axisymmetric, a quasi-anatomic and a patient-specific design. When compared to the native RH, only the axisymmetric implant was significantly different in contact area ($p=0.008$). Active and passive forearm supination was assessed for differences in translations of the RH. Significant differences were found in anterior-posterior translations during active forearm supination between the axisymmetric implant and the native RH ($p=0.014$) and between the quasi-anatomic implant and native RH ($p=0.019$). This work demonstrates that while an anatomic implant appears to improve radiocapitellar contact and kinematics, future efforts are needed to optimize the materials employed in these devices.

Keywords

Biomechanics, Biomedical Engineering, Orthopaedics, Elbow, Radial Head, Implant, Joint Replacements, Joint Contact, Kinematics, Computer Assisted Surgery

CO-AUTHORSHIP STATEMENT

Chapter 1 Hannah Shannon – Sole Author

Chapter 2 Hannah Shannon – Study Design, Specimen Preparation, Data Collection, Data Analysis, Wrote Manuscript

Simon Deluce – Study Design, Data Collection

Emily Lalone – Study Design, Data Analysis

Ryan Willing – Data Analysis

Jim Johnson – Study Design, Reviewed Manuscript

Graham King – Study Design, Specimen Preparation, Reviewed Manuscript

Chapter 3 Hannah Shannon – Study Design, Specimen Preparation, Data Collection, Data Analysis, Wrote Manuscript

Simon Deluce – Study Design, Data Collection

Josh Giles – Data Analysis

Jim Johnson – Study Design, Reviewed Manuscript

Graham King – Study Design, Specimen Preparation, Reviewed Manuscript

Chapter 4 Hannah Shannon – Sole Author

ACKNOWLEDGMENTS

First off, I would like to extend my greatest thanks to both of my supervisors, Dr Jim Johnson and Dr Graham King. Your passion for research and immense knowledge of biomechanics was invaluable to the success of this project. I truly appreciate the opportunities you have given me.

To the entire team at the HULC lab, I don't know how I would have survived this project without you. Simon, my co-pilot through many radial head related obstacles that seemed impossible, I could not have asked for a better research partner. Without your coding and CAD abilities, those implants would never have existed. Josh, your LabVIEW abilities still amaze me and without those skills I would still have no idea what my raw data actually meant. Louis, your input throughout the design and execution of this study were essential to the success of the project. Emily, you have been a great source of advice and VTK programs to me. Your excitement about research and contact mechanics helped to keep me motivated, even when it got tough. To all the other summer students, graduate students, post-docs, residents and surgeons that I have worked with in my time here, you made the lab a fun learning environment that I will be sad to leave.

I would also like to thank my friends, family, and all those close to me. You made sure I stayed sane throughout this experience. Your encouragement and support have helped immensely. I love you all!

TABLE OF CONTENTS

CERTIFICATE OF EXAMINATION	ii
ABSTRACT	iii
CO-AUTHORSHIP STATEMENT	iv
ACKNOWLEDGMENTS	v
TABLE OF CONTENTS.....	vi
LIST OF TABLES	x
LIST OF FIGURES	xi
LIST OF APPENDICES.....	xiv
CHAPTER 1 - INTRODUCTION	1
1.1 THE ELBOW JOINT	1
1.1.1 Osteology	1
1.1.2 Ligaments and Joint Capsule	5
1.1.3 Muscles	9
1.2 RADIAL HEAD.....	11
1.2.1 Morphology of the Proximal Radius and the Radial Head.....	11
1.2.2 Radial Head Fracture	13
1.2.2.1 Classification.....	13
1.2.2.2 Treatment	15
1.3 CONSIDERATIONS FOR RADIAL HEAD IMPLANT DESIGN	18
1.3.1 Load Transfer	18
1.3.2 Current Designs	18
1.3.3 Novel Implant Designs	21
1.3.3.1 Population Based Designs.....	21

1.3.3.2	Reverse Engineered Implants.....	22
1.4	JOINT CONTACT.....	22
1.4.1	Contact Mechanics	22
1.4.2	Measurement Techniques	23
1.5	KINEMATICS	24
1.6	STUDY RATIONALE	25
1.7	OBJECTIVES AND HYPOTHESES.....	25
1.8	THESIS OVERVIEW	26
1.9	REFERENCES.....	27
CHAPTER 2 - EFFECT OF IMPLANT SHAPE ON RADIOCAPITELLAR CONTACT AREA.....		31
2.1	INTRODUCTION	31
2.2	METHODS	33
2.2.1	Design of Implants	33
2.2.1.1	Generic Implant Stem.....	33
2.2.1.2	Axisymmetric Implant Design	35
2.2.1.3	Population Based Quasi-Anatomic Design.....	37
2.2.1.4	Reverse Engineered Patient-Specific Design.....	41
2.2.1.5	Implant Manufacturing	41
2.2.2	Specimen Preparation	43
2.2.3	Computer Navigation	46
2.2.3.1	Registration of Intra-Operative Data to Pre-Operative Plan.....	46
2.2.3.2	Navigation and Implantation.....	46
2.2.4	Casting Joint Contact.....	49
2.2.5	Analysis of Casts	51
2.2.5.1	Contact Area Quantification	53

2.2.5.2	Contact Location Quantification	55
2.2.6	Statistical Analyses.....	59
2.3	RESULTS.....	59
2.3.1	Contact Area	59
2.3.2	Contact Location	62
2.4	DISCUSSION.....	64
2.5	REFERENCES.....	68
CHAPTER 3 - THE EFFECT OF IMPLANT SHAPE ON RADIOCAPITELLAR KINEMATICS DURING FOREARM ROTATION.....		70
3.1	INTRODUCTION	70
3.2	METHODS	72
3.2.1	Specimen Preparation	72
3.2.2	Testing Apparatus.....	72
3.2.3	Testing Protocol	74
3.2.4	Kinematics Measurements	76
3.2.5	Statistical Analyses.....	81
3.3	RESULTS.....	82
3.3.1	Validation of LCL Repair as a Control	82
3.3.2	Comparison of Radial Head Conditions	82
3.3.2.1	Medial-Lateral Translations	82
3.3.2.2	Anterior-Posterior Translations.....	85
3.4	DISCUSSION.....	88
3.5	REFERENCES.....	92
CHAPTER 4 - GENERAL DISCUSSION AND FUTURE WORK.....		94
4.1	SUMMARY	94
4.2	LIMITATIONS AND STRENGTHS	96

4.3 FUTURE DIRECTIONS.....	98
4.4 SIGNIFICANCE.....	99
4.5 REFERENCES.....	100
APPENDIX A - GLOSSARY OF TERMS	101
APPENDIX B - CONTACT AREA OF METAL AXISYMMETRIC IMPLANTS VS. PLASTIC AXISYMMETRIC IMPLANTS	106
APPENDIX C - SUMMARY OF RADIOCAPITELLAR CONTACT IMAGES	107
APPENDIX D - VALIDATION OF THE LCL REPAIR CONDITION AS A CONTROL	114
APPENDIX E - MEAN KINEMATICS DATA WITH STANDARD DEVIATIONS ..	116
CURRICULUM VITAE.....	120

LIST OF TABLES

Table 2.1 Static Loads Applied during Casting	45
Table B.1 Comparison of Contact Area of Plastic Implants to Metal Implants	106
Table E.1 Medial-Lateral Translation during Active Rotation	116
Table E.2 Medial-Lateral Translation during Passive Rotation.....	117
Table E.3 Anterior-Posterior Translation during Active Rotation.....	118
Table E.4 Anterior-Posterior Translation during Passive Rotation.....	119

LIST OF FIGURES

Figure 1.1 The Elbow	3
Figure 1.2 Motion of the Elbow	4
Figure 1.3 The Medial Collateral Ligament	6
Figure 1.4 The Lateral Collateral Ligament	8
Figure 1.5 The Muscles of the Elbow.....	10
Figure 1.6 Morphology of the Radial Head	12
Figure 1.7 The Mason Classification System	14
Figure 1.8 Radial Head Fracture Treatments	17
Figure 1.9 Radial Head Implants.....	20
Figure 2.1 Customized Stem.....	34
Figure 2.2 Axisymmetric Implants.....	36
Figure 2.3 Radial Head Measurements Used for Anatomic Implant Design	38
Figure 2.4 Quasi-Anatomic Implants	40
Figure 2.5 Examples of the Radial Head Implants.....	42
Figure 2.6 Elbow Motion Simulator.....	44
Figure 2.7 Navigation Tool.....	48
Figure 2.8 The Contact Area Quantification Process	50
Figure 2.9 The Digitization Technique Used to Trace the Contact Area.	52
Figure 2.10 The Process of Quantifying the Contact Area.....	54

Figure 2.11 The Process Used to Determine the Centre of the Contact Area	56
Figure 2.12 The Process Used to Find the Centre and Radius of the Radial Head.....	58
Figure 2.13 The Contact Area for All Radial Head Conditions.....	60
Figure 2.14 The Change in Contact Area for Implants Compared to the Native Radial Head	61
Figure 2.15 The Distance from the Centre of the Radial Head to the Contact Area Centroid	63
Figure 3.1 The Elbow Motion Simulator.....	73
Figure 3.2 Testing Protocol.....	75
Figure 3.3 Ring Tracker Mount.....	77
Figure 3.4 Translations of the Radial Head	80
Figure 3.5 Medial-Lateral Translation during Passive Forearm Rotation	83
Figure 3.6 Medial-Lateral Translation during Active Forearm Rotation	84
Figure 3.7 Anterior-Posterior Translation during Passive Forearm Rotation.....	86
Figure 3.8 Anterior-Posterior Translation during Active Forearm Rotation	87
Figure C.1 Specimen 09-12057R	107
Figure C.2 Specimen 10-01020R	108
Figure C.3 Specimen 10-06020R	109
Figure C.4 Specimen 10-07020R	110
Figure C.5 Specimen 10-08002R	111
Figure C.6 Specimen 11-03022R	112
Figure C.7 Specimen 11-03045R	113

Figure D.1 Intact Elbow vs. Control 115

LIST OF APPENDICES

A APPENDIX A - GLOSSARY OF TERMS	101
B APPENDIX B - CONTACT AREA OF METAL AXISYMMETRIC IMPLANTS VS. PLASTIC AXISYMMETRIC IMPLANTS.....	106
C APPENDIX C - SUMMARY OF RADIOCAPITELLAR CONTACT IMAGES.....	107
D APPENDIX D - VALIDATION OF THE LCL REPAIR CONDITION AS A CONTROL	114
E APPENDIX E - MEAN KINEMATICS DATA WITH STANDARD DEVIATIONS	116

CHAPTER 1 - INTRODUCTION

OVERVIEW: The overall goal of this thesis is to compare the joint contact mechanics and forearm rotation kinematics of two novel anatomical radial head implant designs to that of an axisymmetric design and the native radiocapitellar joint. This chapter provides an introduction to the anatomy of the elbow and its primary functions, with a focus on the radial head. An overview of radial head treatment options and currently available implants are presented as well. A description of the design of the novel implants is also provided. The project objective, hypotheses, rationale and thesis outline are summarized.

1.1 The Elbow Joint

The human elbow is made up of three bones; the humerus, the radius and the ulna. Together these bones make up three congruent joints which allow for two degrees of freedom; flexion/extension of the elbow and forearm rotation. Collectively the many muscle groups, ligaments and articulating bony structures provide the elbow with maximum stability. The elbow is essential to everyday life as it controls the length of reach and orientation of the hand.

1.1.1 Osteology

The humerus, radius and ulna (Figure 1.1) bones make up three articulating joints of the elbow: the ulnohumeral joint, the radiocapitellar joint and the proximal radioulnar joint (PRUJ). The ulnohumeral joint consists of the greater sigmoid notch of the ulna articulating with the trochlea of the humerus. This joint allows for flexion/extension (Figure 1.2 A) with some laxity, and provides most of the bony stability in the elbow

joint. The radiocapitellar joint is made up of the radial dish and the capitellum of the humerus. The radius tracks along the ellipsoid-like capitellum (Sabo *et al.*, 2011) in flexion/extension as well as rotates against it during pronation/supination (Figure 1.2 B). The radiocapitellar joint also provides stability to the elbow joint. The PRUJ is formed by the radial notch found on the lateral side of the ulna and approximately 240 degrees (Morrey, 2008) of the circumference of the radial head. This joint allows for rotation of the forearm.

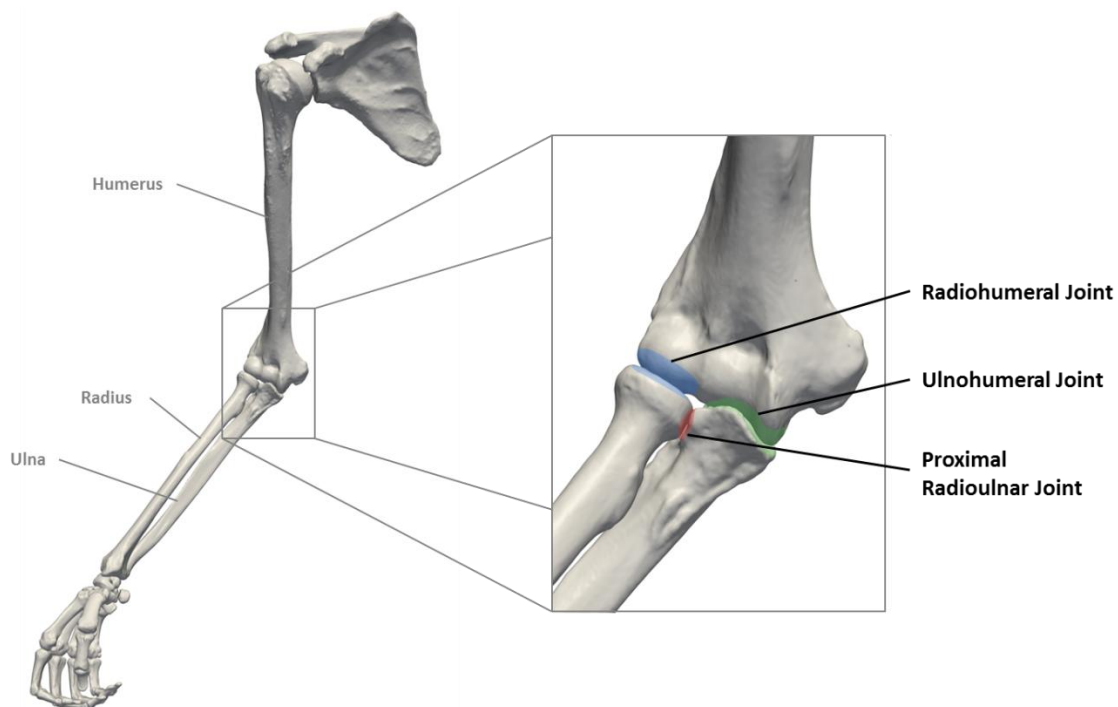


Figure 1.1 The Elbow

The elbow is made up of three bones: the humerus, the ulna and the radius. Together these bones make up three joints: the radiohumeral (radiocapitellar) joint, ulnohumeral joint and proximal radioulnar (PRUJ) joint (Deluce, 2011).

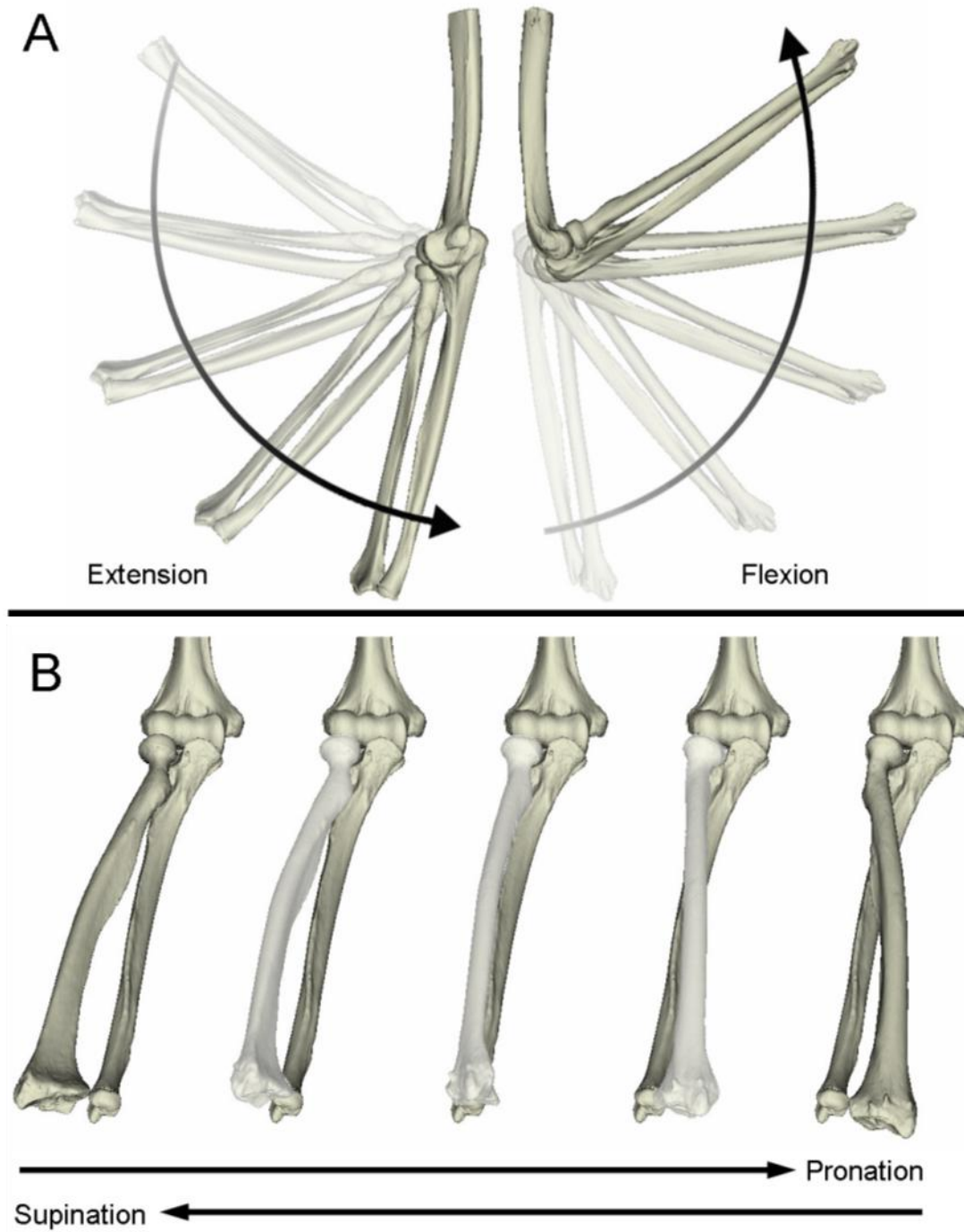


Figure 1.2 Motion of the Elbow

- A. *Elbow flexion and extension*
 B. *Forearm rotation: pronation and supination*
 (Deluce, 2011)

1.1.2 *Ligaments and Joint Capsule*

Two of the main sources of stability in the elbow are the medial collateral ligament (MCL) and the lateral collateral ligament (Figure 1.3). The MCL is comprised of the transverse, anterior and posterior bundles. The anterior bundle is the main contributor to valgus (angulation of the forearm away from the body) elbow stability in this ligament group. The MCL originates at the medial epicondyle (near the axis of flexion) of the humerus with the anterior bundle extending to the proximal ulna near the coronoid and the posterior portion extending the proximal ulna near the mid portion of the greater sigmoid notch.

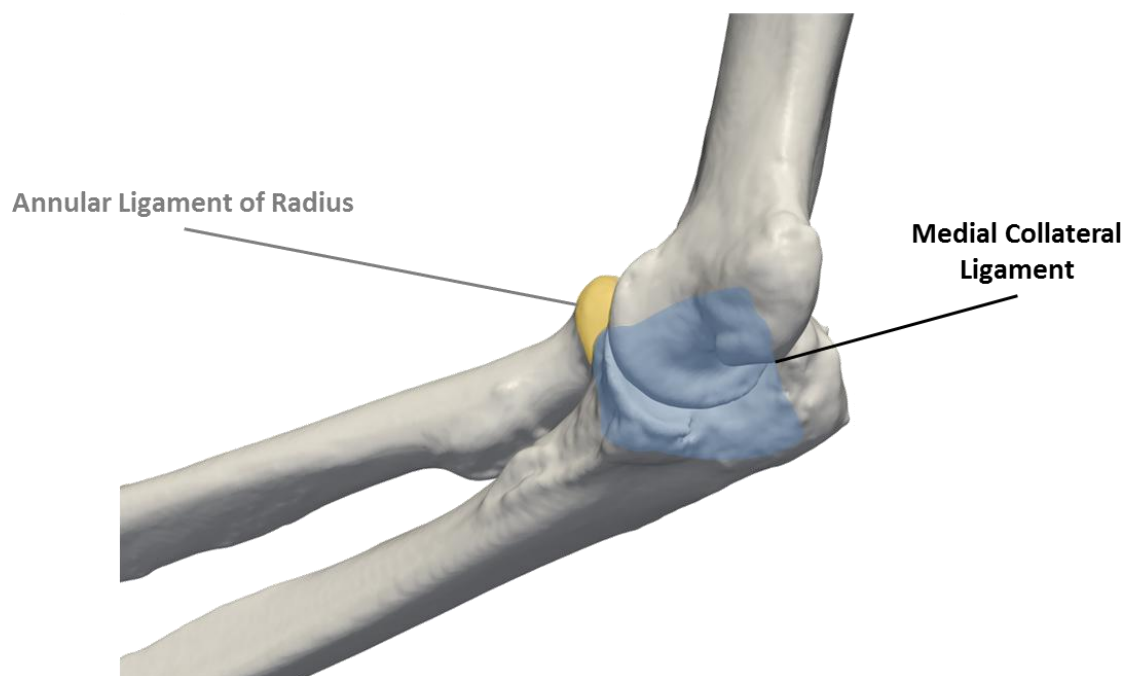


Figure 1.3 The Medial Collateral Ligament

The MCL, shown in blue, is an important valgus stabilizer for the elbow (Deluce, 2011).

The other major ligament group is the lateral collateral ligament (Figure 1.4). The main components of this structure are the radial collateral ligament (RCL), the lateral ulnar collateral ligament (LUCL) and the annular ligament. The LCL originates at the lateral epicondyle of the humerus (in line with the axis of flexion). The RCL extends to the annular ligament, whereas the LUCL extends distal to the posterior portion of the annular ligament to insert on the ulna. The LCL is the main stabilizer of the elbow to varus (angulation of the forearm towards the body) loads. The annular ligament extends from the proximal ulna posterior to the radial notch, surrounds the radial head and inserts on the ulna anterior to the radial notch. The annular ligament keeps the radius in contact with the radial notch of the ulna therefore stabilizing rotation of the proximal radioulnar joint.

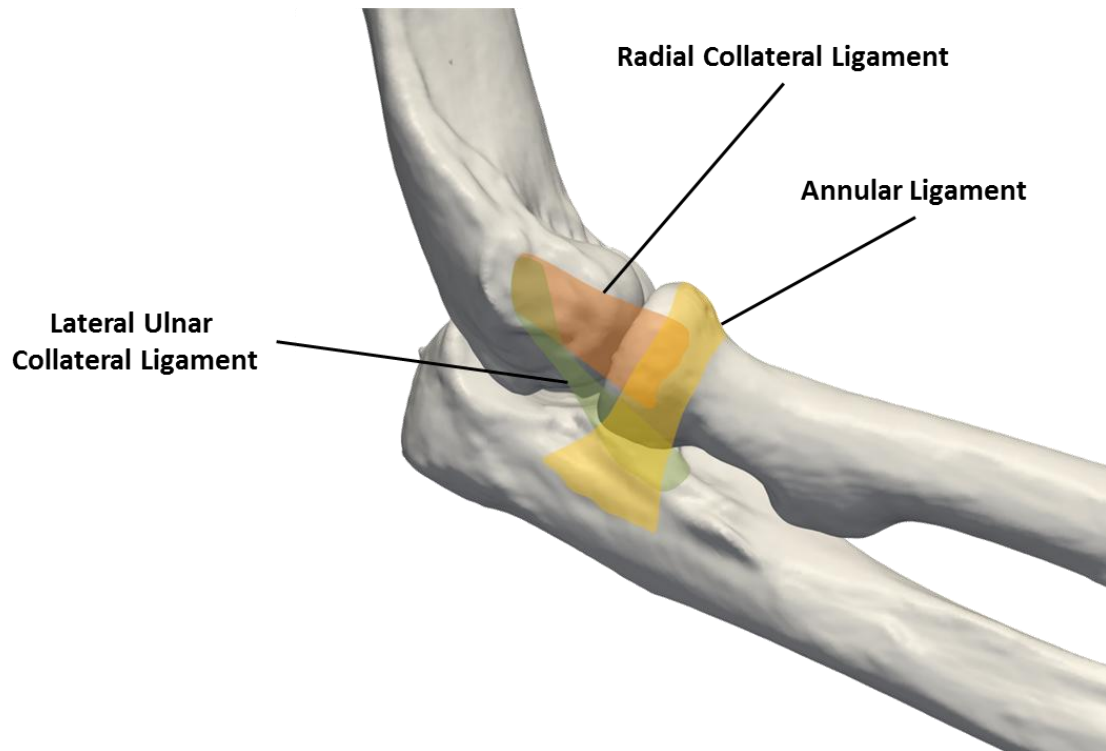


Figure 1.4 The Lateral Collateral Ligament

The LCL is made up of the radial collateral ligament (orange), the lateral ulnar collateral ligament (green) and the annular ligament (yellow) (Deluce, 2011).

The entire elbow joint is also surrounded by the joint capsule. As the elbow is a synovial joint, it must be surrounded by synovial fluid. This fluid is important for cartilage nutrition, acts as a lubrication medium as well as a shock absorber. The cartilage covering the articular surface of the elbow bones requires this fluid to move smoothly during joint motion. The joint capsule attaches proximal to the coronoid and radial fossae on the anterior portion of the humerus and above the olecranon fossa on the posterior humerus (Morrey, 2008). The distal portion of the capsule attaches to the anterior coronoid and the annular ligament and posterior sigmoid notch.

1.1.3 *Muscles*

The muscles surrounding the elbow help to stabilize the joint during motion. There are flexors, extensors, pronators and supinators that allow the two degrees of freedom in this joint (Figure 1.5). The main flexors of the elbow are the biceps, brachialis and brachioradialis. The main extender is the triceps. The pronators are the pronator teres and pronator quadratus and the supinators are the biceps and supinator.

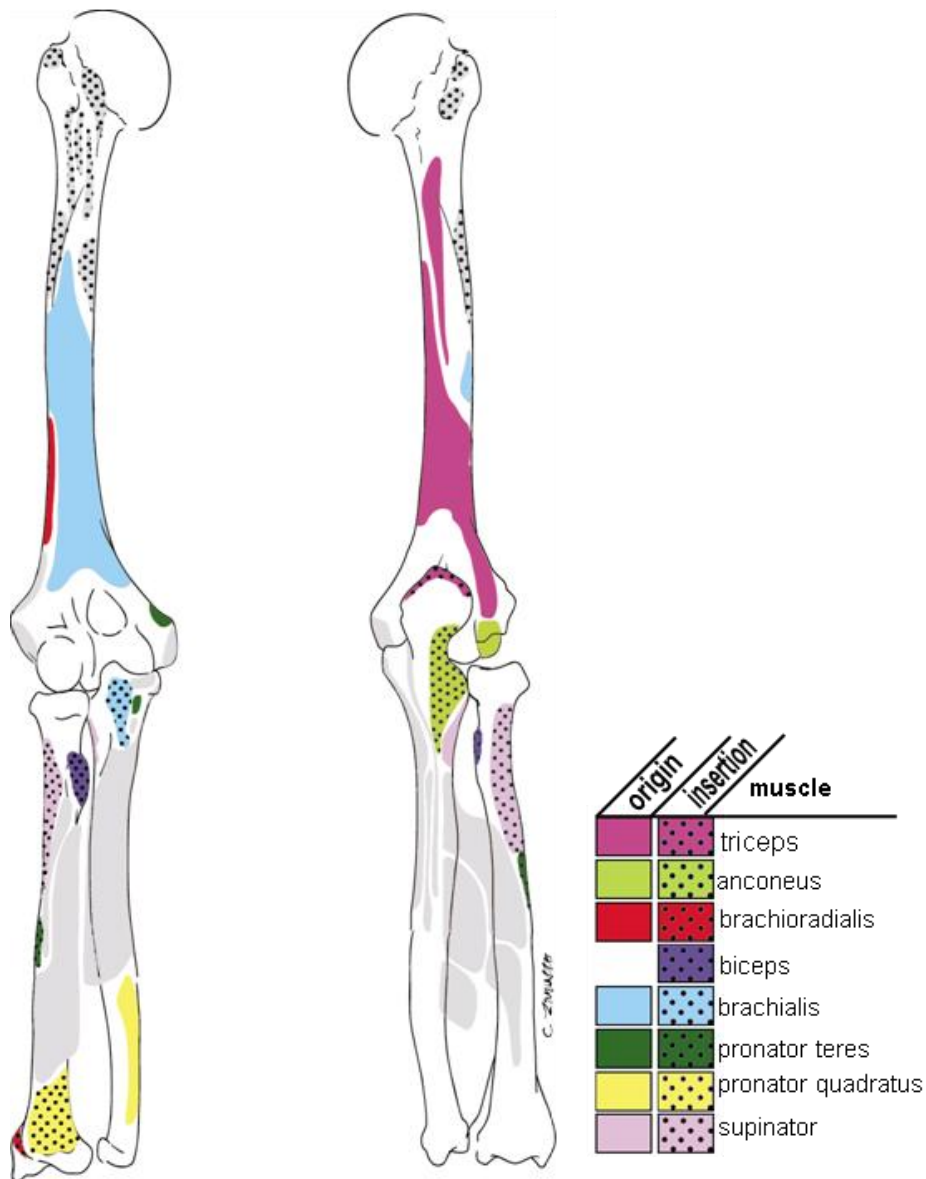


Figure 1.5 The Muscles of the Elbow

Many muscles play a role in flexion/extension, pronation/supination, and overall stability of the elbow joint. The main muscles are displayed in this image (Stacpoole, 2002).

1.2 Radial Head

The radial head is a key bony stabilizer of the elbow. The greatest amount of force through the radial head is seen with the arm in pronation (Morrey, 2008). When the elbow sustains a MCL injury, the radial head is essential to stability as it is considered a secondary stabilizer in preventing elbow dislocation under valgus stress (Morrey, 2008).

1.2.1 *Morphology of the Proximal Radius and the Radial Head*

The majority of studies that have explored the shape of the radial head have determined that it is elliptical in shape (Figure 1.6A). Multiple studies have confirmed that the major axis and minor axis are different in length (King *et al.*, 2001; Swieszkowski *et al.*, 2001; van Riet *et al.*, 2003). The articular portion of the radial head is flat and taller whereas the non-articular side is shorter and rounded (to constrain the annular ligament) (Spinner and Kaplan, 1970) (Figure 1.6B). Furthermore, it has been shown that the radial head is variably offset from the neck of the proximal radius (King *et al.*, 2001; van Riet *et al.*, 2004) (Figure 1.6B). This offset may be essential to forearm rotation, creating a cam effect between the radius and ulna at the proximal radial ulnar joint (PRUJ).

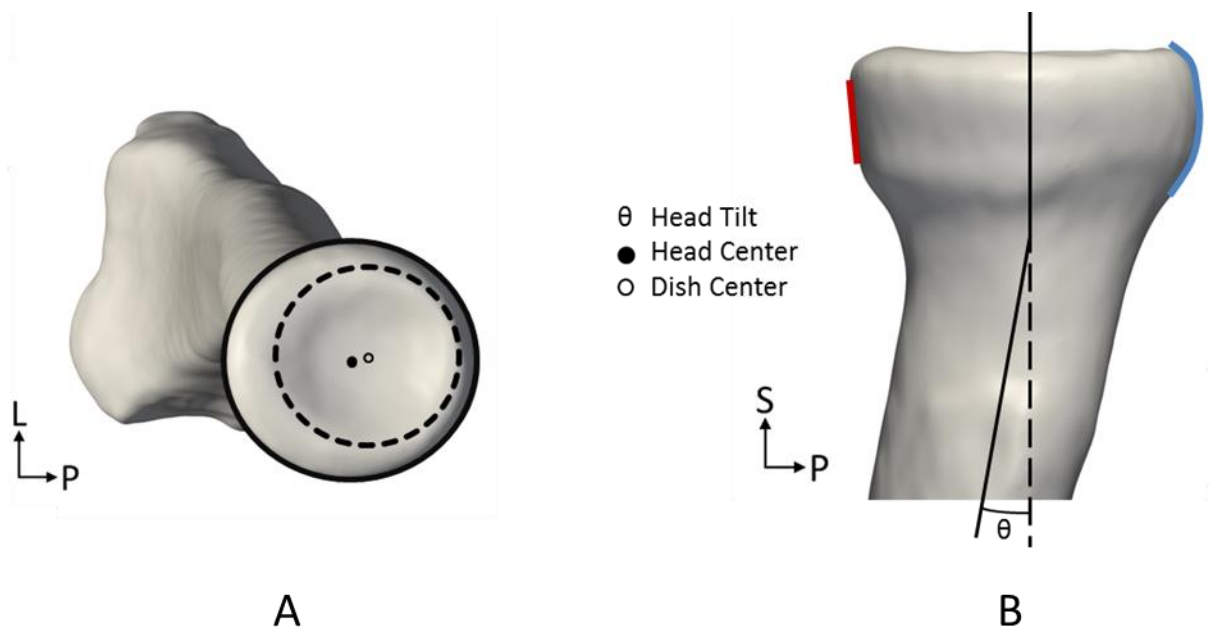


Figure 1.6 Morphology of the Radial Head

- A. Superior view of the radial head demonstrating that the centre of the dish is offset from the centre of the radial head circumference.
- B. Medial view of the proximal radius demonstrating the difference in curvature between the articular (red) and non-articular (blue) portions as well as the tilt between the radial head and long axis of the radius.
- (Deluce, 2011)

1.2.2 *Radial Head Fracture*

Radial head fractures occur in approximately 33% of all elbow fractures (Mason, 1954; Morrey, 2008). The most common form of trauma is the result of a fall with an outstretched arm with the elbow flexed slightly and pronated. During impact, an axial load on the eccentric radial head causes the posterolateral portion of the radial head to hit the capitellum, resulting in an anterolateral fragment breaking off (Morrey, 2008). Other common mechanisms are valgus and axial loading injuries.

1.2.2.1 *Classification*

Radial head fractures can be classified into three types known as the Mason Classification (Mason, 1954). Type I is a marginal fracture with no displacement, Type II involves marginal sector fractures with displacement, and Type III is a comminuted fractures that involves fracture of the entire head (Figure 1.7) (Mason, 1954).



Figure 1.7 The Mason Classification System

- I. Type I - Nondisplaced Fracture*
 - II. Type II - Displaced Fracture*
 - III. Type III - Comminuted Fracture*
- (Deluce, 2011)

1.2.2.2 *Treatment*

The treatment for radial head fractures has changed significantly over the years. The current treatment is based on the severity of the fractures and the presence of associated injuries.

Non-operative treatment is favoured for Type I and II fractures, where displacement is minimal as long as there is no mechanical block to motion (VanBeek and Levine, 2010) (Figure 1.8 A). Early active motion is preferred to reduce elbow stiffness. For more complicated injuries, such as Type III, where the fracture is displaced and there are associated tissue injuries, operative treatment is considered; open reduction and internal fixation (ORIF), excision, and arthroplasty (Figure 1.8 B-D). ORIF is usually quite successful with simple displaced fractures, but complications are frequent when the fracture is more complex (Ring *et al.*, 2002). Excision of the radial head is a controversial treatment for radial head fractures, specifically when there is an associated tissue or bony injury. Excision can result in complications that include instability, loss of strength, excess loading on the ulnohumeral joint leading to osteoarthritis, migration of the proximal radius and wrist pain (Leppilahti and Jalovaara, 2000; Stuffmann and Baratz, 2009; VanBeek and Levine, 2010). Radial head arthroplasty has shown good results thus far in the medium to short-term (Chien *et al.*, 2010; Grewal *et al.*, 2006; Moro *et al.*, 2001; Zhao *et al.*, 2007); however, long-term follow up studies have not yet been completed. Most radial head implants are metallic, a much stiffer material than bone. Furthermore the majority have an axisymmetric shape in spite of the elliptical nature of the native radial head. This can result in complications such as damage to the capitellum,

increased ulnohumeral loading leading to osteoarthritis and implant failure (Burkhart *et al.*, 2010; Harrington *et al.*, 2001; Herald and O'Driscoll, 2008; Popovic *et al.*, 2007).



Figure 1.8 Radial Head Fracture Treatments

- A. Radial head fracture treated without surgery*
 - B. Radial head fracture treated with excision*
 - C. Radial head fracture repaired with open reduction and internal fixation (ORIF)*
 - D. Radial head fracture replaced with an implant*
- (Deluce, 2011)*

1.3 Considerations for Radial Head Implant Design

1.3.1 *Load Transfer*

At the radiocapitellar joint, models of force distribution have calculated loads to be as high as three times body weight during a normal activity, such as pushing inward against an external force (Amis *et al.*, 1979). Halls and Travill conducted an *in vitro* study that showed force being transmitted across the elbow as approximately 40% through the ulnohumeral joint and 60% through the radiocapitellar joint in full extension (Halls and Travill, 1964). Furthermore, a traditional force-displacement study by Hotchkiss and Weiland has attributed 30% of the resistance to valgus stress to the radial head (Hotchkiss and Weiland, 1987). Radial head implants must be designed such that the shape and material can withstand these loads.

1.3.2 *Current Designs*

Early radial head implant designs were constructed from various materials, such as silicone, vitallium and acrylic (Cherry, 1953; Speed, 1941; Swanson *et al.*, 1981). These materials proved to be insufficient to withstand the loads within the elbow. The use of axisymmetric metal implants has become the norm, as they have sufficient strength to resist stresses in the joint and withstand axial loads (Judet *et al.*, 1996; Knight *et al.*, 1993). These designs are available in monoblock systems (Figure 1.9 A) as well as articulating bipolar systems (Figure 1.9 B). These axisymmetric implants may use a loose fitting smooth stem or a bipolar stem to compensate for their lack of anatomic shape and to allow for the head to self-align within the radiocapitellar joint and the PRUJ. There is

currently one anatomically shaped implant commercially available for use (Anatomical Radial Head System, Acumed, Hillboro, OR, USA) (Figure 1.9 C); however, this implant relies on precise placement and secure fixation.



Figure 1.9 Radial Head Implants

- A. *Evolve Proline Radial Head System with axisymmetric head and smooth stem. (Wright Medical Technology Inc., Arlington, TN, USA)*
- B. *RHS Radial Head System bipolar axisymmetric implant with short and long stem designs. (Tornier, Stafford, TX, USA)*
- C. *Anatomic Radial Head System which is designed to allow for bone ingrowth. (Acumed, Hillboro, OR, USA)*

The radial head implants that are currently available all come with limitations. Bipolar implants have shown a reduced capacity to resist radiocapitellar subluxation when compared to non-bipolar designs (Chanlalit *et al.*, 2011). Complications with implant height, especially related to joint over stuffing have been observed as well (Frank *et al.*, 2009). Current anatomical designs rely on anatomical landmarks (*i.e.*, biceps tuberosity, radial head major axis and distal radius) for proper implant alignment. These landmarks have been shown to be poorly correlated with each other (Katchky *et al.*, 2011) and sometimes are damaged in the initial injury and therefore, cannot always be used for implant positioning.

1.3.3 *Novel Implant Designs*

Anatomically shaped implants were previously developed as described by Deluce (Deluce, 2011). These implant concepts were used to conduct the research presented in this thesis. They consist of population based quasi-anatomic designs and reverse engineered patient-specific designs.

1.3.3.1 *Population Based Designs*

Population based implants take into account the geometry of a sample population. Anatomical models of human radii are made from medical imaging techniques such as computed tomography or magnetic resonance imaging and measurements are made on every model in the sample. These measurements can then be grouped into similar categories based on size and averaged to create a series of anatomically shaped implants. When using computed tomography, this makes the anatomically shaped implants similar

to the geometry of the bone, ignoring the contribution of articular cartilage. Although they are based on population averages (and hence termed “quasi-anatomic”), this is much more feasible than creating patient-specific implants.

1.3.3.2 *Reverse Engineered Implants*

Reverse engineered implants make use of medical imaging technologies to determine the exact geometry of specific bone. A 3D model of the radial head is made from the imaging data. This bone model is measured thoroughly and these measurements are then used to replicate the native anatomy exactly. Then patient-specific implants are manufactured. These implants are currently very costly and have a design and fabrication delay because they are custom fabricated instead of mass produced, like most commercially available off-the-shelf implants.

1.4 Joint Contact

1.4.1 *Contact Mechanics*

Measuring contact area within the joint is important in determining load distribution. Contact mechanics can also be used as a metric to assess whether implants are performing similarly to the native articulations. This can aid in the design of implants that reproduce a more natural joint. Also, it is important to note that contact area is somewhat inversely correlated with contact stress. Therefore, by studying contact area, estimations on the changes in contact stress and the prediction of patterns of cartilage wear and sites of potential osteoarthritis can be made.

1.4.2 Measurement Techniques

There are many ways to measure contact area that have been described in the literature. These techniques include pressure-sensitive film (Haut, 1989; Huberti and Hayes, 1984; Matsuda *et al.*, 1997; Ronsky *et al.*, 1995; Van Glabbeek *et al.*, 2004), cartilage staining (Black *et al.*, 1981; Stormont *et al.*, 1985), silicone casting (Lalone *et al.*, 2012b; Lalone *et al.*, 2012a; Liew *et al.*, 2003; Stormont *et al.*, 1985), and imaging techniques (Ateshian *et al.*, 1994; Besier *et al.*, 2005; Eisenhart-Rothe *et al.*, 2004; Heino and Powers, 2002; Lalone *et al.*, 2012a). The majority of these techniques are invasive and are performed *in vitro*; however, imaging techniques can be used *in vivo*.

Silicone casting is considered the gold standard method for studying joint contact area (Stormont *et al.*, 1985). This technique has been proven repeatable and accurate (Liew *et al.*, 2003). The basic technique consists of filling a joint with a liquid silicone material. The opening used to get into the joint is then closed and the silicone is left to harden. Once the cast has cured, it is carefully removed from the joint and can be assessed for contact area.

Various techniques have been described to measure the area seen on the cast. One way to determine the area is to refit the cast to the articular surface of each bone (one at a time) and measure it qualitatively (Stormont *et al.*, 1985). One quantitative method involves scanning the cast and tracing the inner area on the computer image (Liew *et al.*, 2003). Since the joint surface is curved, there can be some limitations to measuring in two-dimensions. To avoid these limitations, Lalone *et al.* measured the contact area of casts using an optically tracked calibrated stylus to trace the area of joint contact (Lalone *et al.*,

2012b). A three-dimensional surface model of the resulting contact patch was constructed and the surface area of the patch, which corresponded to total contact area, was calculated.

There is some error with the casting technique. Contact area could be overestimated due to a thinning around the edge of the contact area that may be torn during the removal of the cast or not easily visible against the cartilage surface. Therefore, it is essential to be careful when measuring the contact area and when removing the cast from the joint.

1.5 Kinematics

The elbow joint is a combination of a hinge (ginglymus) and pivot (trochoid) joint. This combination is also known as a trochoginglymoid joint. The ulnohumeral and radiocapitellar joints function together to allow flexion and extension of the “hinge”. The axis about which the elbow flexes can be approximated as a line that goes through the centre on the greater sigmoid notch of the ulna and the centre of the capitellum (Brownhill *et al.*, 2006). The elbow has been identified as a sloppy hinge with slight laxity. This means that the flexion axis does not remain at a fixed location (Duck *et al.*, 2003). The average elbow has a range of flexion from 0°-145° (Boone and Azen, 1979). The radial head and proximal ulna, which together make up the proximal radial ulnar joint (PRUJ) allow a “pivot” or rotation of the forearm. The axis about which the forearm rotates extends from the centre of the radial head through the centre of the distal ulna (Hollister *et al.*, 1994). The average forearm has a range of 70° in pronation to 85° in supination (Boone and Azen, 1979).

The elbow joint does have some inherent laxity and therefore, during both flexion/extension and pronation/supination, translations are observed. Most of these translations are at the radial head. These translations can be seen in the medial-lateral direction, anterior-posterior direction and proximal-distal direction.

1.6 Study Rationale

It has previously been reported that axisymmetric radial head prostheses do not adequately match the morphology of the native radial head (Beredjiklian *et al.*, 1999). Other ‘anatomic’ implants strive to replicate the anatomy of the radial head, but differences in implant shape from the native radial head and errors in alignment may easily occur when only visual landmarks are used for implantation. These errors may result in abnormal motion and contact patterns; leading to implant failure as a consequence of loosening and/or capitellar cartilage overload. Novel anatomically shaped implants (both population based quasi-anatomic and reverse engineered patient-specific) have recently been developed in our laboratory, as well as a computer guidance system to assure precise implant placement. These implants have not yet been assessed in comparison to the native radial head or an axisymmetric implant design. Although these designs replicate the radial head in appearance, it is essential to determine whether they will replicate the native radial head in joint contact mechanics and kinematics.

1.7 Objectives and Hypotheses

The specific objectives of this research were:

1. to compare the radiocapitellar contact patterns of three radial head implant designs: (1) axisymmetric, (2) population based quasi-anatomic, and (3) reverse engineered patient-specific devices to that of the native radial head,
2. to compare radiocapitellar kinematics of three radial head implant designs: (1) axisymmetric, (2) population based quasi-anatomic and (3) reverse engineered patient-specific to that of the native radial head.

The hypotheses were:

1. anatomically shaped radial head implants will have a greater contact area than the axisymmetric radial head implants and demonstrate similar radiocapitellar contact patterns as the native radial heads.
2. anatomically shaped radial head implants will have similar radiocapitellar kinematics as the native radial heads, while the axisymmetric radial head implants will differ.

1.8 Thesis Overview

Chapter 2 compares the radiocapitellar joint contact for the native radial head as well as all implant morphologies. The native radiocapitellar joint kinematics are compared to the three implants in Chapter 3. Chapter 4 contains a general discussion, conclusions and a summary of future work.

1.9 References

- Amis, A.A., Dowson, D., Wright, V., and Miller, J.H. (1979) The derivation of elbow joint forces, and their relation to prosthesis design. *J Med Eng Technol.* 3[5], 229-234.
- Ateshian, G.A., Kwak, S.D., Soslowky, L.J., and Mow, V.C. (1994) A stereophotogrammetric method for determining in situ contact areas in diarthrodial joints, and a comparison with other methods. *J Biomech.* 27[1], 111-124.
- Beredjikian, P.K., Nalbantoglu, U., Potter, H.G., and Hotchkiss, R.N. (1999) Prosthetic radial head components and proximal radial morphology: a mismatch. *J Shoulder Elbow Surg* 8[5], 471-475.
- Besier, T.F., Draper, C.E., Gold, G.E., Beaupre, G.S., and Delp, S.L. (2005) Patellofemoral joint contact area increases with knee flexion and weight-bearing. *J Orthop Res* 23[2], 345-350.
- Black, J.D., Matejczyk, M.B., and Greenwald, A.S. (1981) Reversible cartilage staining technique for defining articular weight-bearing surfaces. *Clin Orthop Relat Res* [159], 265-267.
- Boone, D.C. and Azen, S.P. (1979) Normal range of motion of joints in male subjects. *J Bone Joint Surg Am* 61[5], 756-759.
- Brownhill, J.R., Furukawa, K., Faber, K.J., Johnson, J.A., and King, G.J. (2006) Surgeon accuracy in the selection of the flexion-extension axis of the elbow: an in vitro study. *J Shoulder Elbow Surg* 15[4], 451-456.
- Burkhart, K.J., Mattyasovszky, S.G., Runkel, M., Schwarz, C., Kuchle, R., Hessmann, M.H., Rommens, P.M., and Lars, M.P. (2010) Mid- to long-term results after bipolar radial head arthroplasty. *J Shoulder Elbow Surg* 19[7], 965-972.
- Chanlalit, C., Shukla, D.R., Fitzsimmons, J.S., An, K.N., and O'Driscoll, S.W. (2011) Influence of prosthetic design on radiocapitellar concavity-compression stability. *J Shoulder Elbow Surg* 20[6], 885-890.
- Cherry, J.C. (1953) Use of acrylic prosthesis in the treatment of fracture of the head of the radius. *J Bone Joint Surg Br.* 35-B[1], 70-71.
- Chien, H.Y., Chen, A.C., Huang, J.W., Cheng, C.Y., and Hsu, K.Y. (2010) Short- to medium-term outcomes of radial head replacement arthroplasty in posttraumatic unstable elbows: 20 to 70 months follow-up. *Chang Gung.Med J* 33[6], 668-678.
- Deluce, S.R. (2011) Design, Validation and Navigation of Anatomic Population-Based and Patient-Specific Radial Head Implants. Master of Engineering Science Western University.

Duck, T.R., Dunning, C.E., King, G.J., and Johnson, J.A. (2003) Variability and repeatability of the flexion axis at the ulnohumeral joint. *J Orthop Res* 21[3], 399-404.

Eisenhart-Rothe, R., Siebert, M., Bringmann, C., Vogl, T., Englmeier, K.H., and Graichen, H. (2004) A new in vivo technique for determination of 3D kinematics and contact areas of the patello-femoral and tibio-femoral joint. *J Biomech.* 37[6], 927-934.

Frank, S.G., Grewal, R., Johnson, J., Faber, K.J., King, G.J., and Athwal, G.S. (2009) Determination of correct implant size in radial head arthroplasty to avoid overlengthening. *J Bone Joint Surg Am* 91[7], 1738-1746.

Grewal, R., MacDermid, J.C., Faber, K.J., Drosdowech, D.S., and King, G.J. (2006) Comminuted radial head fractures treated with a modular metallic radial head arthroplasty. Study of outcomes. *J Bone Joint Surg Am* 88[10], 2192-2200.

Halls, A.A. and Travill, A. (1964) Transmission of Pressure Across the Elbow Joint. *Anat.Rec.* 150, 243-247.

Harrington, I.J., Sekyi-Otu, A., Barrington, T.W., Evans, D.C., and Tuli, V. (2001) The functional outcome with metallic radial head implants in the treatment of unstable elbow fractures: a long-term review. *J Trauma* 50[1], 46-52.

Haut, R.C. (1989) Contact pressures in the patellofemoral joint during impact loading on the human flexed knee. *J Orthop Res* 7[2], 272-280.

Heino, B.J. and Powers, C.M. (2002) Patellofemoral stress during walking in persons with and without patellofemoral pain. *Med Sci.Sports Exerc.* 34[10], 1582-1593.

Herald, J. and O'Driscoll, S. (2008) Complete dissociation of a bipolar radial head prosthesis: a case report. *J Shoulder Elbow Surg* 17[6], e22-e23.

Hollister, A.M., Gellman, H., and Waters, R.L. (1994) The relationship of the interosseous membrane to the axis of rotation of the forearm. *Clin Orthop Relat Res* [298], 272-276.

Hotchkiss, R.N. and Weiland, A.J. (1987) Valgus stability of the elbow. *J Orthop Res* 5[3], 372-377.

Huberti, H.H. and Hayes, W.C. (1984) Patellofemoral contact pressures. The influence of q-angle and tendofemoral contact. *J Bone Joint Surg Am* 66[5], 715-724.

Judet, T., Garreau, d.L., Piriou, P., and Charnley, G. (1996) A floating prosthesis for radial-head fractures. *J Bone Joint Surg Br.* 78[2], 244-249.

Katchky, R.N., Johnson, J.A., King, G.J., and Athwal, G.S. (2011) Anatomic radial head arthroplasty: A lack of reliable landmarks for alignment. 164-165.

King, G.J., Zarzour, Z.D., Patterson, S.D., and Johnson, J.A. (2001) An anthropometric study of the radial head: implications in the design of a prosthesis. *J Arthroplasty* 16[1], 112-116.

Knight, D.J., Rymaszewski, L.A., Amis, A.A., and Miller, J.H. (1993) Primary replacement of the fractured radial head with a metal prosthesis. *J Bone Joint Surg Br* 75[4], 572-576.

Lalone, E.A., McDonald, C.P., Ferreira, L.M., Peters, T.M., King, G.W., and Johnson, J.A. (2012a) Development of an image-based technique to examine joint congruency at the elbow. *Comput Methods Biomech.Biomed.Engin.*

Lalone, E.A., Peters, T.M., King, G.W., and Johnson, J.A. (2012b) Accuracy assessment of an imaging technique to examine ulnohumeral joint congruency during elbow flexion. *Comput Aided Surg* 17[3], 142-152.

Leppilahti, J. and Jalovaara, P. (2000) Early excision of the radial head for fracture. *Int Orthop* 24[3], 160-162.

Liew, V.S., Cooper, I.C., Ferreira, L.M., Johnson, J.A., and King, G.J. (2003) The effect of metallic radial head arthroplasty on radiocapitellar joint contact area. *Clin Biomech.(Bristol., Avon.)* 18[2], 115-118.

Mason, M.L. (1954) Some observations on fractures of the head of the radius with a review of one hundred cases. *Br.J Surg* 42[172], 123-132.

Matsuda, S., Ishinishi, T., White, S.E., and Whiteside, L.A. (1997) Patellofemoral joint after total knee arthroplasty. Effect on contact area and contact stress. *J Arthroplasty* 12[7], 790-797.

Moro, J.K., Werier, J., MacDermid, J.C., Patterson, S.D., and King, G.J. (2001) Arthroplasty with a metal radial head for unreconstructible fractures of the radial head. *J Bone Joint Surg Am* 83-A[8], 1201-1211.

Morrey, B.F. (2008) *The Elbow and Its Disorders*. Saunders Elsevier.

Popovic, N., Lemaire, R., Georis, P., and Gillet, P. (2007) Midterm results with a bipolar radial head prosthesis: radiographic evidence of loosening at the bone-cement interface. *J Bone Joint Surg Am* 89[11], 2469-2476.

Ring, D., Quintero, J., and Jupiter, J.B. (2002) Open reduction and internal fixation of fractures of the radial head. *J Bone Joint Surg Am* 84-A[10], 1811-1815.

Ronsky, J.L., Herzog, W., Brown, T.D., Pedersen, D.R., Grood, E.S., and Butler, D.L. (1995) In vivo quantification of the cat patellofemoral joint contact stresses and areas. *J Biomech.* 28[8], 977-983.

Sabo, M.T., McDonald, C.P., Ng, J., Ferreira, L.M., Johnson, J.A., and King, G.J. (2011) A morphological analysis of the humeral capitellum with an interest in prosthesis design. *J Shoulder Elbow Surg* 20[6], 880-884.

Speed, K. (1941) Ferrule caps for the head of the radius. *Surg.Gynec.Obstet.* 73, 845-850.

Spinner, M. and Kaplan, E.B. (1970) The quadrate ligament of the elbow--its relationship to the stability of the proximal radio-ulnar joint. *Acta Orthop Scand.* 41[6], 632-647.

Stacpoole, R.A. (2002) Biomechanical Considerations Related to the Fixation and Kinematics of Radial Head Arthroplasty. Master of Science Western University.

Stormont, T.J., An, K.N., Morrey, B.F., and Chao, E.Y. (1985) Elbow joint contact study: comparison of techniques. *J Biomech.* 18[5], 329-336.

Stuffmann, E. and Baratz, M.E. (2009) Radial head implant arthroplasty. *J Hand Surg Am* 34[4], 745-754.

Swanson, A.B., Jaeger, S.H., and La Rochelle, D. (1981) Comminuted fractures of the radial head. The role of silicone-implant replacement arthroplasty. *J Bone Joint Surg Am* 63[7], 1039-1049.

Swieszkowski, W., Skalski, K., Pomianowski, S., and Kedzior, K. (2001) The anatomic features of the radial head and their implication for prosthesis design. *Clin Biomech.(Bristol., Avon.)* 16[10], 880-887.

Van Glabbeek, F., van Riet, R.P., Baumfeld, J.A., Neale, P.G., O'Driscoll, S.W., Morrey, B.F., and An, K.N. (2004) Detrimental effects of overstuffing or understuffing with a radial head replacement in the medial collateral-ligament deficient elbow. *J Bone Joint Surg Am* 86-A[12], 2629-2635.

van Riet, R.P., Van Glabbeek, F., Neale, P.G., Bimmel, R., Bortier, H., Morrey, B.F., O'Driscoll, S.W., and An, K.N. (2004) Anatomical considerations of the radius. *Clin Anat.* 17[7], 564-569.

van Riet, R.P., Van Glabbeek, F., Neale, P.G., Bortier, H., An, K.N., and O'Driscoll, S.W. (2003) The noncircular shape of the radial head. *J Hand Surg Am* 28[6], 972-978.

VanBeek, C. and Levine, W.N. (2010) Radial Head-Resect, Fix or Replace. *Operative Techniques in Orthopaedics* 20[1], 2-10.

Zhao, J., Yang, S., and Hu, Y. (2007) The early outcomes with titanium radial head implants in the treatment of radial head comminuted fractures. *J Huazhong.Univ Sci.Technolog.Med Sci.* 27[6], 681-683.

CHAPTER 2 - EFFECT OF IMPLANT SHAPE ON RADIOCAPITELLAR CONTACT AREA

OVERVIEW: *Axisymmetric radial head implants have been previously studied to assess contact mechanics in bench top studies; however both axisymmetric and anatomically shaped implants have not been evaluated in the intact elbow joint. This chapter compares the contact mechanics of an axisymmetric, a population based quasi-anatomic, and a reverse engineered patient-specific radial head implant to the native radiocapitellar joint.*

2.1 Introduction

The radial head has a complex and variable shape (Popovic *et al.*, 2005; Swieszkowski *et al.*, 2001). It has been reported in numerous elbow morphology studies that the radial head is elliptical (King *et al.*, 2001; Koslowsky *et al.*, 2007; van Riet *et al.*, 2003) however, most commercially available radial head designs are axisymmetric circular implants. Only one anatomical asymmetric design is currently available (Calfee *et al.*, 2006). In some systems, the implant stem is smooth and purposely placed loosely; it is thought that small amounts of stem movement in the radial neck will compensate for the non-anatomic shape (van Riet *et al.*, 2006). Other axisymmetric implants have a bipolar articulation, containing a joint between the stem and the radial head to optimize joint contact, but have a potential risk of polyethylene wear and provide less contribution to radiocapitellar stability (Calfee *et al.*, 2006; Chanlalit *et al.*, 2011; Dotzis *et al.*, 2006). Another group of axisymmetric implants aims for secure stem fixation; most commonly with uncemented ingrowth stems (Calfee *et al.*, 2006). When anatomic asymmetrical

designs are used, it is essential that they are positioned and fixed in the correct location to ensure proper joint alignment and hence optimize radiocapitellar contact (Acumed, 2011).

The articulation of a metallic radial head on articular cartilage can be expected to alter joint contact patterns due to the stiffness of the implant (Liew *et al.*, 2003; Sabo *et al.*, 2011). Changes in the implant alignment with respect to the capitellum due to incorrect positioning, or differences in the implant shape relative to the native radial head, may also contribute to changes in contact patterns and hence alter articular cartilage loading. Collectively these changes in stiffness, alignment and shape, like any hemiarthroplasty, have a potential to cause degenerative changes in the opposing cartilaginous surface (Liew *et al.*, 2003; Sabo *et al.*, 2011). The focus of the current study was to evaluate the effect of radial head implant shape on radiocapitellar contact by using computer assisted surgical techniques to ensure optimal implant positioning and a whole elbow model to mimic a clinically relevant loading environment. The objective of this study was to compare the radiocapitellar contact patterns of three radial head implant designs that included (1) axisymmetric, (2) population based quasi-anatomic, and (3) reverse engineered patient-specific devices. It was hypothesized that anatomically shaped radial head implants will have greater contact area than the axisymmetric radial head implants and demonstrate similar radiocapitellar contact patterns as the native radial heads.

2.2 Methods

2.2.1 *Design of Implants*

For the following two studies (Chapters 2 & 3) that were completed for this thesis, custom made radial head implants were used. These designs included an axisymmetric implant, a population based quasi-anatomic and a reverse engineered patient-specific implant.

2.2.1.1 *Generic Implant Stem*

The radial head implant system created for this study consisted of two components; a generic stem that could be used with all implants and the implant head (Figure 2.1). Eight divots located on the head of the stem allowed for navigation calibration (Figure 2.1A). The implant stem was made with notches along the length of the body to ensure fixation to the cement and contained a ball plunger to expand into a recess located on all heads (Figure 2.1B-C). A 6mm x 6mm square head was used to prevent rotation of the implant head. The distal portion of the stem was angled at 5° and made to be short in length to avoid impingement against the canal of the radial necks during navigated placement (Figure 2.1 B).

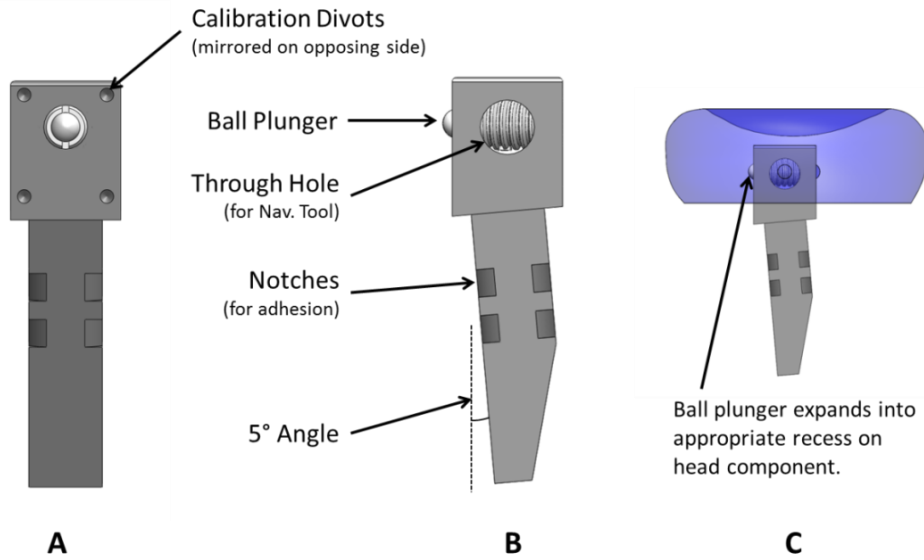


Figure 2.1 Customized Stem

- A. *Front view of the stem*
- B. *Side view of the stem*
- C. *View of the stem inside the implant*
(Deluce, 2011)

2.2.1.2 *Axisymmetric Implant Design*

The axisymmetric radial head implant was modeled after the Evolve Proline Radial Head System (Wright Medical Technology Inc., Arlington, TN, USA). Four sizes were fabricated (22mm, 24mm, 26mm and 28mm diameter) (Figure 2.2). Custom implants were used instead of the commercially available implant since the study was designed to allow all implants to fit on the same custom made stem (Figure 2.1) and were made of the same material.

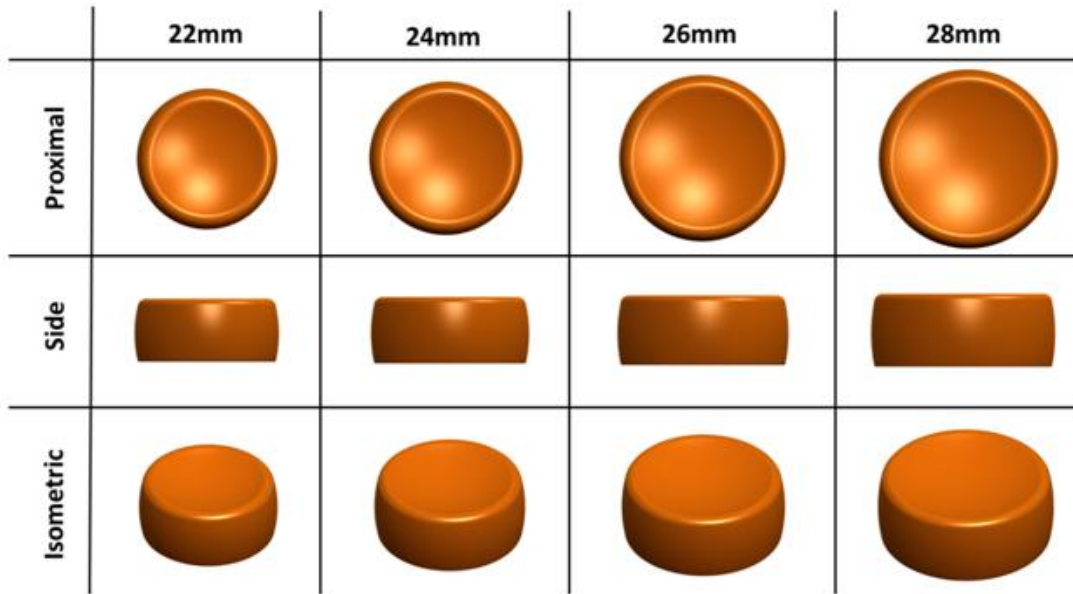


Figure 2.2 Axisymmetric Implants

This figure shows the set of axisymmetric implants that were fabricated (Deluce, 2011).

2.2.1.3 *Population Based Quasi-Anatomic Design*

Computed tomography (CT) scans (GE Discovery CT570 HD, Waukesha, WI) were obtained from 34 (male) specimens. A 512x512 reconstruction matrix was used for all specimens. Pixel size and slice thickness ranged from 0.26-0.98mm and 0.625-1.25mm respectively. Tube current and voltage ranged from 73-292mA and 120-140kVp. The images in these scans were segmented using image processing software (Mimics, Materialise, Leuven, Belgium) such that a surface model of the radius could be made.

All the surface models were imported into a custom program using the Visualization Toolkit (VTK, open-source). The program was designed to use points around the rim of the radial head as well as points on the distal aspects of the radius to determine a coordinate system and then take measurements of the radial head (diameters, height, deepest dish point and elliptical profiles) as demonstrated in Figure 2.3.

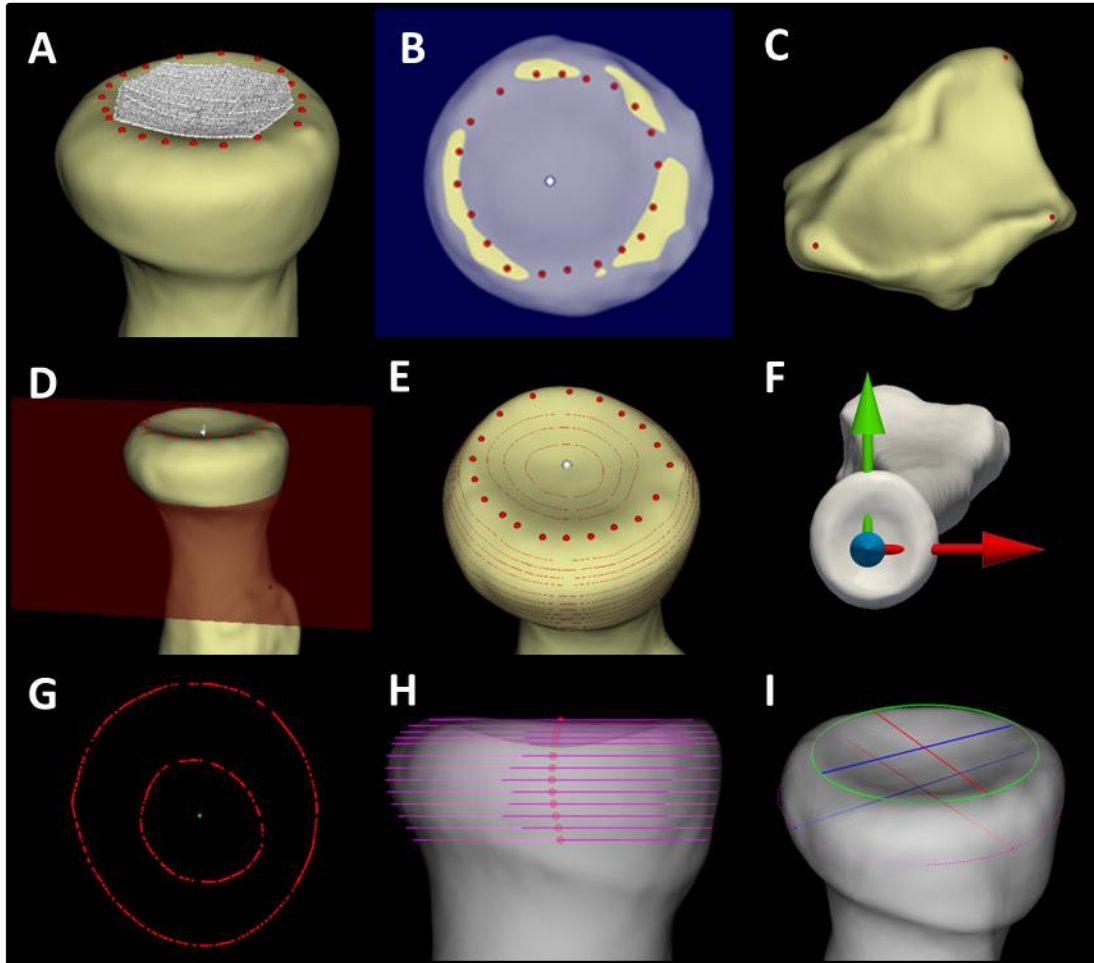


Figure 2.3 Radial Head Measurements Used for Anatomic Implant Design

- A. Twenty rim points (red) are selected and points in the dish generated (white).
 - B. The best-fit plane (blue) is determined and the deepest point found (white).
 - C. Distal points (red) are selected by the user.
 - D. Height is measured using a plane (red) parallel to the best-fit plane.
 - E. Cross sections are generated at known height intervals.
 - F. Anatomic radial head coordinate system is determined (X,Y,Z = Red, Green, Blue).
 - G. An example cross section showing both outer (circumferential) and dish points.
 - H. Ellipses (purple) are fit to each of the radial head cross sections and their centers determined (red).
 - I. Major (red) and minor (blue) diameters are shown for the rim (green) and maximum outer (purple) cross sections.
- (Deluce, 2011)

The specimens were sorted into similar sizes based on the magnitude of the maximum major outer diameter. The resulting three implant sizes were QM (within one standard deviation of the mean), Q+ (greater than one standard deviation above the mean) and Q- (greater than one standard deviation below the mean).

The shapes of the quasi-anatomic implants were determined by averaging the major and minor diameters using the ellipse fitting technique described above, as well as averaging the overall height and dish depth of the specimens within each group. Three-dimensional models were made based on these average measurements and the implants were fabricated (Figure 2.4).

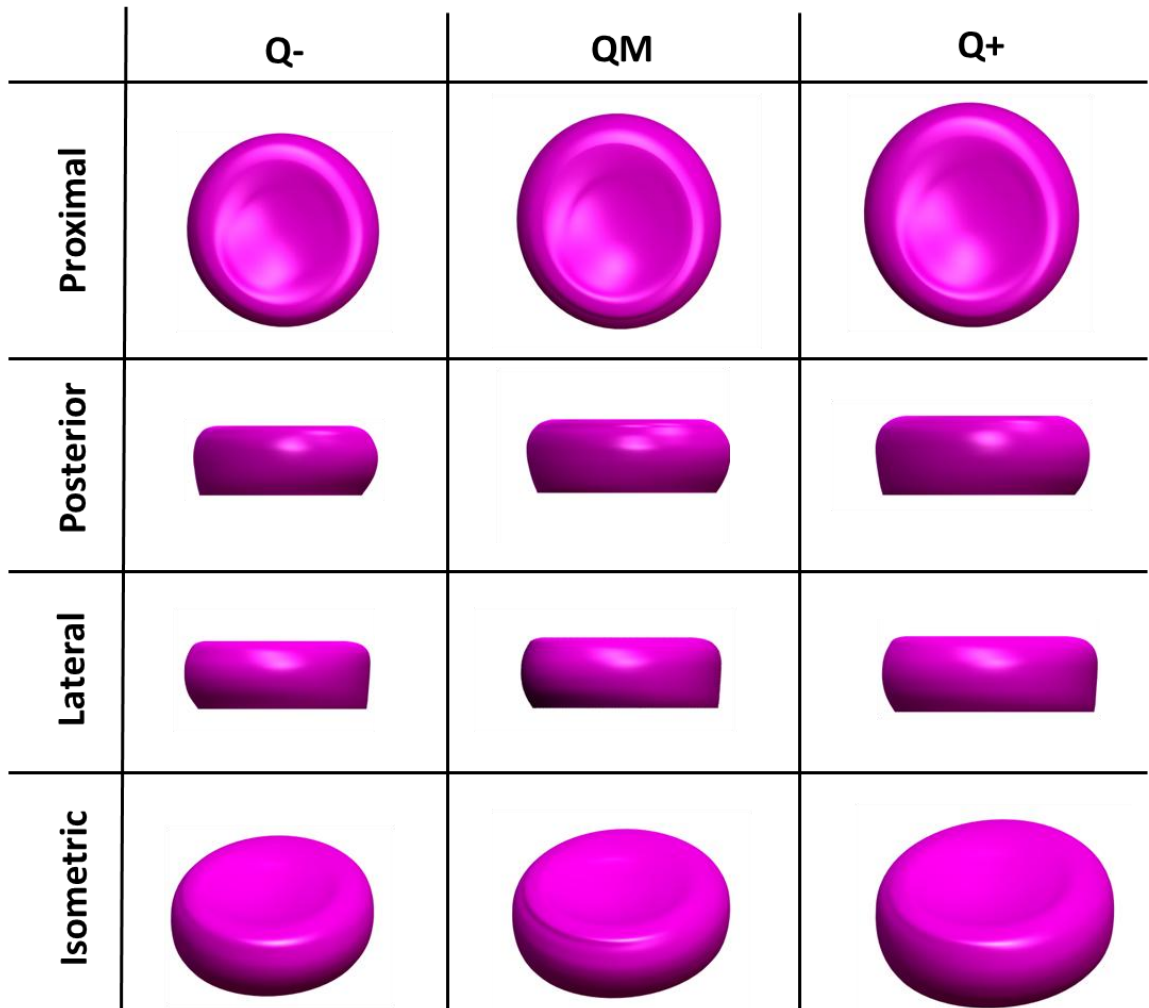


Figure 2.4 Quasi-Anatomic Implants

This figure shows the set of three quasi-anatomic implants (Q+, QM, Q-) that were manufactured (Deluce, 2011).

2.2.1.4 *Reverse Engineered Patient-Specific Design*

CT scans (GE Discovery CT570 HD) of the eight specimens to be tested were obtained. A 512x512 reconstruction matrix was used for all specimens. Pixel size and slice thickness were 0.600 mm and 0.625mm respectively. Tube current and voltage was 200mA and 120kVp. The scans were segmented and surface models of the radii were made (Mimics, Materialize, Leuven, Belgium). The same measurement process was performed on these specimens as the population of specimens used for the quasi-anatomic implants. To create the patient-specific radial head implants, all measurement parameters (Figure 2.3) that were gathered were used to design the 3D CAD models of the implants to be fabricated.

2.2.1.5 *Implant Manufacturing*

The 3D CAD model designs using the custom measurements were made into implants using a fused deposition rapid prototyping machine with an accuracy of ± 0.127 mm (Stratys Fortus 400MC, Eden Prairie, MN, USA). All implants were formed out of ABS M30 plastic (Figure 2.5). Since the machine formed the implants in layers, residual rough edges between layers were evident. To create a smoother articular surface, the implants were lightly sanded and treated with a thin coat of acetone. This had no effect on the final shape of the implants. Also, to rule out an effect of material stiffness on contact area, the ABS M30 plastic axisymmetric implant was compared to a commercially available metal implant, but no differences were measured in contact area (Appendix B).

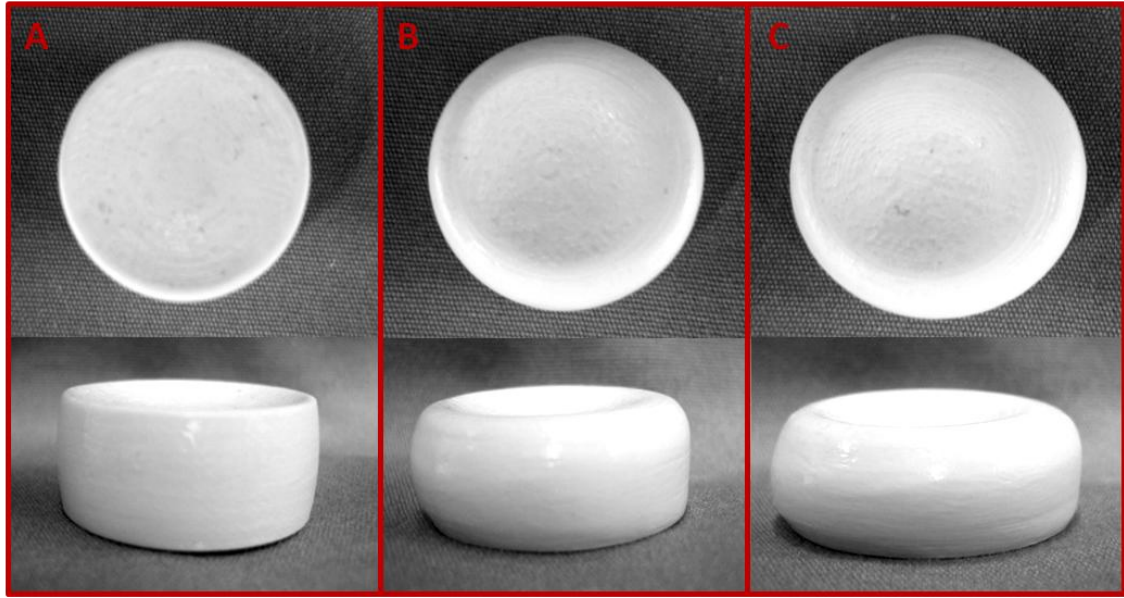


Figure 2.5 Examples of the Radial Head Implants

- A. Axisymmetric*
- B. Population Based Quasi-Anatomic*
- C. Reverse Engineered Patient-Specific*

2.2.2 Specimen Preparation

Eight fresh frozen cadaveric specimens (male, average age 75 ± 8 years, right arm) were mounted in an elbow motion simulator for testing (Figure 2.6) (Johnson *et al.*, 2000). The LCL was sectioned off of the lateral epicondyle to gain access to the radiocapitellar joint. The LCL was subsequently sutured with a braided No. 2 HiFi® ultra high molecular weight polyethylene suture (CONMED Linvatec, FL, USA). The ends of the suture were passed into a single hole placed at the isometric point on the lateral epicondyle, exiting through two transosseous tunnels more proximally, such that the original line of action of the ligament was restored (Fraser *et al.*, 2008). The triceps and biceps were sutured with nylon braided cord and the pronator teres was sutured with No. 5 Ethibond® (Ethicon Inc, Johnson and Johnson, Sommerville, NJ, USA). These sutures were then attached to pneumatic actuators (Airpel, Airpot Corp., Norwalk, CT, USA) via a cable. A 20 N constant load was applied to the LCL actuator to simulate a clinical LCL repair. Static loads were applied, via the actuators, to the triceps, biceps and pronator teres to simulate full pronation, neutral rotation and full supination (Table 2.1). These loads were determined from a simulated active forearm rotation trial that was performed on the elbow motion simulator. The joint angle and muscle load data were analyzed to determine the loads applied to the biceps and pronator teres to achieve full pronation, neutral and full supination positions. The triceps was loaded to achieve a flexion angle of 90° and the forearm rested on a bar to ensure the flexion angle was maintained.

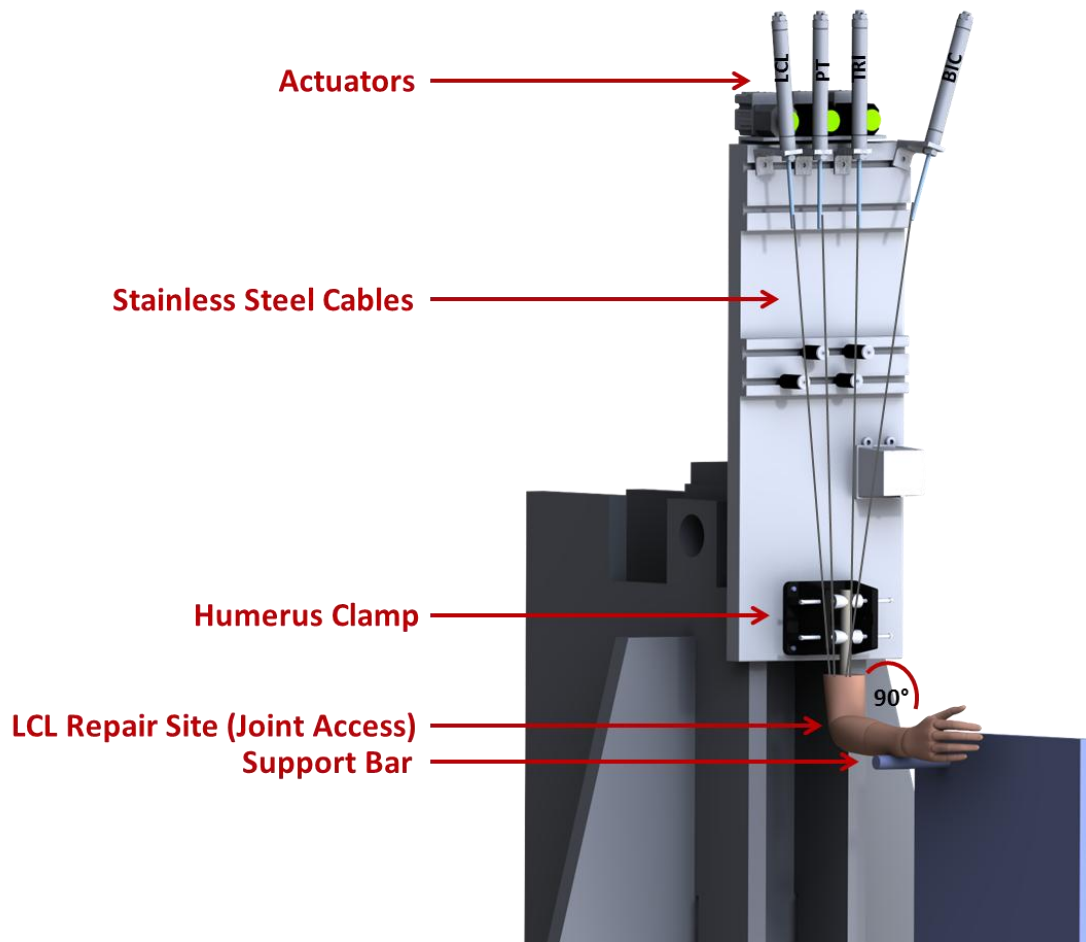


Figure 2.6 Elbow Motion Simulator

This image shows the arm in neutral rotation at 90° of flexion in the elbow motion simulator. Static loads were applied to the three muscles, biceps (BIC), triceps (TRI) and pronator teres (PT), and also the LCL, using pneumatic actuators.

Table 2.1 Static Loads Applied during Casting

Static load values were determined by examining the motion simulator muscle loading data for active forearm rotation and extracting the load values applied for these muscles in each of the three the postions tested.

		Rotation		
		Pronation	Neutral	Supination
Muscle	Triceps	50 N	50 N	50 N
	Biceps	15 N	35 N	40 N
	Pronator Teres	80 N	25 N	30 N

2.2.3 *Computer Navigation*

As this study used anatomic designs of the radial head, it was essential that the implants were accurately positioned. This was done using navigation to achieve the most ideal position possible such that the radial head was restored to the best of our abilities.

2.2.3.1 *Registration of Intra-Operative Data to Pre-Operative Plan*

CT scans were performed of all the specimens tested and 3D surface models of the radii were generated (as described above). Using a custom VTK program, an ideal location for the implant stem was determined based on measurements of the native radius.

Portions of the proximal, midshaft and distal radius were exposed and digitizations of the bony surfaces were made using 3D optical tracking (Optotrak Certus®, NDI, Waterloo, ON, Canada). Anatomical landmarks (radial styloid, dorsal lip of the DRUJ and the centre of the radial dish) were digitized as well. These landmarks were used to align the 3D surface model on the computer with the location visualized by the motion tracking system. Now the target could be used to guide the implant stem into the *in situ* radius.

2.2.3.2 *Navigation and Implantation*

The radial head was marked for anterior and lateral directions using the tracked stylus and drill holes were made so that orientation could be determined after it was excised. The radial head was removed using an oscillating saw and the canal was reamed.

The 3D optical tracking markers were fixed to the radius and the navigation tool with the implant stem (Figure 2.7). A custom LabVIEW (National Instruments, Austin, Texas, USA) program was used to visualize the guidance of the implant stem into the radius. Feedback was given in real-time to allow minor corrections of the implant location. Once the target location was achieved, the stem was cemented into place using Surgical Simplex® bone cement (Stryker, Mahwah, NJ, USA).

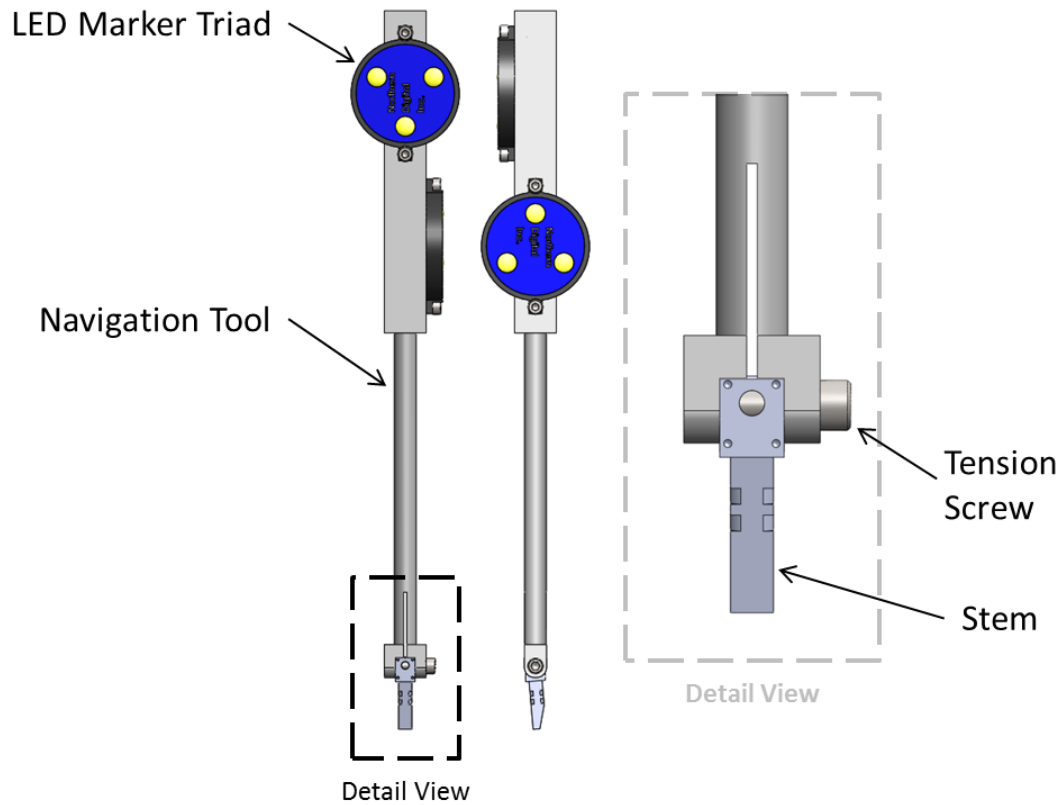


Figure 2.7 Navigation Tool

This tool was used to guide the custom stem into place. The tension screw held the stem rigidly in place and the LED markers allowed 3D motion tracking (Deluce, 2011).

2.2.4 *Casting Joint Contact*

Joint contact was quantified using a previously reported casting technique (Lalone *et al.*, 2012; Liew *et al.*, 2003; Stormont *et al.*, 1985). After mixing, 2 ml of silicone impression material (Reposil® Medium Body Vinyl Polysiloxine Impression Material, DENTSPLY International, Inc., York, PA, USA) was injected onto the radial head using a 10ml syringe. The radiocapitellar joint was reduced and the LCL actuator was loaded to 20N to simulate a clinical ligament repair. Static (muscle) loading was applied across the elbow to mimic normal muscle tone in pronation, neutral rotation and supination. The casting process was conducted with the native radial head and then repeated for all three implant designs in a randomized order (Figure 2.8). The cast was left to cure for 25 minutes prior to removal. Once the cast had set, the LCL tension was released to allow the radiocapitellar joint to be subluxated for cast removal.

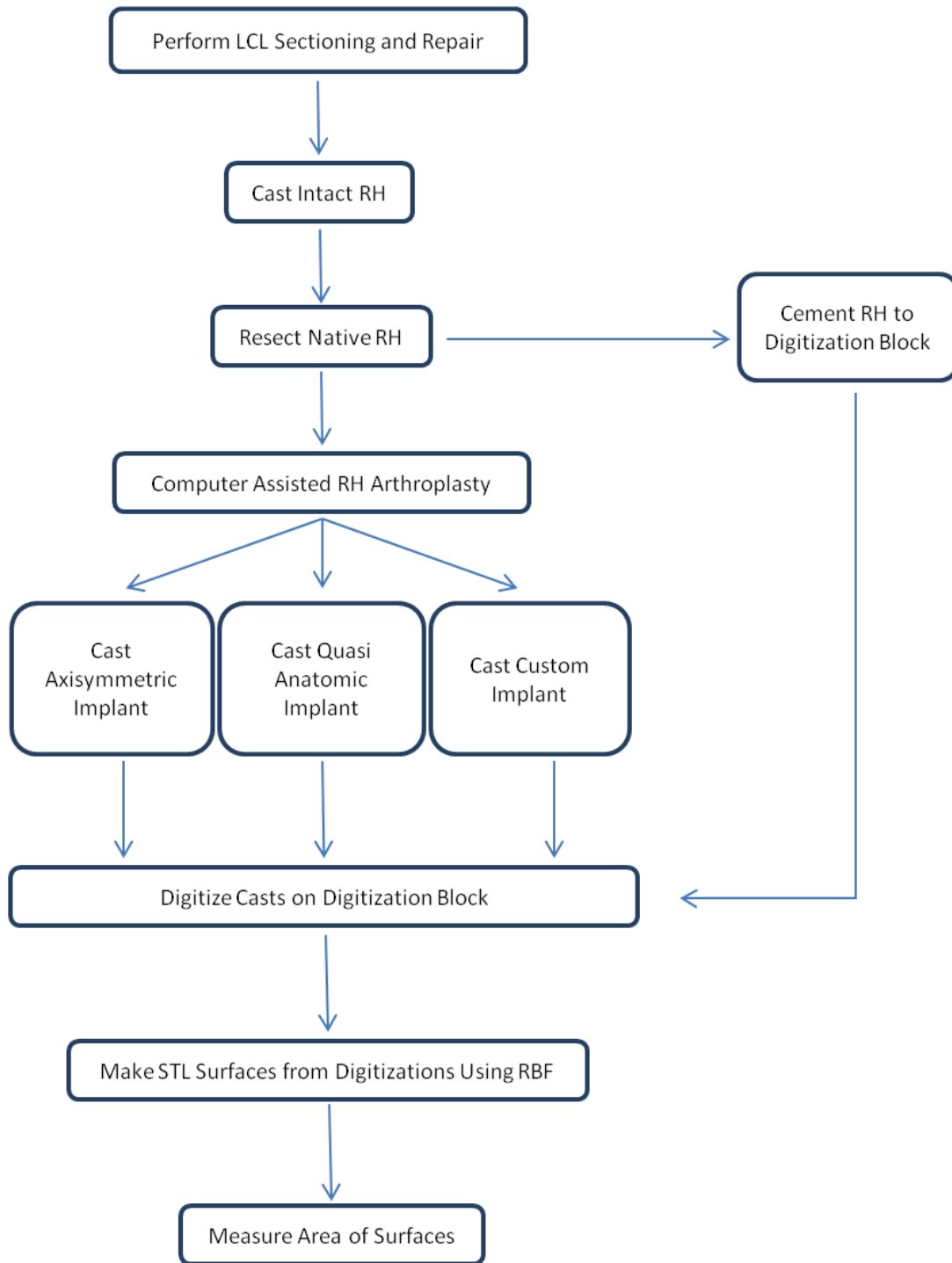


Figure 2.8 The Contact Area Quantification Process

This figure depicts the steps to cast the native radial head and the radial head implants. The steps taken to measure the contact area are also included.

2.2.5 *Analysis of Casts*

The lateral side of the cast was marked prior to removing it from the radiocapitellar joint. The excised native radial head was cemented to the digitization block (Figure 2.9 A). LED markers were also attached so that the position of the contact patch would be known. The orientation markers on the native radial head were digitized and the entire radial head was traced. The cast was then placed onto the radial head in the correct orientation such that the lateral marks on the cast and the lateral hole on the radial head lined up.

For the casts of the radial head implants, the implant was removed from the stem with the cast still *in-situ* and then placed on a stem that was fixed to the digitization block (Figure 2.9 B).

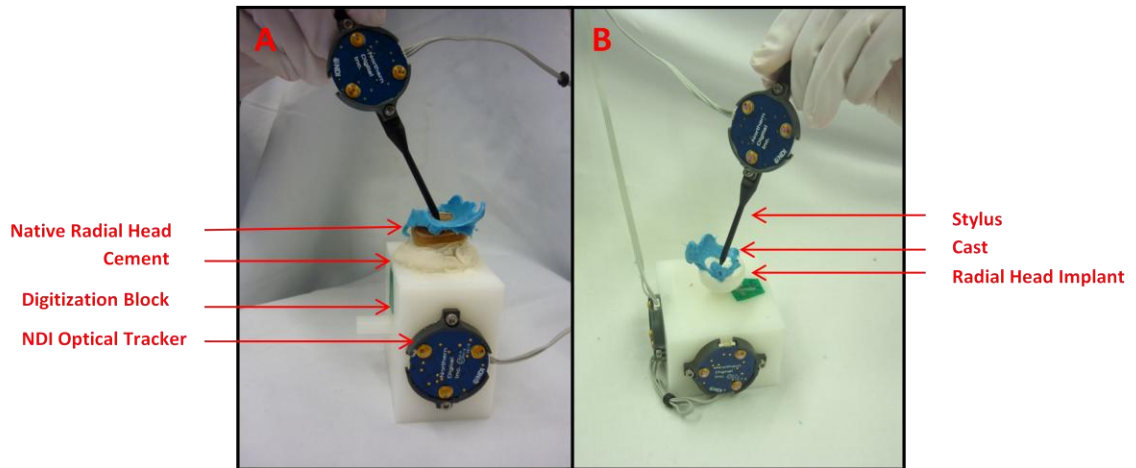


Figure 2.9 The Digitization Technique Used to Trace the Contact Area.

The stylus was used to trace the contact area and was tracked by the Optotrak Certus® system.

- A. The native radial head was cemented to the side of the block*
- B. The radial head implants were placed onto a peg on top of the digitization block*

2.2.5.1 *Contact Area Quantification*

A technique previously described by Lalone *et al.* was used to determine the contact area (Lalone *et al.*, 2012). Radiocapitellar contact area was quantified by digitizing the casts using an optically tracked stylus (Optotrak Certus®, NDI, Waterloo, ON, Canada) relative to the digitization block (Figure 2.9). The point cloud digitizations were then converted to three-dimensional surfaces (Figure 2.8, Figure 2.10) using a radial basis function (RBF) program in MATLAB (MathWorks, Massachusetts, USA). Custom VTK software was used to measure the contact area.

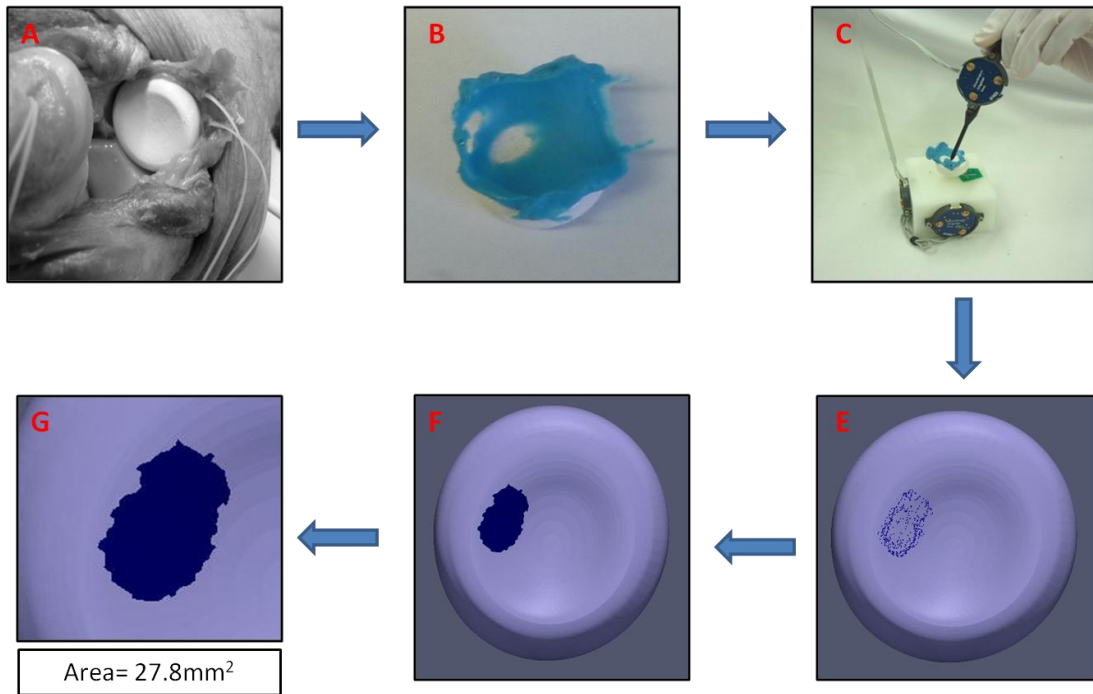


Figure 2.10 The Process of Quantifying the Contact Area

- A. Space where the silicone impression material was injected*
- B. Cast removed from the joint after it has cured, the void space represents the contact area*
- C. Technique and tools used to trace the cast*
- D. Point cloud that is produced from the digitization*
- E. Surface that is made from the point cloud*
- F. Area is calculated*

2.2.5.2 *Contact Location Quantification*

To determine the location of the contact area on the radial head, the centroid of the contact area patch was calculated. The RBF surfaces that were previously calculated were converted back into points to achieve an evenly distributed point cloud (Figure 2.11 A-C). Custom MATLAB (MathWorks, Massachusetts, USA) code was used to fit a plane to the points. These were given indices and projected onto the plane such that a 2D surface was created. The mean of the points was calculated to determine the point closest to the centre of the surface. The points were then projected back onto the original surface. The 3D coordinates of the centre point (centroid) were determined (Figure 2.11 D).

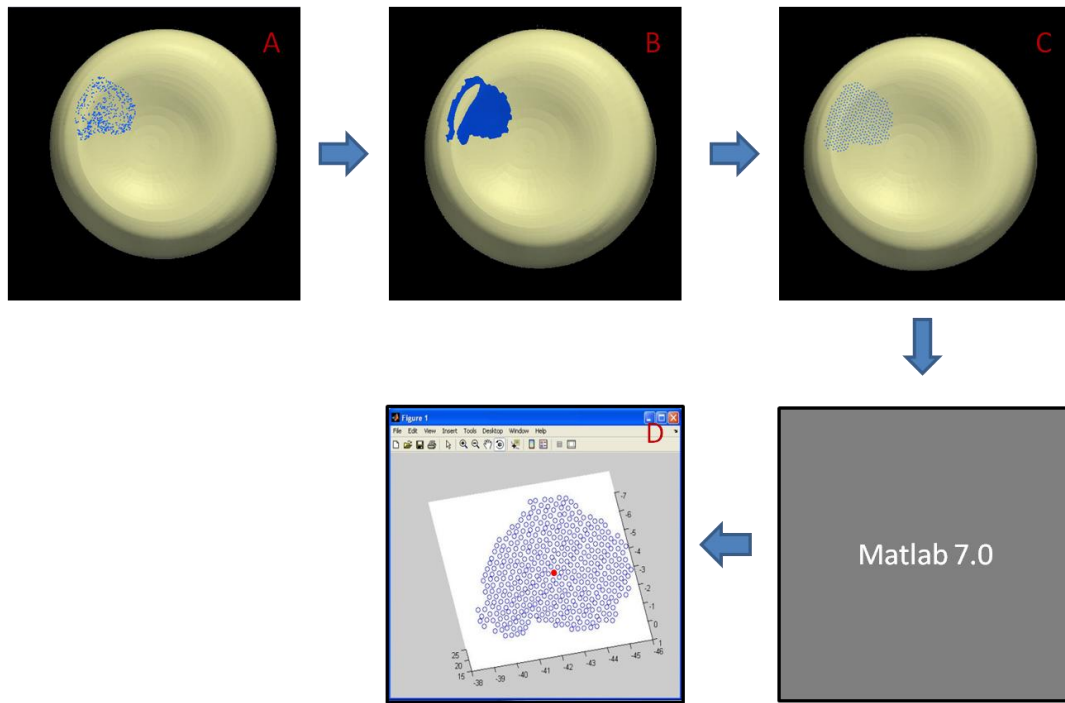


Figure 2.11 The Process Used to Determine the Centre of the Contact Area

- A. *Digitized contact area*
- B. *RBF surface*
- C. *Evenly distributed point cloud*
- D. *Centre point (red)*

To measure the location of the contact area, the centre of the radial head was found. Twenty points were selected around the rim on the radial head (Figure 2.12 A). A circle was then fit to these points (Figure 2.12 B) and the centre and radius of the circle was calculated (Figure 2.12 C). The distance between the centre of the radial head and the contact centroid was compared to the distance from the centroid to the rim of the radial head. This was done to quantify whether the contact patch lay closer to the centre or the rim for the different radial head conditions. The values for distances were normalized against the radial head radius such that the centre was 0 and the rim was 1.

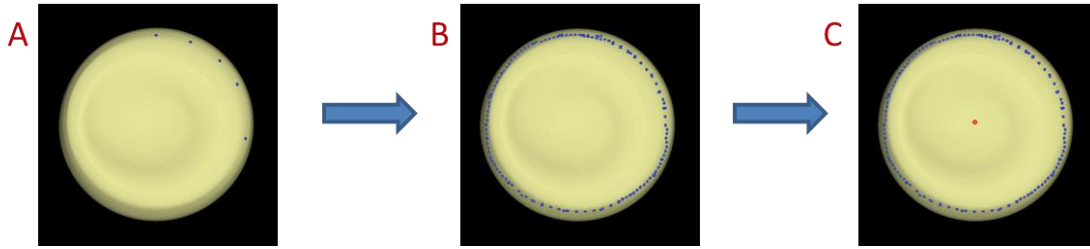


Figure 2.12 The Process Used to Find the Centre and Radius of the Radial Head

- A. *Points being picked on the rim*
- B. *The circle fit*
- C. *Centre of radial head found (red dot)*

2.2.6 *Statistical Analyses*

A two-way repeated measure analysis of variance was performed with radial head condition (native radial head, axisymmetric, quasi-anatomic and patient-specific) and rotation angle (full pronation, neutral and full supination) as the two factors, to determine if there was a statistically significant difference in contact area and location (SPSS, IBM, Armonk, New York, USA).

A post-hoc pairwise comparison ($\alpha=0.05$) was used to determine potential differences in contact area and location between each implant and the native radial head (SPSS, IBM, Armonk, New York, USA). This same technique was used to compare the three implant morphologies to each other.

A power analysis was also performed to determine whether or not this study had enough specimens to see statistical differences among the three implant morphologies.

2.3 Results

2.3.1 *Contact Area*

There was a significant effect of radial head condition ($p=0.005$) (Figure 2.13). All of the implants had a lower contact area than the native radial head, however only the axisymmetric implant was significantly different ($p=0.008$). There was no significant difference in contact area for the three implant shapes ($p>0.05$) (Figure 2.14). There was no statistically significant difference in the contact area with the forearm in pronation,

neutral or supination (p=0.24).

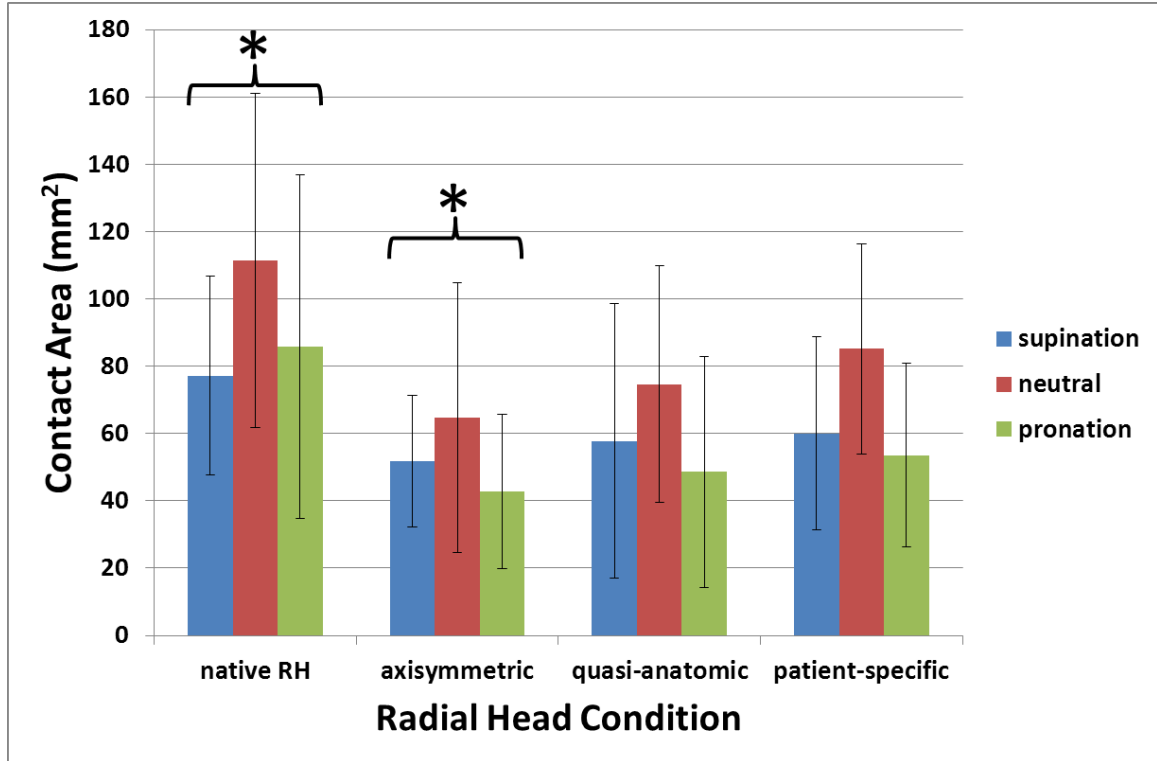


Figure 2.13 The Contact Area for All Radial Head Conditions

Mean contact area (\pm 1SD) is shown for the native radial head, axisymmetric, quasi-anatomic and patient-specific radial head conditions at all three angles of rotation. The axisymmetric radial head implant had a lower contact area than the native radial head ($p=0.008$). “*”symbolizes significant difference.

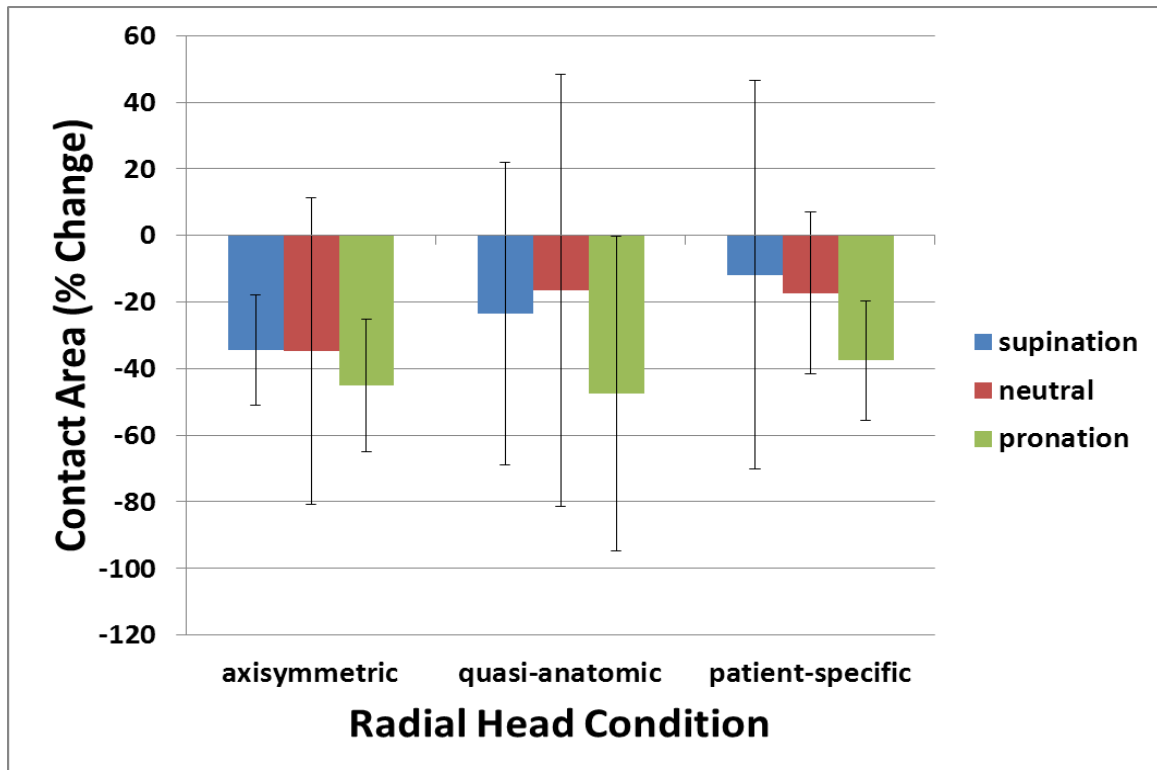


Figure 2.14 The Change in Contact Area for Implants Compared to the Native Radial Head

Mean contact area (\pm 1SD) is shown for axisymmetric, quasi-anatomic and patient-specific radial head conditions at all three angles of rotation as a factor of percent change from the native RH. All the bars are displayed as negative because the intact area was always greater. There was no significant difference in contact area between the three radial head implant shapes ($p > 0.05$).

2.3.2 *Contact Location*

There was no significant difference in contact location for the native radial head, the axisymmetric, the quasi-anatomic or the patient-specific implants ($p=0.22$) (Figure 2.15).

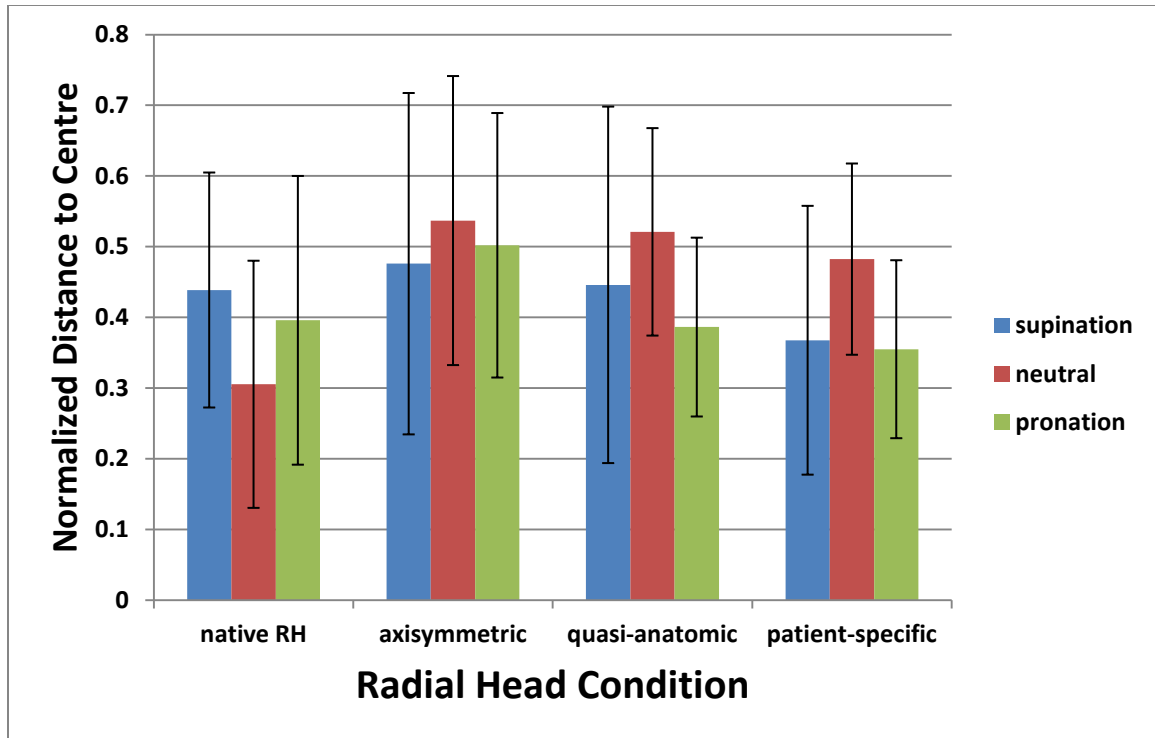


Figure 2.15 The Distance from the Centre of the Radial Head to the Contact Area Centroid

Mean distance ($\pm 1SD$) is shown for the native RH, axisymmetric, quasi-anatomic and patient-specific radial head conditions. The data was normalized against the radius of the radial head. There was no significant difference in contact location ($p=0.22$).

2.4 Discussion

Previous investigations have shown that the articulating surface of the radial head is variably elliptical and is typically offset from the centre of the radial neck (King *et al.*, 2001; Popovic *et al.*, 2005; Swieszkowski *et al.*, 2001). Differences in radial head implant shape relative to the native articulation were expected to affect both the magnitude and location of contact within the radiocapitellar joint. Three radial head implant shapes; axisymmetric, population based quasi-anatomic and reverse engineered patient-specific were implanted and the radiocapitellar contact during rotation was quantified. The results from this study found no significant differences among the three implant morphologies for contact area or contact location. This suggests that the shape of the radial head implant may not be that important with respect to altering radiocapitellar joint contact mechanics.

A previous study from our laboratory (Liew *et al.*, 2003) reported significantly less contact with axisymmetric metal implants compared to the native radial head. The results from the current study agree with the findings of Liew *et al.*, where the axisymmetric radial head displayed a significantly smaller contact area than the intact radial head ($p < 0.05$). However, Liew *et al.* reported an average 60% decrease in contact area with the axisymmetric implant compared to an average 40% reduction in the study presented here. The setup used by Liew *et al.* was aligned by the experimenter, whereas our model allowed the muscles and ligaments to align the joint through applying clinically relevant muscle tones through actuators. Therefore, the contact area measured in the present study is more clinically relevant than contact area determined from previous benchtop studies.

In both studies, the implant materials used were much stiffer than the cartilage of the native radiocapitellar joint. It is possible that the stiffness of the implant and not the implant shape result in the general decrease in contact area. Future work is needed to optimize the materials of these implants with the aim of finding a material that behaves similarly to cartilage.

Our results show that quasi-anatomic and patient-specific implants produce less contact area than the native state although they were not significantly different from each other, or the axisymmetric shape. This study used a sample size of 8 and although this number is generally adequate for *in vitro* biomechanical studies, we have found this insufficient to detect a statistical difference between contact locations for various implants (observed power=0.25). The native, quasi-anatomic and patient-specific radial head implants varied in dish position, as well as shape (from more circular to more elliptical in nature) which may contribute to the variability in our data and lack of a detection of a significant difference between groups. A power analysis was performed and determined that although there was sufficient power (0.90) for the contact area analysis with 8 specimens, 15 specimens would be needed to achieve sufficient power for the contact location analysis.

The radiocapitellar joint experiences concave/convex surface contact mechanics. This relationship between the capitellum and the radial head relies on proper joint alignment such that the concave dish of the radial head centres on the convex surface of the capitellum. There are a few options that exist to assure that the joint mechanics are restored. Bipolar radial heads contain a joint between the head and stem of the implant allowing some tilting of the dish (Dotzis *et al.*, 2006). Some axisymmetric implants

employ a smooth stem that is purposely placed loose such that the head can move small amounts and essentially self-align with the capitellum (van Riet *et al.*, 2006). Anatomic implants are equipped with markings to try to aid in the best possible alignment (Acumed, 2011). In this study, all the implants were fixed in place. Although this is essential for anatomically designed implants, and is commonly used for most axisymmetric implants, this process likely does not represent the behavior of axisymmetric implants which employ a loose stem or those that incorporate a bipolar articulation. By cementing the axisymmetric implants in place we removed their potential self-alignment property. The fact that there were no differences in the contact area or location between the three implants suggests that the concavity compression of the radiocapitellar articulation together with the annular ligament (which was left intact in the current study) keeps the implants aligned, making implant shape less important.

There are currently no other studies that compare contact area and contact location in the radiocapitellar joint for an axisymmetric, population based quasi-anatomic and reverse engineered patient-specific radial head implants. The designs used for the quasi-anatomic and patient-specific implant were novel and are, therefore, not yet commercially available.

In conclusion, there was no significant difference in radiocapitellar contact and location among axisymmetric, quasi-anatomic and patient-specific implants. This suggests that, to increase joint contact and hence reduce cartilage loading, the focus should be on optimally aligning these implants and investigating advanced materials to decrease their stiffness. Further studies are needed to evaluate the importance of implant positioning which was not addressed in the current investigation. Clinical studies are also required to

determine whether these contact patterns will influence the outcomes of radial head arthroplasty in patients.

2.5 References

- Acumed . (2011) Anatomic Radial Head System.
<http://www.acumed.net/sites/default/files/literature/brochure-surgical-technique/anatomic-radial-head-system-brochure-surgical-technique.pdf>.
- Calfee, R., Madom, I., and Weiss, A.P. (2006) Radial head arthroplasty. *J Hand Surg Am* 31[2], 314-321.
- Chanlalit, C., Shukla, D.R., Fitzsimmons, J.S., An, K.N., and O'Driscoll, S.W. (2011) Influence of prosthetic design on radiocapitellar concavity-compression stability. *J Shoulder Elbow Surg* 20[6], 885-890.
- Deluce, S.R. (2011) Design, Validation and Navigation of Anatomic Population-Based and Patient-Specific Radial Head Implants. Master of Engineering Science Western University.
- Dotzis, A., Cochou, G., Mabit, C., Charissoux, J.L., and Arnaud, J.P. (2006) Comminuted fractures of the radial head treated by the Judet floating radial head prosthesis. *J Bone Joint Surg Br.* 88[6], 760-764.
- Fraser, G.S., Pichora, J.E., Ferreira, L.M., Brownhill, J.R., Johnson, J.A., and King, G.J. (2008) Lateral collateral ligament repair restores the initial varus stability of the elbow: an in vitro biomechanical study. *J Orthop Trauma* 22[9], 615-623.
- Johnson, J.A., Rath, D.A., Dunning, C.E., Roth, S.E., and King, G.J. (2000) Simulation of elbow and forearm motion in vitro using a load controlled testing apparatus. *J Biomech.* 33[5], 635-639.
- King, G.J., Zarzour, Z.D., Patterson, S.D., and Johnson, J.A. (2001) An anthropometric study of the radial head: implications in the design of a prosthesis. *J Arthroplasty* 16[1], 112-116.
- Koslowsky, T.C., Germund, I., Beyer, F., Mader, K., Krieglstein, C.F., and Koebke, J. (2007) Morphometric parameters of the radial head: an anatomical study. *Surg Radiol.Anat.* 29[3], 225-230.
- Lalone, E.A., Peters, T.M., King, G.W., and Johnson, J.A. (2012) Accuracy assessment of an imaging technique to examine ulnohumeral joint congruency during elbow flexion. *Comput Aided Surg* 17[3], 142-152.
- Liew, V.S., Cooper, I.C., Ferreira, L.M., Johnson, J.A., and King, G.J. (2003) The effect of metallic radial head arthroplasty on radiocapitellar joint contact area. *Clin Biomech.(Bristol., Avon.)* 18[2], 115-118.

Popovic, N., Djekic, J., Lemaire, R., and Gillet, P. (2005) A comparative study between proximal radial morphology and the floating radial head prosthesis. *J Shoulder Elbow Surg* 14[4], 433-440.

Sabo, M.T., Shannon, H., Ng, J., Ferreira, L.M., Johnson, J.A., and King, G.J. (2011) The impact of capitellar arthroplasty on elbow contact mechanics: Implications for implant design. *Clin Biomech.(Bristol., Avon.)* 26[5], 458-463.

Stormont, T.J., An, K.N., Morrey, B.F., and Chao, E.Y. (1985) Elbow joint contact study: comparison of techniques. *J Biomech.* 18[5], 329-336.

Swieszkowski, W., Skalski, K., Pomianowski, S., and Kedzior, K. (2001) The anatomic features of the radial head and their implication for prosthesis design. *Clin Biomech.(Bristol., Avon.)* 16[10], 880-887.

van Riet, R.P., Van Glabbeek, F., Baumfeld, J.A., Neale, P.G., Morrey, B.F., O'Driscoll, S.W., and An, K.N. (2006) The effect of the orientation of the radial head on the kinematics of the ulnohumeral joint and force transmission through the radiocapitellar joint. *Clin Biomech.(Bristol., Avon.)* 21[6], 554-559.

van Riet, R.P., Van Glabbeek, F., Neale, P.G., Bortier, H., An, K.N., and O'Driscoll, S.W. (2003) The noncircular shape of the radial head. *J Hand Surg Am* 28[6], 972-978.

CHAPTER 3 - THE EFFECT OF IMPLANT SHAPE ON RADIOCAPITELLAR KINEMATICS DURING FOREARM ROTATION

OVERVIEW: *The effect of radial head implant shape on the kinematics of the radiocapitellar joint has not been reported. This chapter compares forearm rotation kinematics of the native radiocapitellar joint to axisymmetric, population based quasi-anatomic and reverse engineered patient-specific radial head implants.*

3.1 Introduction

Approximately 33% of elbow fractures involve the radial head (Mason, 1954; Morrey, 2008). This structure is an important stabilizer of the elbow, especially in the case of associated ligamentous injuries (Morrey, 2008). In the setting of comminuted radial head fractures associated with ligament injuries or fractures, it is essential that the radial head is replaced with an implant to maintain joint stability (Beingessner *et al.*, 2004).

A number of commercially available radial head implants have been developed and are in common clinical use for the management of acute radial head fractures and late reconstruction for non-unions and malunions. Currently, the majority of these implants are axisymmetric in shape (Calfée *et al.*, 2006). However it has been reported that the radial head is typically elliptical and the articulating dish is located eccentrically with respect to the neck (King *et al.*, 2001; Koslowsky *et al.*, 2007; van Riet *et al.*, 2003).

This complex shape of the native radial head poses a question of whether an axisymmetric implant can adequately replicate the normal radiocapitellar joint kinematics that occurs during forearm rotation. During this motion, the dish of the radial head rotates

about the capitellum and the margin of the radial head rotates within the radial notch of the ulna. If the native radial head is elliptical and the dish is eccentric, it is possible that an axisymmetric implant may exhibit abnormal kinematics which may cause pain, stem loosening and lead to clinical failure.

Proper tracking within the joint is essential to maintain the health of the articular cartilage. If there is abnormal contact between the radius and capitellum during elbow movement, this could lead to increased stress on parts of the articulation leading to premature cartilage wear (van Riet *et al.*, 2004) and an early onset of osteoarthritis. This decreases the longevity of a joint and may lead to the need for removal of the radial head implant or revision to a unicompartamental radiocapitellar arthroplasty (Heijink *et al.*, 2008; Sabo *et al.*, 2012).

Similar to the variables in Chapter 2, the objective of this study was to compare the radiocapitellar kinematics of three radial head implant designs to the native articulation: (1) axisymmetric, (2) population based quasi-anatomic and (3) reverse engineered patient-specific. It was hypothesized that anatomically shaped radial head implants would have similar radiocapitellar kinematics as the native radial heads, while the axisymmetric radial head implants would differ.

3.2 Methods

3.2.1 *Specimen Preparation*

Eight fresh frozen cadaveric upper extremities (male, age 75 ± 8 years) were thawed overnight at room temperature prior to the experiment. The specimens were prepared by suturing both the biceps and triceps tendons using nylon braided string and the pronator teres with No. 5 Ethibond® polyester braided suture (Ethicon Inc, Johnson and Johnson, Sommerville, NJ, USA). These sutures were attached to servomotors to achieve active forearm rotation as described below. The wrist was fixed in neutral by passing a pin through the long finger metacarpal into the distal radius. The surgical incisions were closed using a No. 2 Vicryl® suture (Ethicon Inc., Johnson and Johnson, Sommerville, NJ, USA). The specimens were kept at room temperature and were hydrated with normal saline throughout testing.

3.2.2 *Testing Apparatus*

As in Chapter 2, the arm was mounted into a custom upper extremity motion simulator that was previously developed in our laboratory (Johnson *et al.*, 2000) (Figure 3.1). The biceps, triceps and pronator teres sutures were attached to servomotors to allow for computer controlled movement. The triceps was activated to maintain 90 degrees of flexion and the biceps and pronator teres were activated to achieve active forearm supination and pronation, respectively.

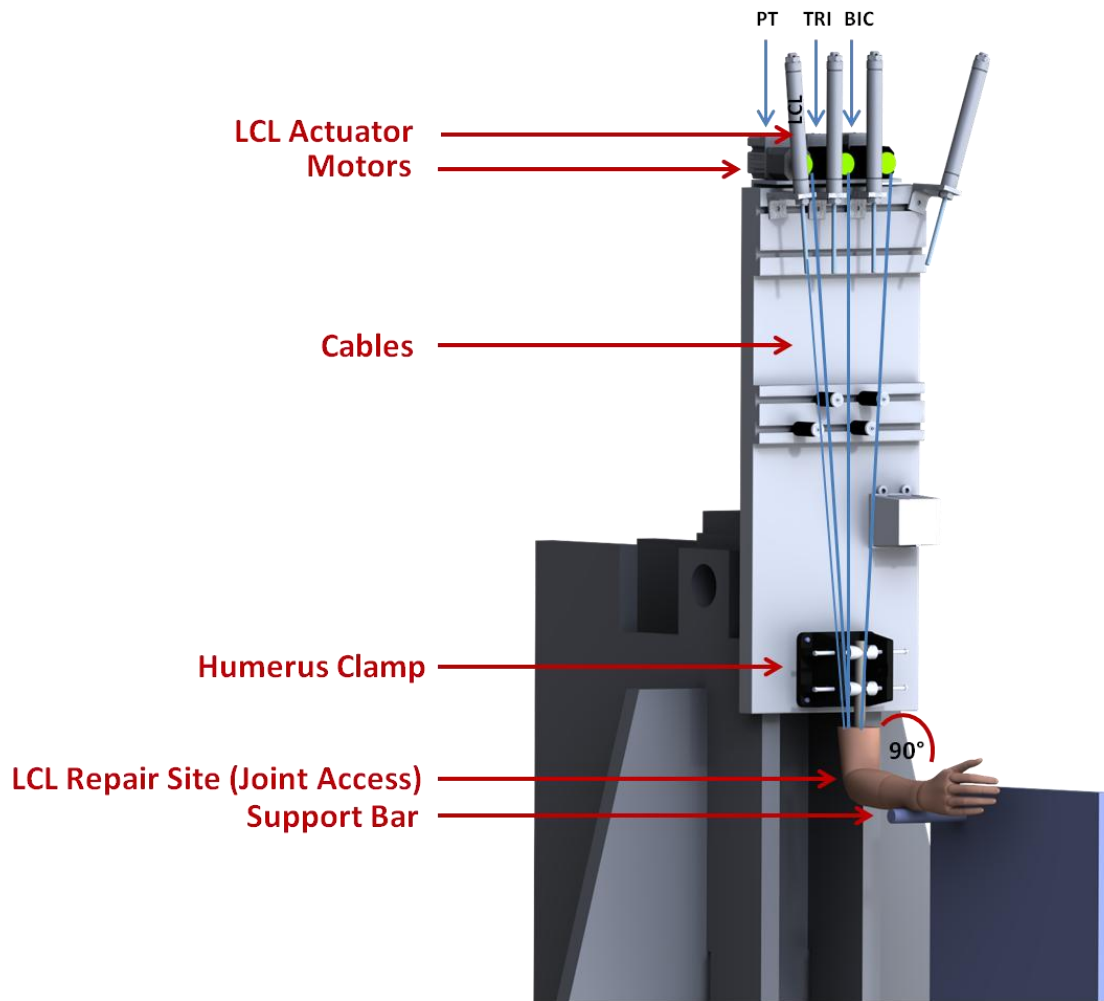


Figure 3.1 The Elbow Motion Simulator

This simulator was used to achieve active forearm rotation by using servomotors attached to the triceps (TRI), biceps (BIC) and pronator teres (PT). A bar was placed under the arm to maintain a flexion angle of 90°.

3.2.3 *Testing Protocol*

Active and passive forearm supination and pronation was performed with the joint intact. After the intact testing was complete, the LCL was sectioned from the lateral epicondyle to provide access to the radial head and subsequently repaired using a braided No. 2 HiFi® ultra high weight polyethylene suture (CONMED Linvatec, FL, USA). The suture ends were passed into a hole placed at the isometric point on the lateral epicondyle and out through two tunnels located proximal to the site of entry. This allowed the ligament to be repaired such that the original line of action was restored (Fraser *et al.*, 2008). The annular ligament was kept intact. A pneumatic actuator was used to apply a load of 20N to the LCL prior to clamping the ligament cable during testing. Active and passive forearm supination from the pronated position was performed after the ligament repair. Since repeated access to the radiocapitellar joint was required, this LCL repair model was compared to the intact state such that it could be used as a control.

Three radial head implants were tested: (1) an axisymmetric, (2) a population based quasi-anatomic and (3) a reverse engineered patient-specific implant (for implant design and implantation information see Chapter 2, Sections 2.2.1 and 2.2.3). The stem was cemented into the canal of the radius such that both of the anatomically shaped radial heads would be in an optimal location. The implants were tested in a random order for each specimen. Active and passive forearm supination and pronation was performed for each radial head implant (Figure 3.2).

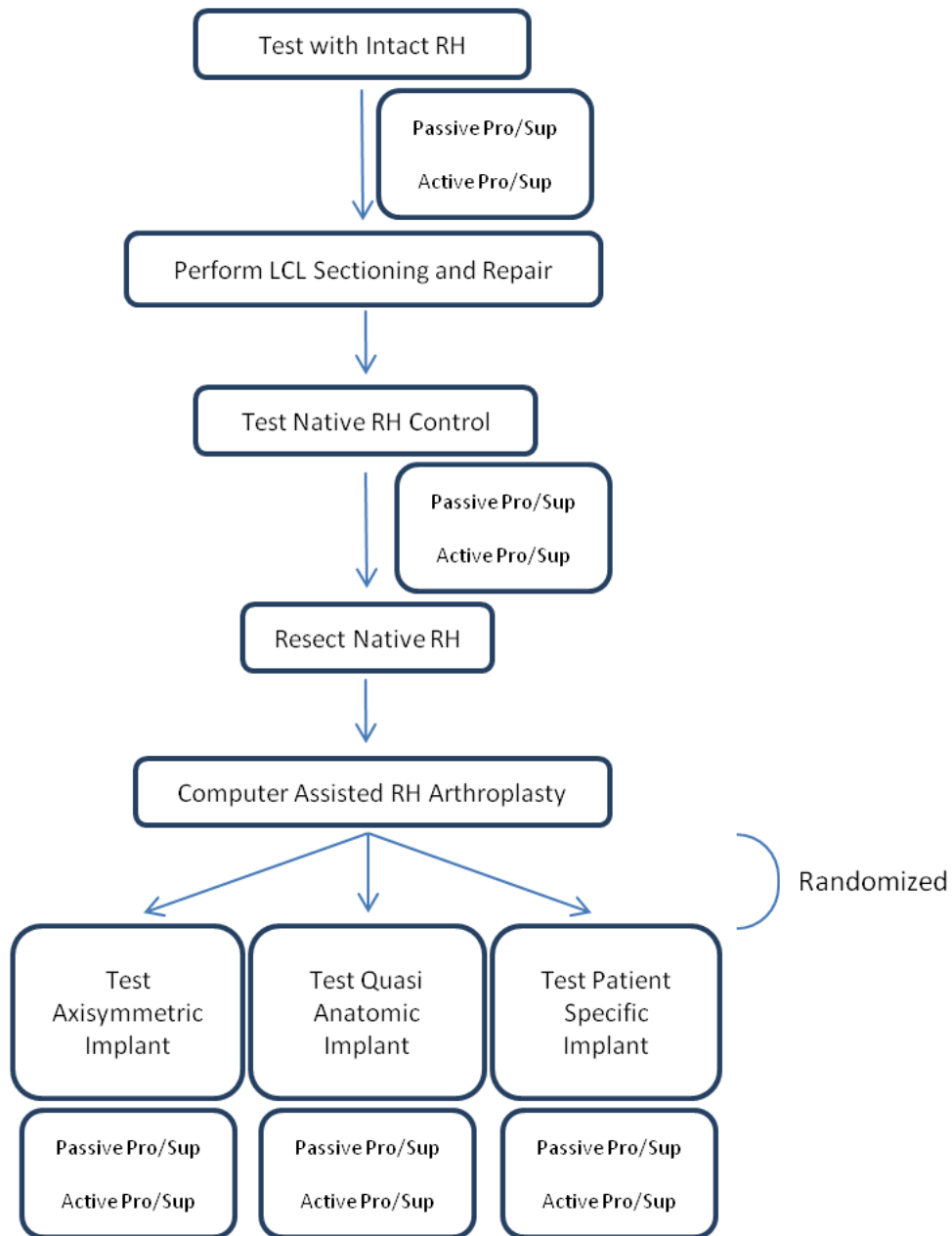


Figure 3.2 Testing Protocol

This flow chart depicts the phases of the testing protocol.

3.2.4 *Kinematics Measurements*

To track the motion of the forearm, optical tracker mounts were fixed to the radius and ulna directly on the bone surface using custom made mounts and cortical bone screws. LED markers (NDI, Waterloo, ON, Canada) were attached to the ulnar mount and one was also attached to the simulator to represent the humerus. A ring containing six smart markers that were calibrated to perform as one rigid body was attached to the radius (Figure 3.3). This was done to maintain visualization of the radius by the tracking system throughout forearm rotation.

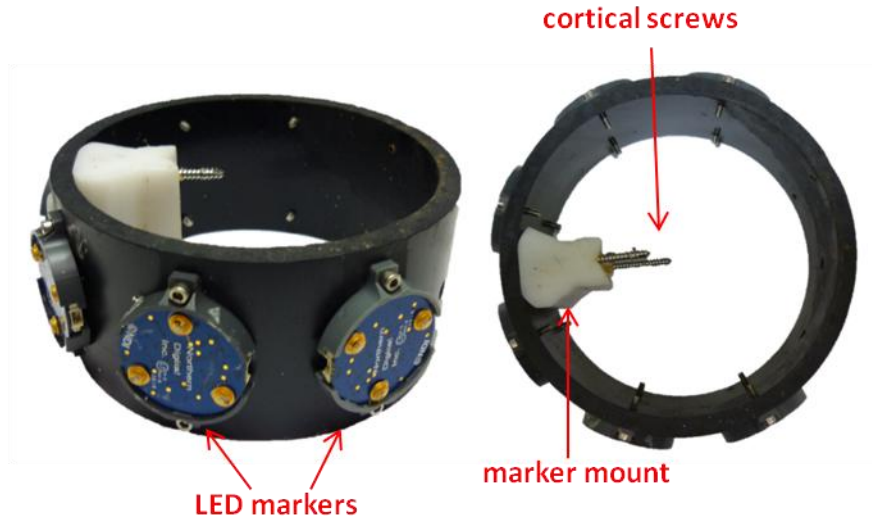


Figure 3.3 Ring Tracker Mount

LED triads were arranged around a section of PVC pipe and calibrated to perform as one circular LED tracker. This tracker was attached to the radius (midshaft) with cortical bone screws, such that the tracker surrounded the arm.

Motions were recorded using a 3D optical tracking camera (Optotrak Certus®, NDI, Waterloo, ON, Canada). The data were analyzed using custom LabVIEW software to determine the kinematics of the radius with respect to the humerus.

The humeral and radial coordinate systems were defined using a series of anatomical digitizations (Ferreira *et al.*, 2010). To produce the humeral coordinate system, the capitellum surface and the trochlear sulcus were traced and a point was digitized in the centre of the humeral shaft at the mid-diaphysis. The capitellum was sphere fit and the trochlear sulcus was circle fit and their centres were calculated. A vector was made between these two centre points in the medial direction (the $Z_{\text{hum}+}$ axis). The bisector of these two centre points was found and a vector was made from this bisector to the shaft point (long axis). The $Y_{\text{hum}+}$ axis was the cross product of the $Z_{\text{hum}+}$ axis and the long axis. The $X_{\text{hum}+}$ axis was the cross product of the $Y_{\text{hum}+}$ axis and the $Z_{\text{hum}+}$ axis. The origin of the humeral coordinate system was centre of the capitellum such that radial head translation about the capitellum during rotation could be measured (Figure 3.4 A). To produce the radial coordinate system, ten points around the rim of the radial head were digitized as well as the radial styloid, the dorsal and volar aspects of the lesser sigmoid notch of the distal radius. The ten rim points were circle fit and the centre was found. The bisector of the dorsal and volar aspects of the lesser sigmoid notch was found and a vector was made from this bisector to the radial styloid point (medial vector). The bisector of this vector was found and a vector from this bisector to the centre of the radial head was made (the $X_{\text{rad}+}$ axis). The $Y_{\text{rad}+}$ axis was the cross product of the $X_{\text{rad}+}$ axis and the medial vector. The $Z_{\text{rad}+}$ axis was the cross product of the $X_{\text{rad}+}$ axis and the $Y_{\text{rad}+}$ axis. The origin of the radial coordinate system was located at the centre of the

radial head (Figure 3.4 B). The outcome variables examined were medial-lateral (ML) translation and anterior-posterior (AP) translation of the centre of the radial head with respect to the centre of the capitellum (Figure 3.4 C-D).

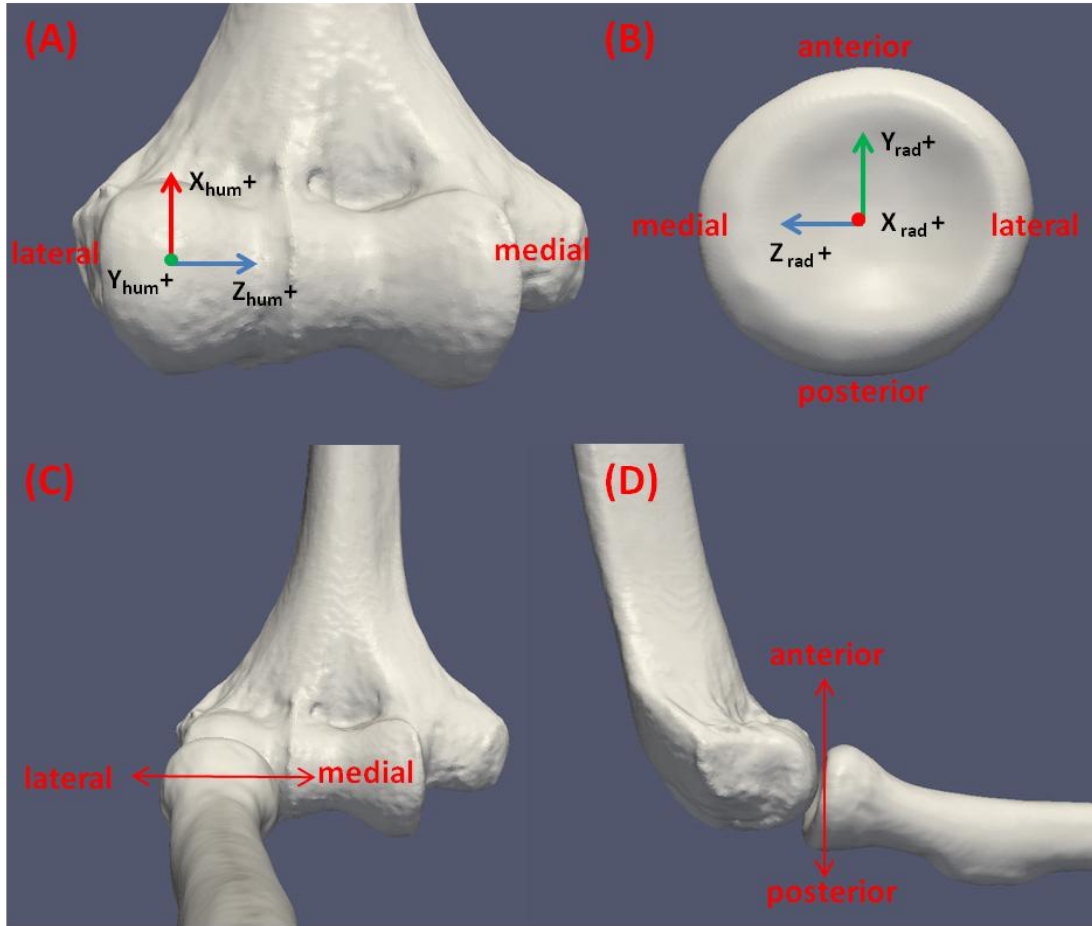


Figure 3.4 Translations of the Radial Head

Anterior-posterior (AP) and medial-lateral (ML) translations of the radial head with respect to the centre of the capitellum were examined.

- A. Anterior view of the humerus showing the humeral coordinate system with the centre of the capitellum as the origin.*
- B. Proximal view of the radial head showing the radial coordinate system with the centre of the radial head as the origin.*
- C. Direction of ML translation of the radial head relative to the capitellum.*
- D. Direction of AP translation of the radial head relative to the capitellum.*

3.2.5 *Statistical Analyses*

A two-way repeated measures analysis of variance was performed with radial head condition (intact state and native radial head with lcl repair) and forearm rotation angle (-40°, -30°, -20°, -10°, 0°, 10°, 20°, 30°, 40°, 50°) as the two factors, to determine if there were differences between ML or AP translations of the radial head for the intact state and the LCL repair (SPSS, IBM, Armonk, New York, USA). This was done to determine whether or not the LCL repair condition could truly be used as a control.

A two-way repeated measures analysis of variance was also performed with radial head condition (native radial head, axisymmetric, quasi-anatomic and patient-specific) and rotation angle (-40°, -30°, -20°, -10°, 0°, 10°, 20°, 30°, 40°, 50°) as the two factors, to determine if there were differences in ML or AP translations between the native radial head and the three implant shapes during forearm rotation (SPSS, IBM, Armonk, New York, USA).

A post-hoc pairwise comparison ($\alpha=0.05$) was used to determine potential differences between each implant and the native radial head (SPSS, IBM, Armonk, New York, USA). This same technique was used to compare the three implant morphologies to each other.

3.3 Results

3.3.1 *Validation of LCL Repair as a Control*

There was no significant difference ($p>0.05$) for either active or passive motion when comparing medial-lateral translations or anterior-posterior translations for the intact elbows with the native radial head and following LCL sectioning and repair (Appendix D). For all cases, the two conditions were within 1 mm translation of each other. Thus, the LCL sectioned and repaired condition with the native radial head was used as the control for comparison to the radial head implants.

3.3.2 *Comparison of Radial Head Conditions*

3.3.2.1 *Medial-Lateral Translations*

No significant differences in medial-lateral translations were found for radial head morphology in passive or active motion ($p=0.58$, $p=0.61$ respectively) (Figure 3.5 and Figure 3.6). Also, no significant differences in medial-lateral translations were found among rotation angles for passive or active motions ($p=0.53$, $p=0.33$ respectively).

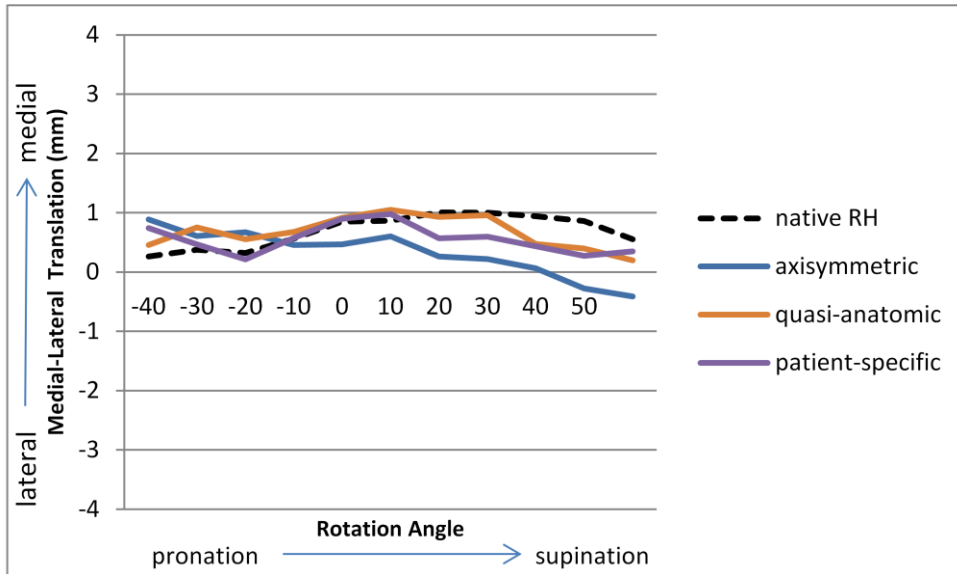


Figure 3.5 Medial-Lateral Translation during Passive Forearm Rotation

The mean radial head translations in the ML direction, where 0 translation represents the origin of the radius (centre of radial head) located at the centre of the capitellum. There were no significant differences between radial head conditions ($p=0.58$). Appendix E shows the mean and standard deviations for all trials. Standard deviations ranged from 1.01-2.99 mm.

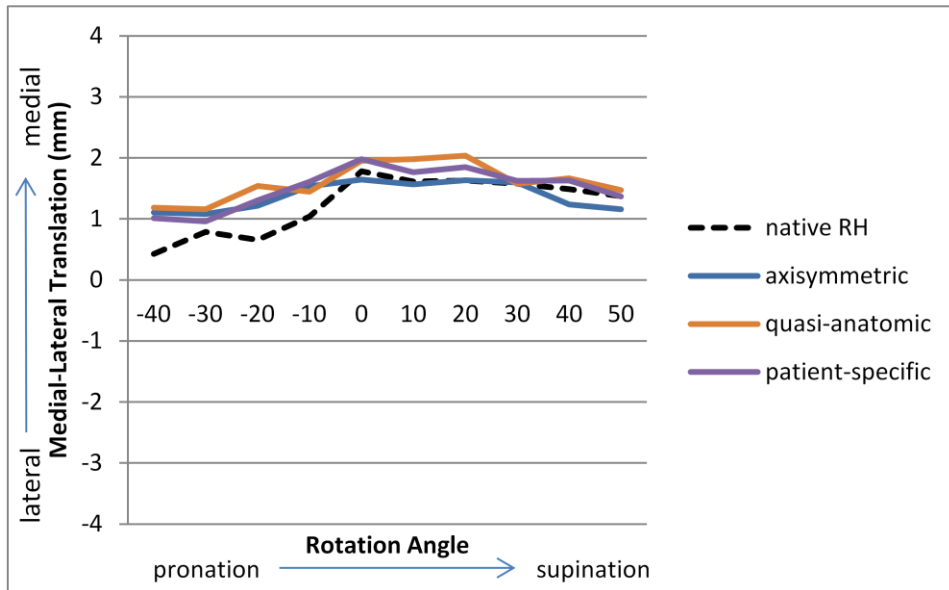


Figure 3.6 Medial-Lateral Translation during Active Forearm Rotation

This graph displays the mean data for active radial head translations in the ML direction. There were no significant differences between radial head conditions ($p=0.61$). Appendix E shows the mean and standard deviations for all trials. Standard deviations ranged from 0.68-3.17mm.

3.3.2.2 *Anterior-Posterior Translations*

There was no significant effect of radial head morphology for passive motion ($p=0.72$) (Figure 3.7); however, there was a significant effect of radial head morphology for active motion ($p=0.001$) (Figure 3.8). A pairwise comparison for radial head implant shape showed that there was no significant difference in radiocapitellar kinematics between the axisymmetric, the quasi-anatomic and the custom radial head implant shapes ($p>0.05$). There were significant differences between the native radial head and the axisymmetric implant ($p=0.014$) and between the native radial head and quasi-anatomic implant ($p=0.019$) for active rotation. There was no significant difference between the native radial head and the patient-specific implant for active rotation ($p>0.05$). There was no significant difference in anterior-posterior translations among rotation angles for passive or active motions ($p=0.26$, $p=0.56$ respectively).

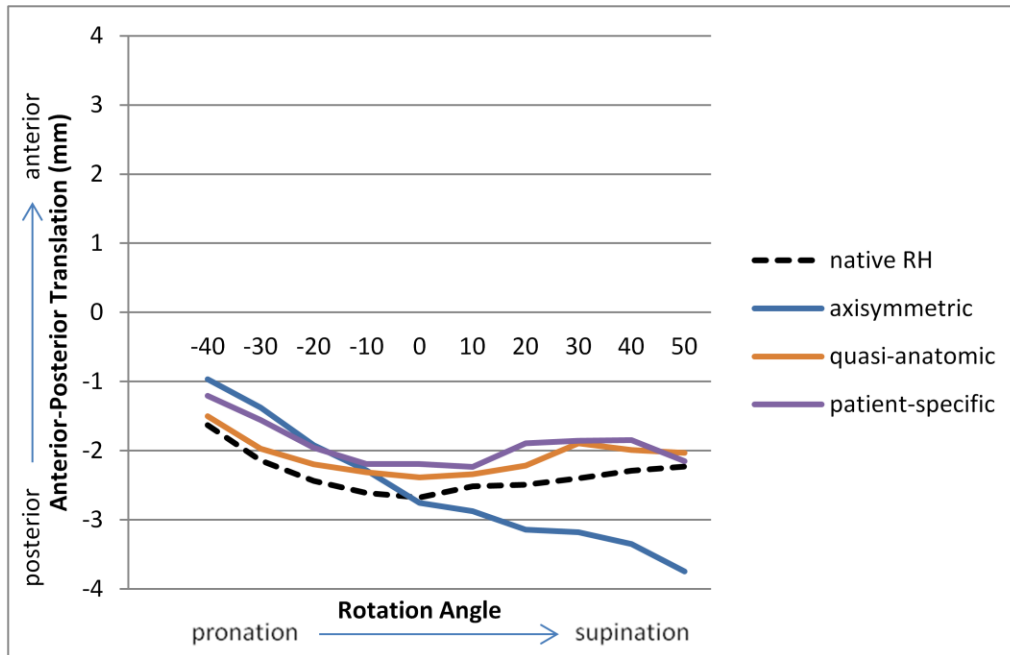


Figure 3.7 Anterior-Posterior Translation during Passive Forearm Rotation

This graph displays the mean data for passive radial head translations in the AP direction. There were no significant differences between radial head conditions ($p=0.72$). Appendix E shows the mean and standard deviations for all trials. Standard deviations ranged from 1.44-3.54mm.

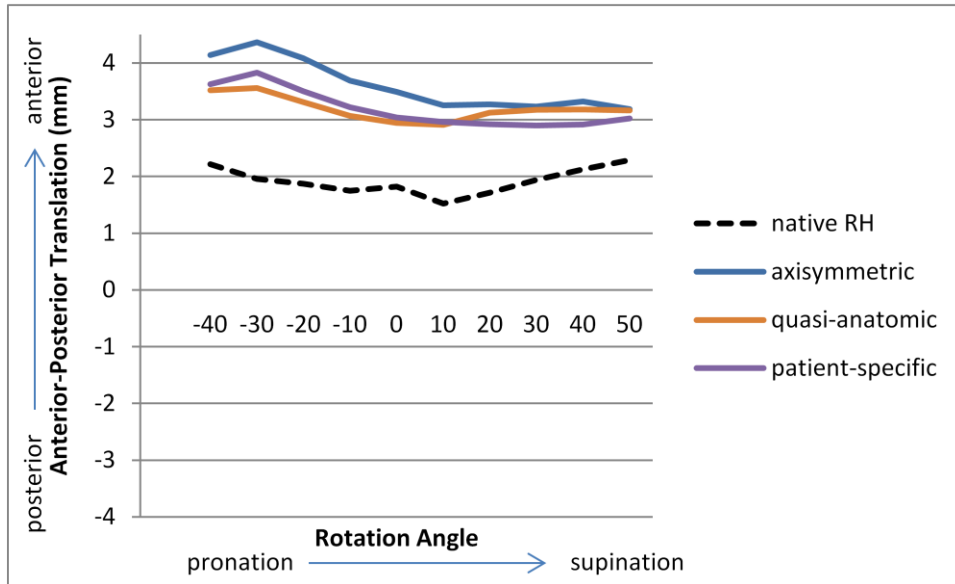


Figure 3.8 Anterior-Posterior Translation during Active Forearm Rotation

This graph displays the mean data for active radial head translations in the AP direction. There was a significant difference between the axisymmetric and quasi-anatomic implant verses the native radial head ($p=0.014$ and $p=0.019$ respectively). There was no significant difference between the patient-specific implants and the native radial head nor between the three different implant shapes ($p>0.05$). Appendix E shows the mean and standard deviations for all trials. Standard deviations ranged from 1.84-3.00mm.

3.4 Discussion

The radial head has a complex elliptical shape. The articular dish is typically offset from the centre of the head, and the head is offset from the centre of the neck (King *et al.*, 2001; Koslowsky *et al.*, 2007; van Riet *et al.*, 2003). Hence, changes in kinematics after radial head arthroplasty are expected unless the implant is perfectly positioned during surgery, and the implant shape and size replicates the native anatomy. To study the importance of these caveats, this study used computer navigated radial head arthroplasty (as described in Chapter 2) as well as testing a reverse engineered patient-specific radial head implant.

The native radial head with an LCL repair was used as the control in this experiment such that repeated access to the radiocapitellar joint could be achieved. The LCL resection and repair technique described by Fraser *et al.* (Fraser *et al.*, 2008) was successfully repeated in this study. By removing the LCL from the lateral epicondyle, the radial head could be accessed easily and the annular ligament, an important radial head stabilizer, was kept intact. By using strong braided sutures and tensioning the repair to 20N, the control replicated the radiocapitellar kinematics of the intact elbow during forearm rotation.

The kinematic pathways of the radial head with respect to the capitellum observed in the current study are similar to those reported by Galik *et al.* (Galik *et al.*, 2007). They found that the radial head translates an average of 2.1mm in the AP direction and 1.6mm in the ML direction. Our data for mean AP and ML translations for all radial head conditions are within these ranges. In our study we kept the annular ligament intact. This important elbow stabilizer as well as the concavity compression of the curved articular dish of the

radial head with respect to the spherical capitellum likely helped to control the motions of the native radial head and the various implants tested.

The effects of three radial head implant shapes (i.e. the axisymmetric, population based quasi-anatomic and reverse engineered patient-specific) on radiocapitellar kinematics during rotation were examined. Significant differences in kinematics were evident in anterior-posterior translations between the axisymmetric and the native control as well as between the quasi-anatomic and the native control. No significant differences were observed between the patient-specific implant and the native control. Therefore, with respect to forearm kinematics, the patient-specific implant performed most similarly to the native state. However, no significant differences were measured between the three radial head morphologies. Therefore, while the patient-specific implants performed the best of the three implants studied, the kinematics of the implants were similar. It is not known whether the small kinematic differences between implants are clinically important.

The change in kinematics following radial head arthroplasty are most likely related to the small errors (<2mm translation and <11° rotation) in placement of the stem in spite of image-based computer navigation (Deluce, 2011). The errors seen in rotation would be expected to have a greater effect on the two anatomical implants than the axisymmetric implant. This is because the anatomic implants have off-centered dishes which would be expected to rely on precise placement to perform similarly to the native kinematics. It is likely that up to 11° of malrotation may have altered the position of the dish of both the quasi-anatomic and patient-specific implant. This error in rotational orientation would not have had much of an effect on the axisymmetric implant since the dish is located

centrally on this implant. The observation that the kinematics of the more anatomic implants were similar to the axisymmetric implants, in spite of rotational malpositioning, suggests other factors such as translational malpositioning or annular ligament and interosseous membrane tension may have a greater influence on radiocapitellar kinematics than implant shape. Further studies are needed to better understand the articular contact at the radiocapitellar joint and to further elucidate the influence of errors in implant translation.

In this study, the implant stem was cemented into the canal of the radius. This was done to ensure both the quasi-anatomic and patient-specific radial head implants were located in an optimal position. Since, we used a custom stem to fit all implants; the axisymmetric implant was fixed in place as well. Although a fixed position is necessary for anatomically shaped implants, some commercially available axisymmetric implants are designed to have a loose fitting stem or a bipolar head, such that the implant has some ability to self-align the dish against the capitellum (Calfee *et al.*, 2006). During forearm motion the radial heads of these implants may move slightly with respect to the proximal radius such that they stay in optimal contact with the capitellum. Future studies should compare the radiocapitellar kinematics and contact mechanics of anatomically shaped radial head implants to that of a loose fitting stem or bipolar radial head implants.

In this study both simulated active and passive forearm supination were performed. During active supination, the radial head was located much more anteriorly (approximately 3-7mm) than during passive rotation. This is likely due to the fact that during supination, the biceps (which inserts on the radius) was loaded and therefore, pulled up on the radius, causing it to translate more anteriorly. This difference was not

observed in ML translation data since there were no muscle groups that caused the radial head to move side to side and the annular ligament and proximal radioulnar joint (PRUJ) were kept intact; therefore, maintaining stability in both the medial and lateral directions. It was also observed, that the standard deviations for passive forearm rotation were generally higher than the standard deviations for active rotation, specifically for the AP translation data. This is likely due to the fact that the active forearm rotation was conducted with computer controlled tendon loading, simulating muscle activity which helped to stabilize the joint, whereas passive rotation relies on the experimenter to manually move the arm while no muscles are loaded. The lower repeatability of passive motions has been previously reported with this testing system and is expected given that variable external forces and moments are applied to the forearm by the tester (Dunning *et al.*, 2001).

In summary, implant shape had little effect on radiocapitellar kinematics with near optimally positioned implants as employed in this investigation. Further studies are needed to explore the clinical significance of implant shape in the setting of suboptimally positioned implants which frequently occurs in clinical practice when proximal radial landmarks are damaged as is typically the case with radial head fractures and when navigation is not employed.

3.5 References

- Beingessner, D.M., Dunning, C.E., Gordon, K.D., Johnson, J.A., and King, G.J. (2004) The effect of radial head excision and arthroplasty on elbow kinematics and stability. *J Bone Joint Surg Am* 86-A[8], 1730-1739.
- Calfee, R., Madom, I., and Weiss, A.P. (2006) Radial head arthroplasty. *J Hand Surg Am* 31[2], 314-321.
- Deluce, S.R. (2011) Design, Validation and Navigation of Anatomic Population-Based and Patient-Specific Radial Head Implants. Master of Engineering Science Western University.
- Dunning, C.E., Duck, T.R., King, G.J., and Johnson, J.A. (2001) Simulated active control produces repeatable motion pathways of the elbow in an in vitro testing system. *J Biomech.* 34[8], 1039-1048.
- Ferreira, L.M., Stacpoole, R.A., Johnson, J.A., and King, G.J. (2010) Cementless fixation of radial head implants is affected by implant stem geometry: an in vitro study. *Clin Biomech.(Bristol., Avon.)* 25[5], 422-426.
- Fraser, G.S., Pichora, J.E., Ferreira, L.M., Brownhill, J.R., Johnson, J.A., and King, G.J. (2008) Lateral collateral ligament repair restores the initial varus stability of the elbow: an in vitro biomechanical study. *J Orthop Trauma* 22[9], 615-623.
- Galik, K., Baratz, M.E., Butler, A.L., Dougherty, J., Cohen, M.S., and Miller, M.C. (2007) The effect of the annular ligament on kinematics of the radial head. *J Hand Surg Am* 32[8], 1218-1224.
- Heijink, A., Morrey, B.F., and Cooney, W.P., III . (2008) Radiocapitellar hemiarthroplasty for radiocapitellar arthritis: a report of three cases. *J Shoulder Elbow Surg* 17[2], e12-e15.
- Johnson, J.A., Rath, D.A., Dunning, C.E., Roth, S.E., and King, G.J. (2000) Simulation of elbow and forearm motion in vitro using a load controlled testing apparatus. *J Biomech.* 33[5], 635-639.
- King, G.J., Zazour, Z.D., Patterson, S.D., and Johnson, J.A. (2001) An anthropometric study of the radial head: implications in the design of a prosthesis. *J Arthroplasty* 16[1], 112-116.
- Koslowsky, T.C., Germund, I., Beyer, F., Mader, K., Krieglstein, C.F., and Koebke, J. (2007) Morphometric parameters of the radial head: an anatomical study. *Surg Radiol.Anat.* 29[3], 225-230.

Mason, M.L. (1954) Some observations on fractures of the head of the radius with a review of one hundred cases. *Br.J Surg* 42[172], 123-132.

Morrey, B.F. (2008) *The Elbow and Its Disorders*. Saunders Elsevier.

Sabo, M.T., Shannon, H., De Luce, S., Lalone, E., Ferreira, L.M., Johnson, J.A., and King, G.J. (2012) Elbow kinematics after radiocapitellar arthroplasty. *J Hand Surg Am* 37[5], 1024-1032.

van Riet, R.P., Van Glabbeek, F., Neale, P.G., Bimmel, R., Bortier, H., Morrey, B.F., O'Driscoll, S.W., and An, K.N. (2004) Anatomical considerations of the radius. *Clin Anat.* 17[7], 564-569.

van Riet, R.P., Van Glabbeek, F., Neale, P.G., Bortier, H., An, K.N., and O'Driscoll, S.W. (2003) The noncircular shape of the radial head. *J Hand Surg Am* 28[6], 972-978.

CHAPTER 4 - GENERAL DISCUSSION AND FUTURE WORK

OVERVIEW: This chapter reviews the initial objectives and hypotheses presented in Chapter 1, and the work subsequently conducted. The strengths and limitations of the studies are presented and discussed. Also, the future directions of this research are considered.

4.1 Summary

A number of studies have examined the morphology of the radial head. Recent studies have concluded that the radial head is in fact elliptical in shape, not circular. The majority of currently available radial head implants are axisymmetric in design. There is only one commercially available anatomically shaped implant and it uses special marks to guide alignment during implantation. Due to the elliptical shape and eccentric dish of the radial head, it is essential that anatomically shaped implants are oriented correctly during surgery to optimize implant alignment and hence restore normal joint kinematics, articular contact and load transfer. Previous to the studies of this thesis, two anatomically shaped implants were designed in our laboratory (Deluce, 2011). One of these implants was a reverse engineered patient-specific implant and the other was a set of three population based quasi-anatomic implants. Although these implants have been analyzed to assure they more closely match the anatomy of the native radial head than the axisymmetric radial head implants, the contact mechanics and resulting kinematics with these novel implants have not yet been assessed.

In Chapter 2, the joint contact mechanics of the anatomically shaped implants were assessed in relation to an axisymmetric radial head implant as well as the native radial head (Objectives 1, Chapter 2). The findings of the study showed that there was a significant effect of radial head morphology on contact area, but not for the location of the contact. Although all of the implant morphologies resulted in a lower contact area than the native radial head, only the axisymmetric implant was significantly different from the native state. Therefore, while it was shown that an anatomically shaped implant can improve the contact mechanics of the radiocapitellar joint compared to an axisymmetric implant, the differences between the implants were small relative to the large differences in contact between the implants and the native articulation.

Although we know from theory that the anatomically shaped implants more closely replicate the shape of the native radial head than axisymmetric implants, it is important to determine how these implants compare during active motion of the elbow. Forearm rotation kinematics were analyzed in Chapter 3 to determine whether or not the anatomically shaped implants would perform more similarly to the intact joint than the axisymmetric implants (Objective 2, Chapter 3). The findings of this study showed that the only significant kinematic differences between implant shapes were in AP translation of the radial head with respect to the capitellum. While there was no significant difference between implant morphologies; there were significant differences between the axisymmetric and native radial head as well as the quasi-anatomic and native radial head. However, there was no difference in kinematics between the patient-specific implant and the native radial head. These data suggest that the patient-specific implants most

accurately replicated the kinematics of the native articulation. However the differences between the implant designs were small and may not be clinically important.

This work has shown that an anatomically shaped radial head implant can improve the mechanics of the radiocapitellar joint as long as rigid fixation and proper alignment are achieved. This has proved problematic in clinical experience with such implants to date (Flinkkila *et al.*, 2012). It is important that further work is done to validate these designs and to improve upon design and implantation techniques. Future efforts to reduce the stiffness of radial head implants may have a bigger impact than altering the shape which was the focus of the current thesis.

4.2 Limitations and Strengths

This study was not without limitations. First, all experiments were *in vitro* biomechanical models that used cadaveric specimens. Although we were able to generate active motion (using an elbow simulator) to analyze kinematics, there may still be some differences between the *in vitro* and *in vivo* states, including applied joint loads, soft tissue interactions and hydration of cartilage. Another limitation of this research was that we were only able to analyze the contact mechanics statically due to the casting process used. Contact analysis with motion was not possible with this experimental set-up.

This project used novel implant designs that were previously developed in our laboratory. These designs were not without their own limitations. For instance, the models and measurements were made from CT images that did not include cartilage. Also, there were reliability issues in the measurement process, specifically radial head height, which may

have affected the final shape of the quasi-anatomic implants (Deluce, 2011). Another limitation with the implants was the computer navigation set-up. The digitizations required for the best possible registration meant that more access to the radius was required than a surgeon would typically have in the operating room. Also the navigation tool used to place the stem was bulky and had to be held still by the experimenter while the cement set, which proved to be challenging.

These studies had strengths. This research was the first to quantify the contact mechanics and kinematics of a patient-specific radial head implant. Other studies have looked at anatomically shaped implants or the concept of reverse engineered implants, but no one has tested a patient-specific radial head.

Also, this is one of few studies to cast the radiocapitellar joint *in situ*, leaving all the soft tissues intact or repaired in a clinical manner. This provided more clinically relevant data, as the joint was allowed to self-align when loaded as opposed to being aligned by the experimenter. The contact mechanics of the entire joint (bone, muscle and ligament) could be examined, instead of just the bony anatomy.

This is also the first study to use an active motion simulator and a 3D optical tracking camera to assess the kinematics of forearm rotation with anatomically shaped implants. Therefore, this data is more accurate than past studies that have used weights to move the arm or electromagnetic tracking systems to quantify kinematics (which has greater error).

4.3 Future Directions

One future study of great interest would be to quantify radiocapitellar joint congruency using non-invasive imaging techniques which have recently been developed in our laboratory (Lalone *et al.*, 2012). This novel technique provides information on the relative alignment of two articular surfaces as a surrogate of joint contact and could be compared with the findings from the current casting study. This potential work would help confirm the contact area and location results reported in Chapter 2. Furthermore joint congruency can be evaluated dynamically throughout motion unlike the current studies which were performed at only three positions of forearm rotation with the elbow at 90 degrees of flexion.

An additional study would be to pair the contact and kinematics data together to better understand as much as possible about what is happening at the radiocapitellar joint after radial head arthroplasty. It would be valuable to compare real-time contact data to contact data for static positions. Pressure sensors allow for real-time analysis of the contact mechanics of the joint; however they do come with limitations, such as wrinkling. Finite element contact analysis could be also used to validate experimental data and develop improvements in implant design.

Further work must also be done to improve the techniques used for computer navigation. These techniques need to be less invasive as well as more repeatable. Perhaps the use of robotic assistance or a jig to hold the navigation tool during implantation of the stem would help in future studies using these implants such that the final location of the stem does not rely on the experimenter.

As stated in section 4.2 on limitations, the implants were made from radius models that did not include cartilage. It would be valuable to produce implants from models that include the dimensions of the cartilage and compare these implants to the original implants. The size of the implant would change and this may affect both the contact mechanics and kinematics in the radiocapitellar joint. It would also be interesting to investigate less stiff implant materials, as the contact area may well increase and hence possibly lead to less wear on the native cartilage of the capitellum. A study should be performed to determine the appropriate material stiffness of an implant such that contact area approximates the native state, while maintaining strength to undertake the mechanical demands within the joint.

4.4 Significance

This study is the first to quantify the contact mechanics and kinematics of a patient-specific radial head implant. Also, this study is the first to examine anatomically shaped radial head implants (both quasi-anatomic and patient-specific) using an active motion elbow simulator and 3D optical tracking. The results of this study will help direct future efforts in the optimization of radial head implants. Great strides have already been made in determining that the radial head should be replaced as it is an important elbow stabilizer. The current studies demonstrate that while an implant that provides a more anatomic shape slightly improves radiocapitellar contact and kinematics, future efforts are needed to optimize the materials employed in these devices.

4.5 References

Deluce, S.R. (2011) Design, Validation and Navigation of Anatomic Population-Based and Patient-Specific Radial Head Implants. Master of Engineering Science Western University.

Flinkkila, T., Kaisto, T., Sirnio, K., Hyvonen, P., and Leppilahti, J. (2012) Short- to mid-term results of metallic press-fit radial head arthroplasty in unstable injuries of the elbow. *J Bone Joint Surg Br.* 94[6], 805-810.

Lalone, E.A., McDonald, C.P., Ferreira, L.M., Peters, T.M., King, G.W., and Johnson, J.A. (2012) Development of an image-based technique to examine joint congruency at the elbow. *Comput Methods Biomech. Biomed. Engin.*

APPENDIX A - GLOSSARY OF TERMS

Anatomic	- Relating to the structure of the body
Anterior	- Towards the front of the body
Annular Ligament	- A ligament which encircles the head of the radius ensuring contact between the radius and PRUJ
Arthroplasty	- Surgical reconstruction or replacement of a joint
Articular	- Relating to a joint
Axisymmetric	- Having symmetry around an axis
Capitellum	- Smooth rounded surface on the lateral distal humerus which articulates with the radial dish
Cartilage	- Smooth, firm connective tissue found on articulating surfaces of joints
Comminuted	- To break into several small fragments
Contact Area	- Surface area in contact between two bones
Coronoid	- Triangular anterior projection on the proximal ulna which articulates with the radius
CT	- Computed tomography, method of x-ray imaging which produces cross section images of the body
Digitization	- Acquiring three-dimension location of points relative to an object
Distal	- Away from the center of the body

DRUJ	- Distal radioulnar joint, pivot-joint between the distal radius and ulna
Excision	- Surgical removal
External Rotation	- Rotation away from the body.
Fossa	- Shallow depression
Humerus	- Bone of the upper arm forming the shoulder and elbow
ICP	- Iterative closest point, an algorithm used for surface registration
Internal Rotation	- Rotation towards the body
Intramedullary Canal	- Marrow cavity of a bone
Landmark	- Reliably identified feature
Lateral	- Away from the middle of the body
Laxity	- Looseness
LCL	- Lateral collateral ligament; ligament composed of the LUCL and the RCL
LED	- Light emitting diode
Lesser Sigmoid Notch	- Depression on the lateral side of the coronoid which articulate with the radial head
Ligament	- Fibrous connective tissue between two bones

LUCL	- Lateral ulnar collateral ligament; extends from lateral epicondyle to the coronoid and serves as an important posterolateral rotational stabilizer
Medial	- Towards the middle of the body
Modular	- Constructed with standardized units allowing flexibility in assembly
MCL	- Medial collateral ligament; extends from medial epicondyle of humerus to the coronoid providing primary valgus restraint
Morphology	- Study of size, shape and structure
ORIF	- Open reduction and internal fixation; method for surgically repairing fracture bone using plates and/or screws
Osseous	- Relating to bone
Posterior	- Towards the back of the body
Post-Operative	- After surgery
Pre-Operative Planning	- Using medical imaging to determine surgical targets before operating
Pronation	- Rotation towards the midline
Prosthesis	- Artificial device extension replacing a missing body part
Proximal	- Towards the center of the body

- PRUJ** - Proximal radioulnar joint, articulation between the lesser sigmoid notch of the ulna and the circumference of the radial head
- Radial Dish** - Concavity on the proximal end of the radial head which articulates with the capitellum
- Radial Head** - Complex anatomic structure forming the proximal end of the radial which articulates with both the humerus and ulna
- Radial Neck** - Narrow region of proximal radius distal to the radial head
- Radius** - The lateral bone of the forearm articulating with the ulna, humerus and carpal bones
- RCL** - Radial collateral ligament; originates on the lateral epicondyle and inserts into the annular ligament serving as a primary varus stabilizer of the elbow
- Registration** - The process by which one dataset is aligned with another based on shared features
- Reverse Engineer** - Create a 3D CAD model of an existing part or in this study, bone. Involves measuring the object to construct the 3D model.
- Rigid-Body** - Solid body in which deformation is neglected
- Segmentation** - Process by which a 3D data set is transcribed from 2D slice information
- Soft-Tissue** - Tissues that connect, support or surround other structures, not including bone
- Stylus** - Penlike device used to obtain digitizations with

respect to a tracking system

- Subluxate** - To partially dislocate a joint
- Supination** - Rotation away from the midline
- Trochoginglymoid** - Type of joint composed of hinge (ginglymus) and pivot joints (trochoid)
- Ulna** - The medial bone of the forearm articulating with the radius, humerus, and carpal bones
- Valgus** - Displacement of the distal aspect of the bone away from the midline of the body
- Varus** - Displacement of the distal aspect of the bone towards the midline of the body

APPENDIX B - CONTACT AREA OF METAL AXISYMMETRIC IMPLANTS VS. PLASTIC AXISYMMETRIC IMPLANTS

Table B.1 Comparison of Contact Area of Plastic Implants to Metal Implants

Three casts were made using a cadaveric humerus with one plastic axisymmetric implant and one metal axisymmetric implant of the same size. A t-test was performed to compare the two implants. The plastic and metal implants showed no significant differences in contact area ($p=0.92$).

	Metal Contact Area (mm²)	Plastic Contact Area (mm²)
Trial #1	50.99	52.94
Trial #2	53.82	44.32
Trial #3	49.66	55.98
mean	51.49	51.08
p value	0.92	

APPENDIX C - SUMMARY OF RADIOCAPITELLAR CONTACT IMAGES

Note: Only 7 of 8 specimens are displayed in this appendix. Due to registration issues with the image set for specimen 11-03052R, the images could not be displayed in this fashion.

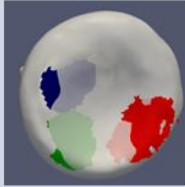
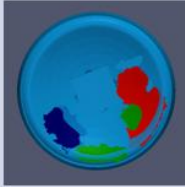
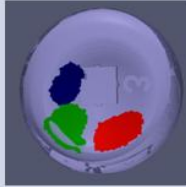
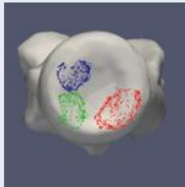
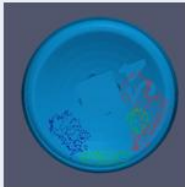
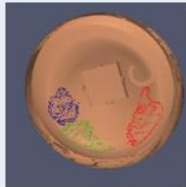
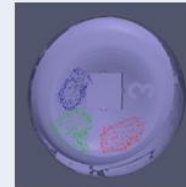
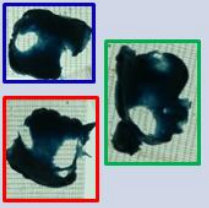
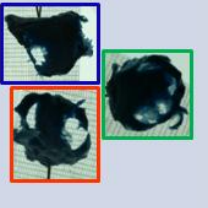
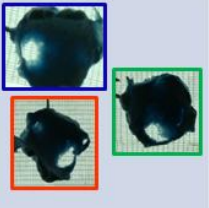
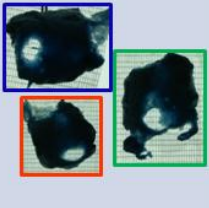
	Native RH	Axisymmetric	Quasi-Anatomic	Patient-Specific	Legend
Surfaces					<ul style="list-style-type: none"> ■ supination ■ neutral ■ pronation
Digitizations					
Casts					

Figure C.1 Specimen 09-12057R

This image displays the casts, point cloud digitizations and the resulting surfaces for radiocapitellar contact area for the native radial head (grey), axisymmetric implant (blue), population based quasi-anatomic implant (orange) and the reverse engineered patient-specific implant (purple).

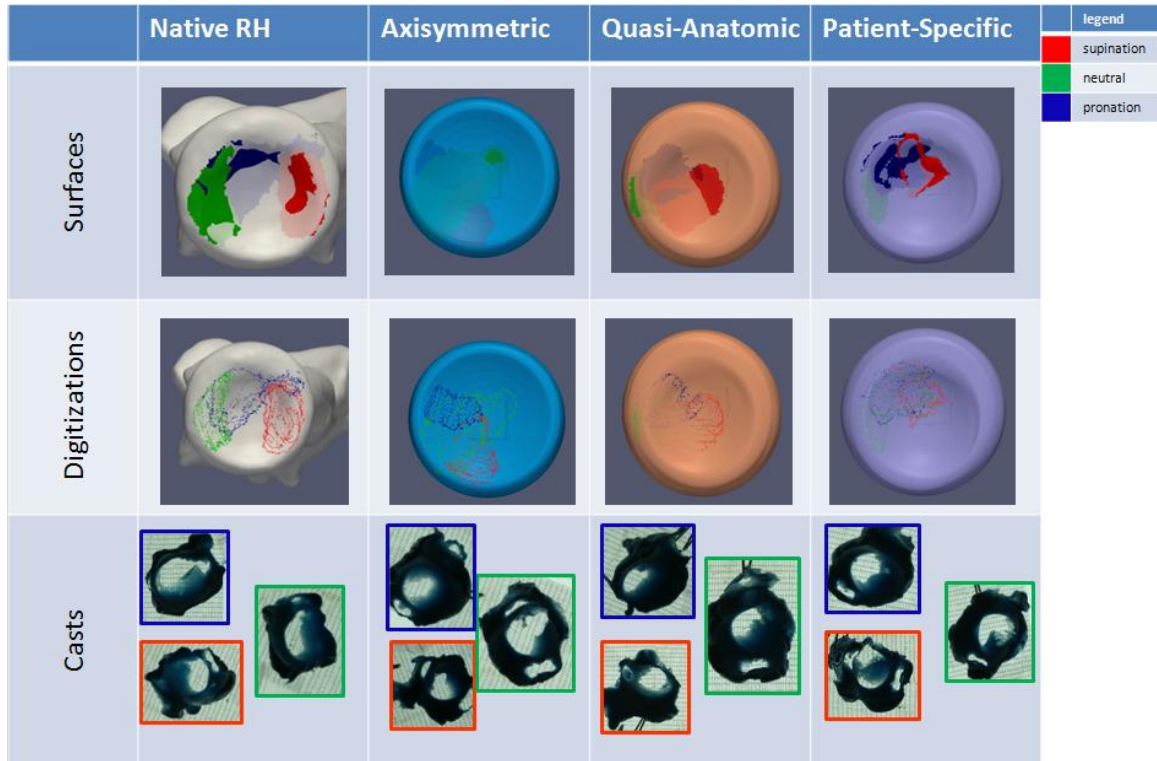


Figure C.2 Specimen 10-01020R

This image displays the casts, point cloud digitizations and the resulting surfaces for radiocapitellar contact area for the native radial head (grey), axisymmetric implant (blue), population based quasi-anatomic implant (orange) and the reverse engineered patient-specific implant (purple).

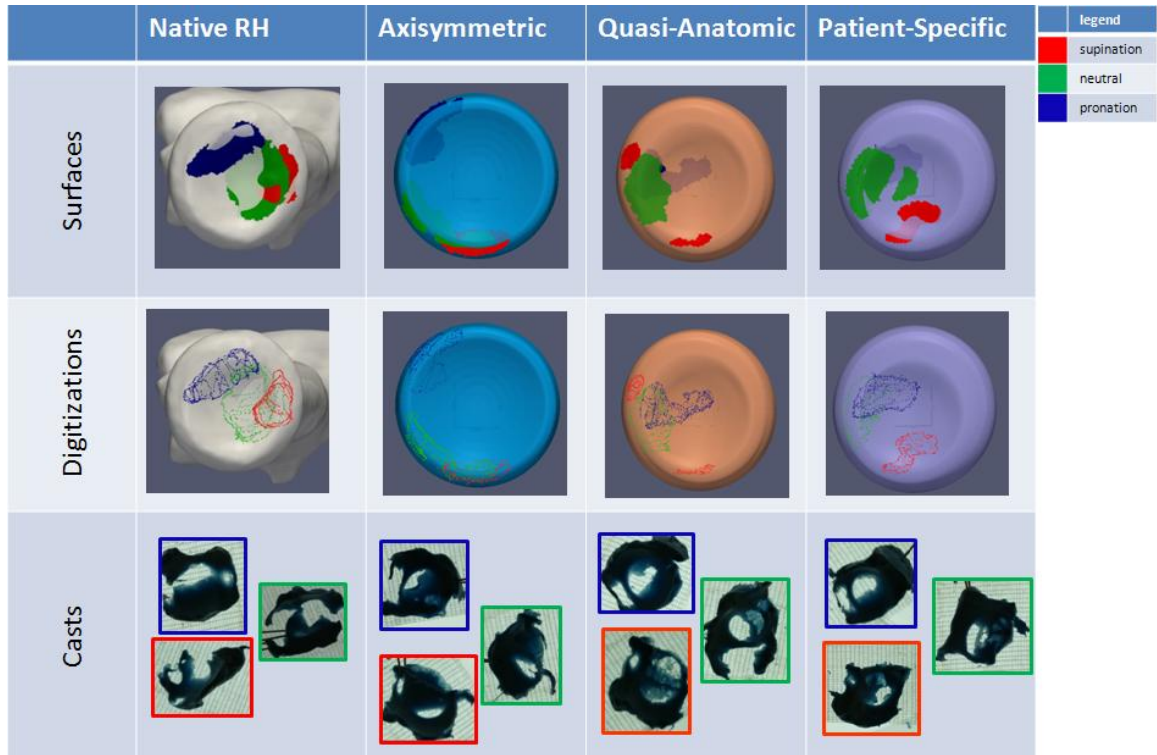


Figure C.3 Specimen 10-06020R

This image displays the casts, point cloud digitizations and the resulting surfaces for radiocapitellar contact area for the native radial head (grey), axisymmetric implant (blue), population based quasi-anatomic implant (orange) and the reverse engineered patient-specific implant (purple).

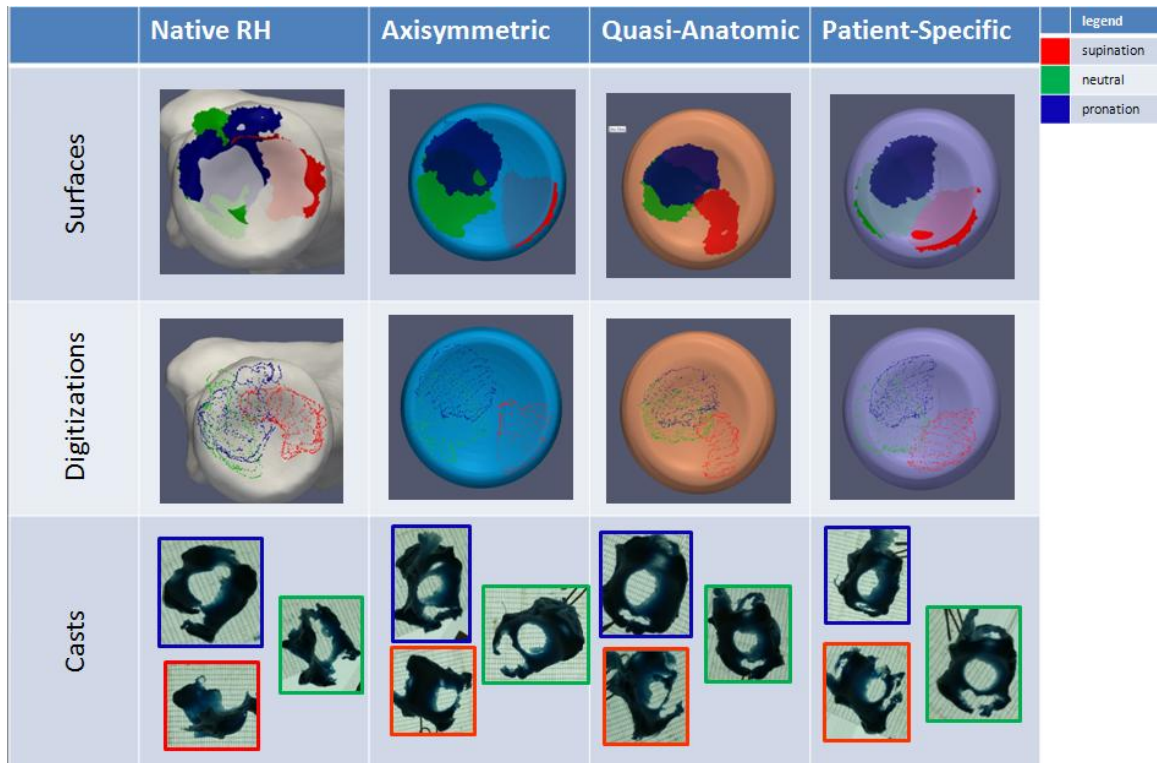


Figure C.4 Specimen 10-07020R

This image displays the casts, point cloud digitizations and the resulting surfaces for radiocapitellar contact area for the native radial head (grey), axisymmetric implant (blue), population based quasi-anatomic implant (orange) and the reverse engineered patient-specific implant (purple).

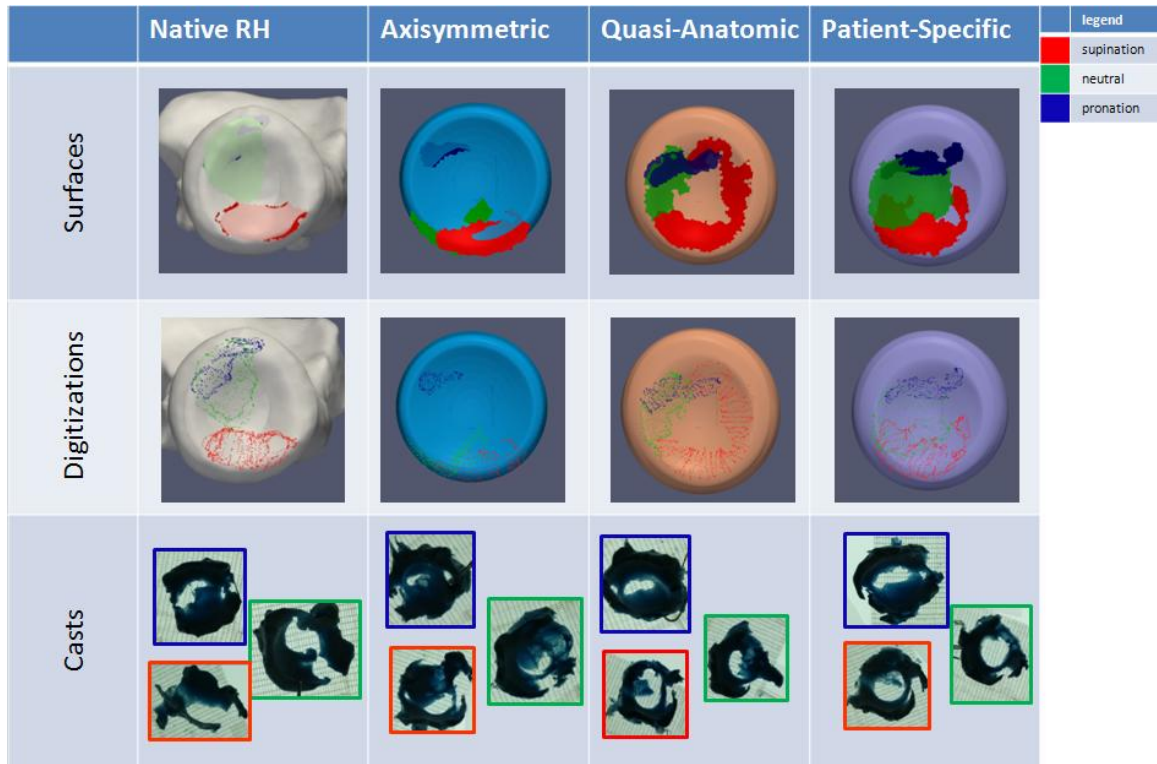


Figure C.5 Specimen 10-08002R

This image displays the casts, point cloud digitizations and the resulting surfaces for radiocapitellar contact area for the native radial head (grey), axisymmetric implant (blue), population based quasi-anatomic implant (orange) and the reverse engineered patient-specific implant (purple).

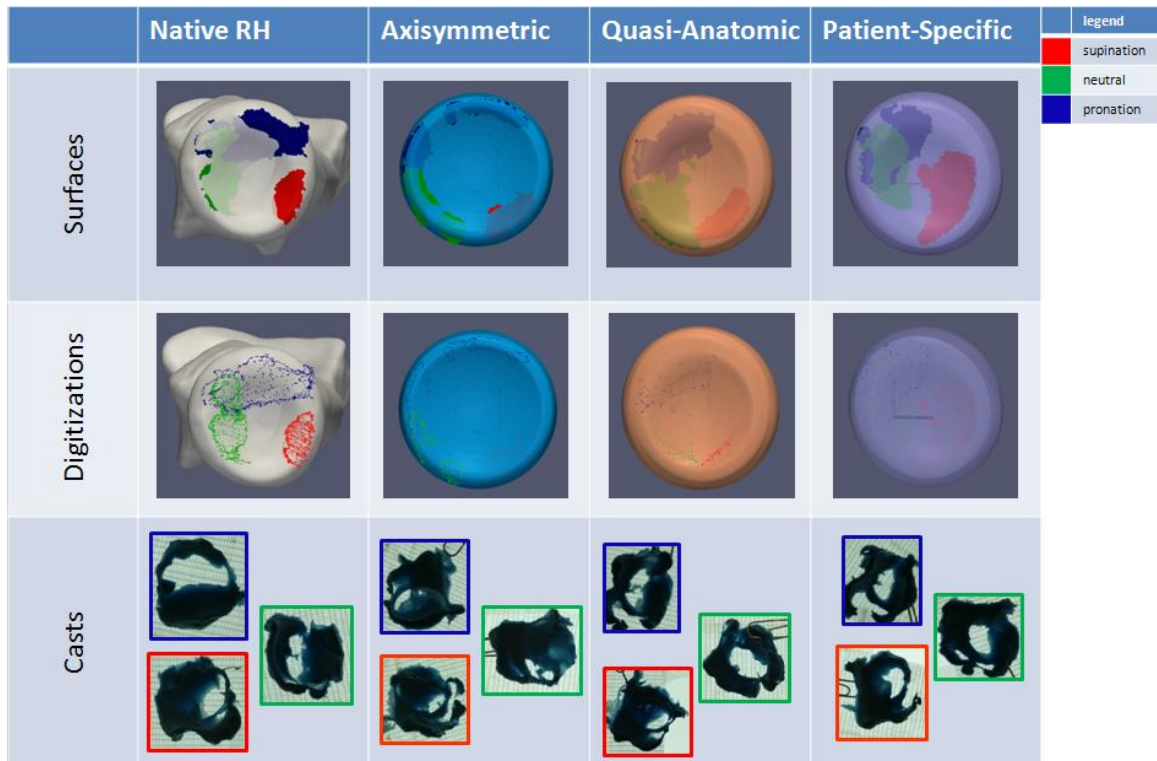


Figure C.6 Specimen 11-03022R

This image displays the casts, point cloud digitizations and the resulting surfaces for radiocapitellar contact area for the native radial head (grey), axisymmetric implant (blue), population based quasi-anatomic implant (orange) and the reverse engineered patient-specific implant (purple).

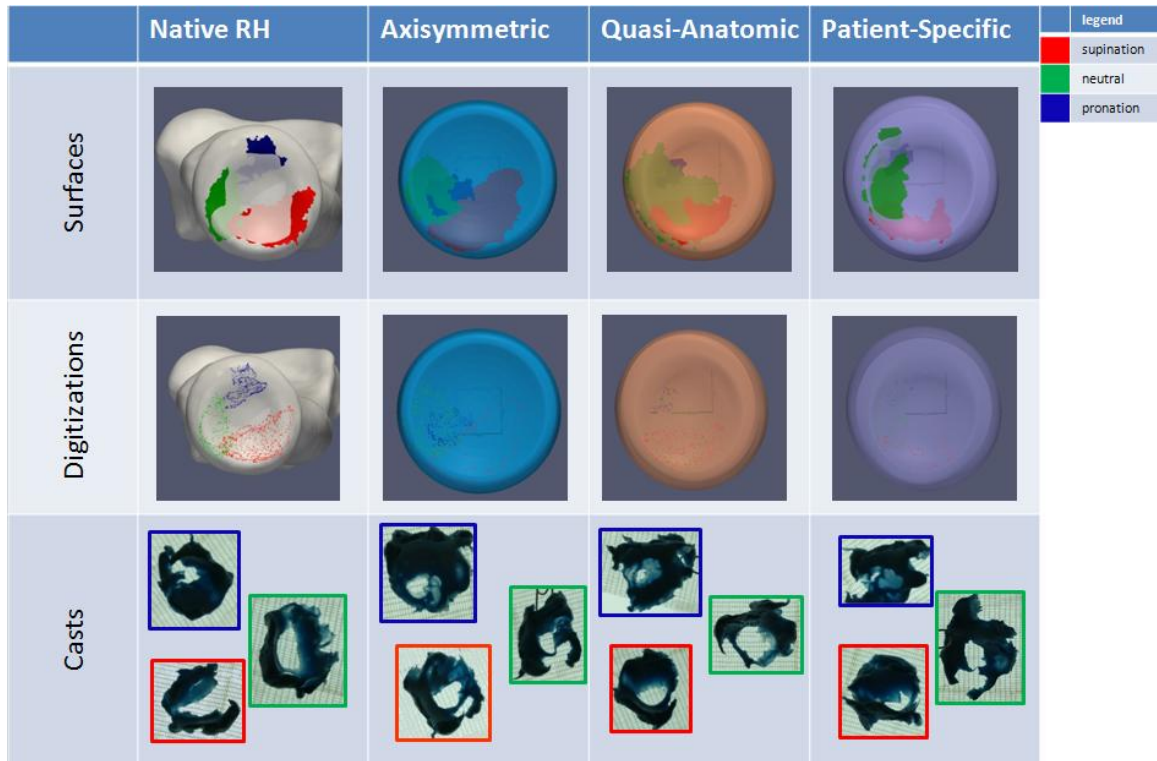


Figure C.7 Specimen 11-03045R

This image displays the casts, point cloud digitizations and the resulting surfaces for radiocapitellar contact area for the native radial head (grey), axisymmetric implant (blue), population based quasi-anatomic implant (orange) and the reverse engineered patient-specific implant (purple).

APPENDIX D - VALIDATION OF THE LCL REPAIR CONDITION AS A CONTROL

The results of comparing medial-lateral translations as well as anterior-posterior translations for the intact elbows with the native radial head and following LCL sectioning and repair are shown here. There was no significant difference ($p>0.05$) for active or passive motion.

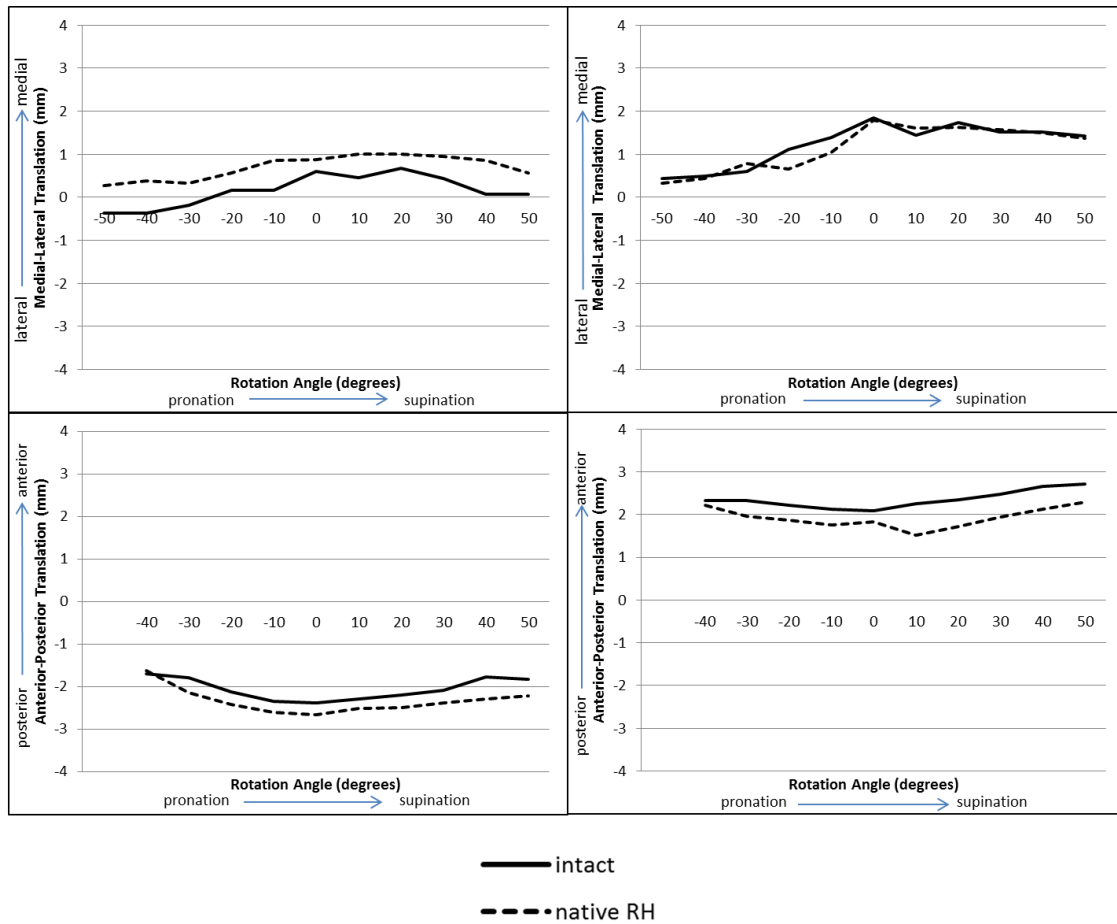


Figure D.1 Intact Elbow vs. Control

Intact (solid line) represents the fully intact joint and native RH (dashed line) represents the native radial head (control) condition (with sectioned and repaired LCL). There were no significant differences between the intact elbow and the native radial head control condition ($p > 0.05$).

- A. Medial-lateral translations during passive forearm rotation
- B. Medial-lateral translations during active forearm rotation
- C. Anterior-posterior translations during passive forearm rotation
- D. Anterior-posterior translations during active forearm rotation

APPENDIX E - MEAN KINEMATICS DATA WITH STANDARD DEVIATIONS

Table E.1 Medial-Lateral Translation during Active Rotation

This table displays the mean ML translation and standard deviations during active forearm rotation (every 10°) for the native RH, the axisymmetric implant, the quasi-anatomic implant and the patient-specific implant. Positive rotation represents supination.

		-50°	-40°	-30°	-20°	-10°	0°	10°	20°	30°	40°	50°
native RH	mean (mm)	0.32	0.43	0.78	0.66	1.04	1.78	1.61	1.63	1.58	1.49	1.37
	std dev (±mm)	0.87	0.68	1.07	1.20	1.10	1.38	1.86	1.66	1.23	0.83	1.05
axisymmetric	mean (mm)	0.94	1.11	1.08	1.21	1.53	1.64	1.57	1.64	1.60	1.24	1.16
	std dev (±mm)	1.48	1.69	1.53	2.03	2.26	2.29	2.67	3.17	2.99	2.20	2.18
quasi-anatomic	mean (mm)	1.00	1.19	1.16	1.54	1.45	1.95	1.98	2.04	1.57	1.66	1.47
	std dev (±mm)	0.77	0.97	1.17	1.49	1.55	1.95	2.12	2.36	1.56	1.67	1.71
patient-specific	mean (mm)	0.81	1.01	0.96	1.30	1.61	1.98	1.76	1.85	1.62	1.63	1.37
	std dev (±mm)	1.44	1.37	1.39	1.65	2.01	2.01	2.34	2.25	1.94	1.69	1.58

Table E.2 Medial-Lateral Translation during Passive Rotation

This table displays the mean ML translation data and standard deviations during passive forearm rotation (every 10°) for the native RH, the axisymmetric implant, the quasi-anatomic implant and the patient-specific implant. Positive rotation represents supination.

		-50°	-40°	-30°	-20°	-10°	0°	10°	20°	30°	40°	50°
native RH	mean (mm)	0.26	0.38	0.32	0.56	0.85	0.87	1.01	1.00	0.94	0.86	0.56
	std dev (±mm)	1.67	1.05	1.01	1.05	1.16	1.48	1.52	1.64	1.66	1.37	1.30
axisymmetric	mean (mm)	0.89	0.61	0.67	0.46	0.47	0.60	0.26	0.22	0.06	-0.28	-0.41
	std dev (±mm)	1.45	1.55	1.62	1.56	2.40	2.53	2.79	2.99	2.78	2.12	2.00
quasi-anatomic	mean (mm)	0.46	0.75	0.55	0.68	0.91	1.05	0.93	0.96	0.47	0.40	0.20
	std dev (±mm)	1.23	1.10	1.17	1.39	1.46	1.70	1.74	2.16	1.89	1.77	1.55
patient-specific	mean (mm)	0.74	0.47	0.22	0.58	0.90	0.98	0.57	0.60	0.43	0.28	0.35
	std dev (±mm)	1.60	1.43	1.44	1.80	1.81	1.94	2.19	2.15	1.74	1.64	1.57

Table E.3 Anterior-Posterior Translation during Active Rotation

This table displays the mean AP translation data and standard deviations during active forearm rotation (every 10°) for the native RH, the axisymmetric implant, the quasi-anatomic implant and the patient-specific implant. Positive rotation represents supination.

		-50°	-40°	-30°	-20°	-10°	0°	10°	20°	30°	40°	50°
native RH	mean (mm)	2.31	2.22	1.95	1.87	1.75	1.82	1.52	1.71	1.94	2.12	2.29
	std dev (±mm)	2.09	1.84	1.87	1.92	1.94	1.89	1.95	2.08	2.04	2.06	2.03
axisymmetric	mean (mm)	4.76	4.14	4.37	4.08	3.69	3.49	3.25	3.27	3.23	3.32	3.19
	std dev (±mm)	3.00	2.50	2.18	2.16	2.09	2.18	2.24	2.23	2.14	2.15	2.10
quasi-anatomic	mean (mm)	3.36	3.52	3.56	3.31	3.07	2.94	2.91	3.12	3.18	3.18	3.16
	std dev (±mm)	2.46	2.10	1.93	1.85	2.03	1.97	1.97	1.96	2.03	1.89	1.88
patient-specific	mean (mm)	3.25	3.63	3.83	3.50	3.22	3.04	2.96	2.92	2.90	2.91	3.02
	std dev (±mm)	2.11	1.87	1.98	1.91	1.92	2.03	2.21	2.26	2.19	2.14	2.25

Table E.4 Anterior-Posterior Translation during Passive Rotation

This table displays the mean AP translation data and standard deviations during passive forearm rotation (every 10°) for the native RH, the axisymmetric implant, the quasi-anatomic implant and the patient-specific implant. Positive rotation represents supination.

		-50°	-40°	-30°	-20°	-10°	0°	10°	20°	30°	40°	50°
native RH	mean (mm)	-1.42	-1.63	-2.14	-2.43	-2.61	-2.67	-2.51	-2.49	-2.40	-2.29	-2.23
	std dev (±mm)	2.39	2.54	2.59	2.84	3.05	3.20	3.45	3.49	3.51	3.38	3.31
axisymmetric	mean (mm)	-1.01	-0.97	-1.37	-1.92	-2.28	-2.75	-2.87	-3.14	-3.18	-3.35	-3.74
	std dev (±mm)	3.44	3.54	3.15	3.15	3.17	3.20	3.03	2.80	2.15	1.78	1.95
quasi-anatomic	mean (mm)	-1.30	-1.50	-1.97	-2.19	-2.31	-2.38	-2.34	-2.22	-1.89	-1.99	-2.03
	std dev (±mm)	3.34	2.99	2.84	2.69	2.57	2.58	2.38	2.08	1.61	1.58	1.44
patient-specific	mean (mm)	-0.64	-1.21	-1.55	-1.96	-2.19	-2.19	-2.23	-1.89	-1.86	-1.85	-2.15
	std dev (±mm)	2.92	2.63	2.49	2.28	2.24	2.46	2.41	2.08	2.16	2.10	2.00

CURRICULUM VITAE

Hannah Louise Shannon, BSc

EDUCATION

- 2002-2006 Humber College
Toronto, Ontario
Ontario Secondary School Diploma
Bilingual Certificate
(Ontario Scholar, Centennial Scholar)
- 2006-2010 The University of Western Ontario
London, Ontario
Bachelor of Science – Honors Specialization Medical Biophysics
(Western Scholar)
- 2009-2010 The University of Western Ontario
St. Joseph's Health Care
Hand and Upper Limb Centre - Bioengineering Lab
London, Ontario
Fourth Year Honors Thesis
Supervisor- Dr. Jim Johnson, PEng PhD
- 2010-present The University of Western Ontario
St. Joseph's Health Care
Hand and Upper Limb Centre - Bioengineering Lab
London, Ontario
Masters of Engineering Science – Biomedical Engineering
Supervisor- Dr. Jim Johnson, PEng PhD

TEACHING

- 2010-2011 **Instructor**
Biomedical Engineering Course
Western Engineering Summer Academy
The University of Western Ontario
London, Ontario
- 2010-present **Teaching Assistant**
Biophysics of Transport Systems
Medical Biophysics/Biomedical Engineering

The University of Western Ontario
London, ON

2011 **Coordinator**
Biomedical Engineering Course
Western Engineering Summer Academy
The University of Western Ontario
London, Ontario

HONOURS AND AWARDS

2006 **Ontario Volunteer Award** -Commitment to Girl Guides of Canada, 115th Girl Guides
Ontario Provincial Government
Toronto, Ontario

2007-2010 **Dean's Honor List** -Achieving an average of 80% or greater
The University of Western Ontario
London, Ontario

2010 **Western Scholar**-Entering university with a high school average of at least 90% and achieving a sessional average at of 80% or more with no mark less than 65% with a full course load
The University of Western Ontario
London, Ontario

2010-present **Western Graduate Research Scholarship**-Tuition equivalent scholarship for students with an average of at least 80%
The University of Western Ontario
London, Ontario

2010-present **Joint Motion Program (JuMP)**-CIHR funded scholarship and training program for musculoskeletal research
The University of Western Ontario
London, Ontario

EMPLOYMENT HISTORY

2009-present **Research Assistant**
Bioengineering Lab
Hand and Upper Limb Centre
St. Joseph's Health Care
London, Ontario

PUBLICATIONS

Journal Articles

- 1) Sabo MT, Shannon H, Ng J, Ferreira LM, Johnson JA, King GJ. The Impact of Capitellar Arthroplasty on Elbow Contact Mechanics: Implication for Implant Design. *Clin Biomech (Bristol, Avon)*. 2011 Jun;26(5):458-63.
- 2) Sabo MT, Shannon HL, Deluce S, Lalone E, Ferreira LM, Johnson JA, King GJ. Capitellar Excision and Hemiarthroplasty Affects Elbow Kinematics and Stability. *J Shoulder Elbow Surg*. 2011 Aug 3. [Epub ahead of print]
- 3) Sabo MT, Shannon H, Deluce S, Lalone E, Ferreira LM, Johnson JA, King GJ. Elbow Kinematics After Radiocapitellar Arthroplasty. *J Hand Surg Am*. 2012 May;37(5):1024-32.

Co-Authored Abstracts and Presentations to Professional Meetings

- 1) Sabo M, Shannon H, Ng J, Ferreira LM, Johnson JA, King GJW: Radiocapitellar Contact Mechanics of the Elbow: Implications for Implant Design. *The 37th Annual Orthopaedic Surgery Residents' Research Day*, London, Ontario, October 6, 2009.
- 2) Deluce SR, Shannon H, Ferreira LM, King GJ, Johnson JA: The Development and Validation of a Laser Point Digitization System for Computer Assisted Orthopaedic Surgery. *57th Annual Meeting of the Orthopaedic Research Society*, Long Beach, California, January, 2011.
- 3) Sabo MT, Shannon H, Ng J, Ferreira LM, Johnson JA, King GJW. Capitellar Hemiarthroplasty Significantly Alters Radiocapitellar Contact Mechanics. *45th Annual Meeting of the Canadian Orthopaedic Research Society*, St John's, Newfoundland, July, 2011.
- 4) Deluce SR, Shannon HL, Ferreira LM, King GJ, Johnson JA: The Development and Validation of a Laser Point Digitization System for Computer-Assisted Orthopaedic Surgery. *45th Annual Meeting of the Canadian Orthopaedic Research Society*, St John's, Newfoundland, July, 2011.
- 5) Shannon HL, Ferreira LM, King GJW, Johnson JA: The Effect of Radial Head Implant Position on the Kinematics of Forearm Rotation. *46th Annual Meeting of the Canadian Orthopaedic Research Society*, Ottawa, Ontario, June, 2012.
- 6) Sabo MT, Shannon H, Lalone E, Deluce S, Ferreira LM, Johnson JA, King GJW: Capitellar Hemiarthroplasty Can Restore Normal Elbow Kinematics Compared with Capitellar Excision. *46th Annual Meeting of the Canadian Orthopaedic Research Society*, Ottawa, Ontario, June, 2012.

- 7) Sabo MT, Shannon H, Lalone E, Deluce S, Ferreira LM, Johnson JA, King GJW: Radiocapitellar Arthroplasty and Elbow Kinematics. *46th Annual Meeting of the Canadian Orthopaedic Research Society*, Ottawa, Ontario, June, 2012.

Meetings Attended

- 1) The 37th Annual Orthopaedic Surgery Residents' Research Day, London, Ontario, October 6, 2009.
- 2) The 38th Annual Orthopaedic Surgery Residents' Research Day, London, Ontario, October 13, 2010.
- 3) Innovation Takes Leadership: Ivey Global Health Innovation and Leadership Conference, Toronto, Ontario, November, 2010.
- 4) 57th Annual Meeting of the Orthopaedic Research Society, Long Beach, California, January, 2011.
- 5) 45th Annual Meeting of the Canadian Orthopaedic Research Society/66th Annual Meeting of the Canadian Orthopaedic Association, St John's, Newfoundland, July, 2011.
- 6) The 39th Annual Orthopaedic Surgery Residents' Research Day, London, Ontario, September 27, 2011.
- 7) 58th Annual Meeting of the Orthopaedic Research Society, San Francisco, California, February, 2012.
- 8) 46th Annual Meeting of the Canadian Orthopaedic Research Society/67th Annual Meeting of the Canadian Orthopaedic Association, Ottawa, Ontario, June, 2012.